Chem Soc Rev

Metal-Organic Frameworks: Versatile heterogeneous catalysts for efficient catalytic organic transformations.

Journal:	*Chemical Society Reviews*
Manuscript ID:	CS-REV-11-2014-000395.R1
Article Type:	Review Article
Date Submitted by the Author:	09-Apr-2015
Complete List of Authors:	Chughtai, Adeel; Wuhan University of Technology, State Key Laboratory of Advanced Technology for Materials Synthesis and Processing Ahmand, Nazir; Wuhan University of Technology, State Key Laboratory of Advanced Technology for Materials Synthesis and Processing Younus, Hussein; Wuhan University of Technology, State Key Laboratory of Advanced Technology for Materials Synthesis and Processing; Fayoum University, Chemistry Lyapkov, Alex; Tomsk Polytechnic University, Department of Technology of Organic Substances and Polymer Materials verpoort, francis; Wuhan University of Technology, State Key Laboratory of Advanced Technology for Materials Synthesis and Processing; Ghent University, Inorganic and Physical Chemistry

Metal-Organic Frameworks: Versatile heterogeneous catalysts for efficient catalytic organic transformations.

Adeel H. Chughtai[a,b], Nazir Ahmad[a,b], Hussein A. Younus[a,b], A. Laypkov[c], Francis Verpoort[a,b,c,d*]

[a]*Laboratory of Organometallics, Catalysis and Ordered Materials, State Key Laboratory of Advanced Technology for Materials Synthesis and Processing, Wuhan University of Technology, Wuhan 430070, China.*
[b] *School of Chemistry, Chemical Engineering and Life Sciences, Wuhan University of Technology, Wuhan 430070, China.*
[c] *National Research Tomsk Polytechnic University, Lenin Avenue 30,Tomsk 634050, Russia.*
[d] *Ghent University Global Campus Songdo, 119 Songdomunhwa-Ro,Yeonsu-Gu, Incheon 406-840, South Korea.*
[*] ***Corresponding author: Tel.: +86 18701743583; Fax: +86 2787879468. E-mail:*** Francis.verpoort@ugent.be

Abstract

Novel catalytic materials are highly demanded to perform a variety of catalytic organic reactions. MOFs combine the benefits of heterogeneous catalysis like easy post reaction separation, catalyst reusability, high stability and homogeneous catalysis such as high efficiency, selectivity, controllability and mild reaction conditions. The possible organization of active centers likes metallic nodes, organic linkers, and their chemical synthetic functionalization on nanoscales shows potential to build up MOFs particularly modified for catalytic challenges. In this review, we have summarized the recent research progress in heterogeneous catalysis by MOFs and their catalytic behavior in various organic reactions, highlighting the key features of MOFs as catalysts on the basis of the active sites in the framework. Examples of their post functionalization, inclusion of active guest species and metal nano particles have been discussed. Finally, the use of MOFs as catalysts for asymmetric heterogeneous catalysis and stability of MOFs has been presented as separate sections.

1. Introduction

Metal-organic frameworks (MOFs) are an important class of new materials in the vast field of metal organic materials (MOMs).[1-3] MOFs are the top growing division of novel inorganic-organic materials as they combined the two often-separated disciplines of chemistry; organic and inorganic. The most attractive features of MOFs are their crystalline nature, the high specific surface area (up to 10,400 m^2 g^{-1}),[4] large pore aperture (98 Å),[5] and the low density

(0.13 g cm^{-3}).[6] MOFs are solids with permanent porosity which are built from nodes (metal ions or clusters) coordinated with multi-topic organic bridging linkers to form three-dimensional (3D) coordination networks (Fig. 1a).[7] SBUs are molecular entities in which ligand coordination modes and metal coordination environments can provide the transformation of these components into extensive porous networks in combination with poly-topic linkers.[8] The synthetic methodology generally consists of mixing two solutions containing the hydrophilic metal[9] and the hydrophobic organic component (organic linker),[10] using hydrothermal[11] or solvothermal techniques.[12, 13] Large varieties of metal entities in their stable oxidation states, *i.e.*, alkaline, alkaline earth, transition metal, and rare earth elements have been successfully used in the synthesis of MOFs. In case of the organic linker, usually rigid systems are preferred over flexible ones as they give crystalline, porous, and stable MOFs. Different varieties of organic linkers have been used but mostly poly-carboxylic molecules and poly-azaheterocycles are used.

MOFs are one of the most promptly rising fields in chemical and material sciences, not only due to the fascinating structural topologies but also because of their potential as functional materials in various applications (Fig. 1b). MOFs are currently eliciting noteworthy attention for their prospective applications in gas storage,[14] purification,[15] molecular sensing,[16] drug delivery,[17] biomedicines,[18] photoluminescence,[19] molecular based magnetisms,[20, 21] and photo catalysis.[22]

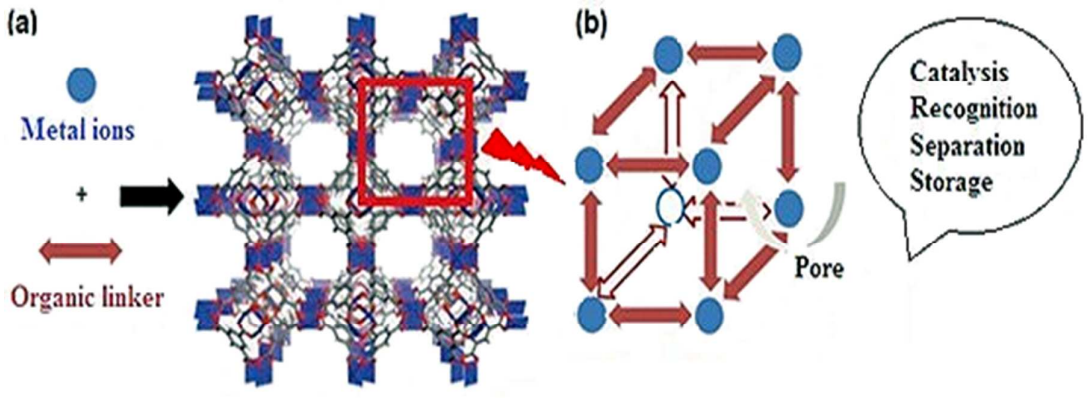

Fig. 1 (a) Schematic representation of synthesis of MOFs, (b) attractive MOFs applications. Reproduced from ref.23.

The most significant feature of MOFs is their potential inner porosity and guest molecules can access the pores which are important for catalytic purposes. Zeolites are amongst the most commercially important classes of catalysts.[24] The similarity between MOFs and zeolites, is well-known, being the inorganic materials zeolites are highly robust and suitable to catalysis under extreme conditions. Their porosity yields internal surface areas that are comparatively large, thus facilitating the catalytic reactivity.[25] The crystalline MOFs, share a number of catalytically relevant features like those of zeolites *e.g.*, large internal surface areas, uniform pores and voids. But, MOFs also differ from zeolites in several important aspects. Firstly, MOFs can be constructed in considerable more chemical varieties than zeolites.[26] Secondly, in most cases, MOFs show a good thermal stability (400-500 °C), but not a bit approaching the stability of zeolites. Thirdly, the persistence of micro porosity after solvent evacuation. In addition, the pore's uniformity and controllability in channel sizes of MOFs accounts mainly for their catalytic selectivity.[27] To date, zeolites are used as heterogeneous catalyst in many industrial processes.[28] However for the manufacturing of bulky and high added value molecules, there is a limitation due to their small pore size. Multi-functionality, high porosity, tunability and original flexibility, are placing MOFs at the frontier between zeolites and enzymes.[29]

One of the most distinct areas of MOF's research is heterogeneous catalysis. MOF based catalysis depends on the active sites; both metal centers and organic linkers contribute to catalytic activities.[30] Especially, the organic bridging linkers may be used as scaffolds to which distinct catalytic complexes, bio-molecules, and homogeneous catalysts can be immobilized or encapsulated. The synthetic flexibility of MOF enables considerable control over size and environment of the pores, allowing selectivity to be tuned more effectively. MOF pores can serve as guest hosts for small molecules (active homogeneous catalysts) or as supports for metal or metal oxide nanoparticles.[31] These properties can be changed *via* chemical synthesis, which distinguish MOFs from other nanoporous materials such as

zeolites and activated carbons. A wide variety of MOFs have been designed with various transition metals as well as different poly-topic ligands and screened in heterogeneous catalysis of organic transformations but still there are hundreds of MOF materials that have not been explored for catalysis. Therefore, the use of MOFs in catalysis is extremely broad and increasing continuously (Fig. 2).

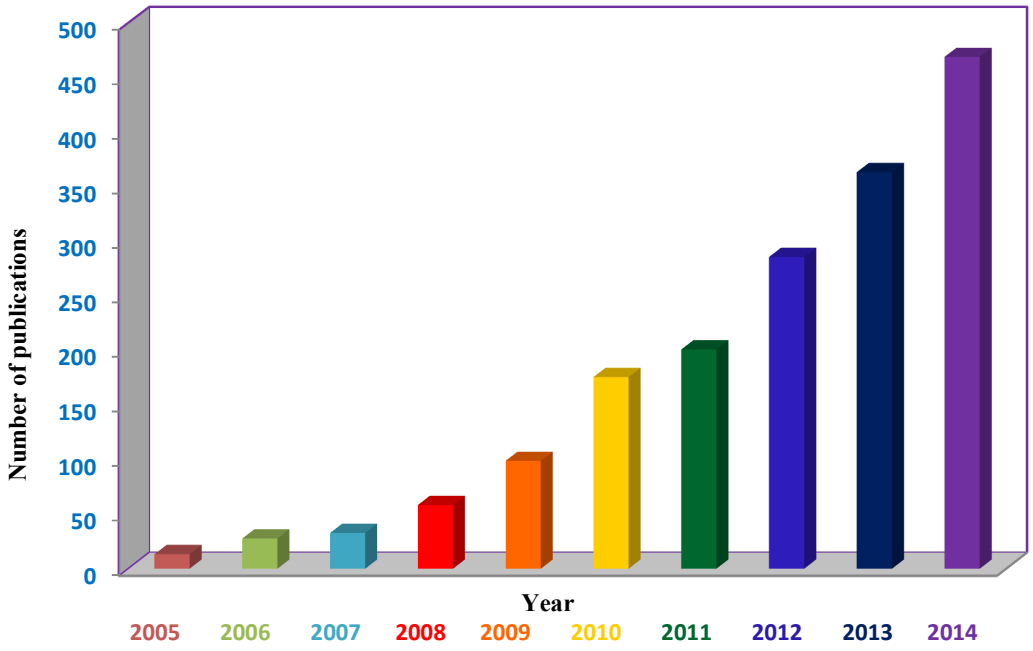

Fig. 2 Publications related to catalysis by MOFs since 2005. (Source: Sci Finder, key word: catalysis by MOFs).

The chemical industry has emerged as a vibrant part of the world economy.[32] However, the production of chemicals also leads to a massive magnitude of environmentally harmful wastes. Heterogeneous catalysis is playing an increasingly imperative role in chemical manufacturing, often with the result of a major reduction in waste.[33] For economic and environmental reasons, there is a huge incentive to replace homogeneous by green and efficient heterogeneous catalytic systems. Heterogeneous catalysis is superior to homogeneous for easier separation, reusability, minimized waste, green and, clean products.[34] The high porosity of MOFs allows fast mass transport and/or interactions with substrates. The use of MOFs as heterogeneous catalysts has presented a significance increase in the last two

decades as they have been considered as an eco-friendly alternative for catalysis. Separation of the reaction products and the catalyst reusability, less leaching problems make MOFs as an active heterogeneous catalyst.

There is currently much interest in applying MOFs as solid catalysts for liquid-phase organic reactions. Earliest example of a coordination polymer based catalyst was a cadmium-bipyridine framework $[Cd(bpy)_2\cdot(NO_3)_2)]_\infty$ (bipy = 4,4-bipyridine) reported by Fujita *et al.* used for the cyanosilylation of aldehydes with cyanotrimethylsilane giving 2-(trimethylsiloxy)phenylacetonitrile in 77% yield.[34] Further examples were reported by Xamena *et al*.[35] focusing on 2D, square grid frameworks $[Pd(2\text{-pymo})2]_n$ (2-pymo = 2-hydroxypyrimidinalote) containing Pd(II) nodes that catalyzes a range of reactions such as Suzuki coupling, olefin hydrogenation, and alcohol aerobic oxidation. The earlier examples are defined as opportunistic catalysts, with trial and error catalytic investigations, a second generation of materials with designed frameworks such as $[Cu_3(btc)_2]$ or HKUST (HKUST = Hong Kong University of Science and Technology's) and MOF-199 ($[Cu_2(btc)_{3/4}]$) (H_3btc = benzene-1,3,5-tricarboxylic acid) which contain large cavities with labile water ligands coordinated to the metal nodes, allowing the formation of open metal sites upon de-solvation.[36] The MOFs possess Lewis-acid sites that can catalyze the cyanosilylation of benzaldehyde or acetone,[37] Lewis-base sites that can catalyze Knoevenagel condensation of benzaldehyde with ethylcyanoacetate and ethyl acetoacetate.[38]

Although, MOFs appear as a new opportunist in the field of heterogeneous catalysis and hundred publications of MOF catalysis are reported, there is a need to ensure its stability, activity and selectivity under reaction conditions. All heterogeneous catalysts including MOFs deactivate after long operation time. Numerous reports are available discussing the reusability of MOF, but only few publications out of hundreds focusing on the turnover numbers, turnover frequencies and comparison with other catalysts. Catalyst deactivation can be checked by textural and spectroscopic techniques.[39] Relatively low thermal stability of

MOFs is another limiting factor for those reactions carried out at higher temperatures. Similarly, leaching of metal or organic components to reaction medium is an undesirable process in heterogeneous catalysis. Therefore, it must be confirmed during reaction progress and can be detected by chemical analysis of reaction filtrate or by hot filtration test. Finally, there is need for theoretical studies rationalizing the catalytic activity of MOFs and also its thermal and chemical stability must be carefully screened in catalysis.

Scope of the review

This review aims to give an overview about MOF based heterogeneous catalysis of different organic reactions and describes the recent literature comprehensively. We critically evaluated the MOF-based heterogeneous catalysis on the basis of (i) active sites *i.e*., metal centre and functional linker, (ii) inclusion of active species, (iii) synthetic chemical modifications, and (iv) homochiral MOFs. The recent significant progress in the development of MOFs catalysis is reviewed and a detailed discussion of the components, structures, stability, reusability, robustness and comparison of MOFs to other catalysts is given.

The catalysis promoted by the multifunctional porous MOFs is summarized and highlighted also. Multi-functional MOFs have a very rich chemistry in terms of their sole structures and multi-functionalities. Their applications in heterogeneous catalysis have been extensively explored, which have been discussed in this review. Moreover, we also thrash out the most recent reports of inclusion of different catalytically active species inside MOFs such as polyoxometallates, metalloprphyrins, and their structure stability after inclusion and also after catalysis. This article will comprehensively discuss the topical development in the use of MOFs as support for mono and bi-metallic nanoparticles. Apart from the synthesis, their applications in organic catalysis are highlighted.

Synthetic chemical modification (SCM) is an important approach in the field of MOF as it offers a way to devise such MOFs that could not be equipped by usual conventional methods.

This review surveys influential examples of SCM, its different types *i.e*., post-synthetic modification, post-synthetic deprotection, post-synthetic exchange to highlight the broad scope of these techniques for enhancing the performance of MOFs and to demonstrate how the SCM concept can be used for future applications. Also an inclusive overview of important reports is given in detail, describing the use of homochiral MOFs in asymmetric catalysis.

MOFs have one major disadvantage, their weak stability (thermal and chemical). Modern synthetic techniques have reported new MOFs having considerable stability. Different approaches have been used to build stable MOFs. Mostly, the use of hard metal ions (high valance metals) with hard bases containing donor atoms (O or N) gives thermally and chemically stable MOFs. The stability and reusability of MOFs as evidenced by different techniques such as XRD and TGA is discussed. The aim of this review is to show that in comparison to the belief about lack of structural stability, the controllable hydrophilicity/hydrophobicity of the internal void of MOFs makes them extremely promising catalysts without compromising their structural stability, while still being efficient in catalyzing the reaction.

Furthermore, catalogues of known catalytic MOFs with formulas are given describing; (i) the active catalytic center in MOFs (Metal, organic linker *etc*.,) and (ii) summery of reactions catalyzed, that will help the reader to grasp a general but comprehensively overview about MOF-based catalysis. Special emphasis is made to present the catalytic behaviour of active MOFs rather than catalytic chemistry that may prove useful to synthetic organic chemists working in the field of organic synthesis and related fields. We sincerely hope that the review will instigate the attention and enthusiasm of chemists in the investigation of MOFs as heterogeneous catalysts for organic transformations, who are advised to further read the cited articles

2. Catalysis with MOFs

Catalysis is at the heart of chemistry and provides tools for efficiently and selectively making and breaking chemical bonds that are crucial for converting given chemicals into more valuable products.[40] Recently, the field of MOFs as catalysts has expanded rapidly as the synthetic chemistry has developed remarkably. From a catalytic point of view, MOFs are very attractive for applications in the liquid phase. Since, they possess catalytic sites characteristics of homogeneous catalysts, along with the advantages of easy separation and recycling. The nano-spherical cavities within the MOF networks serve as reaction chambers. The void volumes and the chemical environment of the interior of MOFs can be designed or modified as required for the use in catalysis. In principle, the active sites of MOF catalysts can be (i) metal centers with unsaturated coordination environment, (ii) other catalytic species encapsulated in the pores, and (iii) the sites inherent in the framework.

Although, catalysis is a developing application of MOFs, several MOFs have been employed as solid catalysts or catalyst supports for a variety of organic transformations. These includes Knoevenagel condensation,[41-44] aldol condensation[45, 46] oxidation reactions,[47-52] epoxide formation,[53-56] hydrogenation,[57-60] Suzuki coupling,[35, 61, 62] ketalization reactions,[63] ring-opening,[64-67] alkylation of amines,[68] cyclopropanation reactions,[69, 70] Henry reactions,[71] Friedel-Crafts reactions,[72-75] cyanosilylation,[76-79] cyclization reactions,[80, 81] Friedlander reaction,[72, 82, 83] acetalization,[84, 85] hydroformylation,[86] Biginelli reaction,[87] Claisen-Schmidt condensation,[88] Beckmann rearrangement,[89] Sonogashira reaction,[90] and polymerization.[91] Herein, we critically described the recently reported examples of different MOFs and their catalytic behavior in various organic reactions.

Nam *et al.* evaluated the catalytic activity of MOF-5 having $[Zn_4O(bdc)_3]$ (H_2bdc = benzene-1,4-dicarboxylic acid) for Friedel-Crafts benzylation of toluene with benzyl bromide as heterogeneous acid catalyst.[74] MOF-5 was characterized by using a variety of techniques such as X-ray diffraction (XRD), Fourier transform Infrared spectroscopy (FT-IR), atomic

absorption spectroscopy (AAS), thermogravimetric analysis (TGA), scanning electron microscopy (SEM), transmission electron microscopy (TEM) and N_2-physiosorption measurements. Quantitative conversion of benzyl bromide was achieved in 4 h and 60% selectivity to *p*-benzyltoluene (major product) was detected in the product mixture with trace amount of *m*-benzyltoluene (by-product). MOF-5 catalyst could be recovered, reused and selectivity remained almost unchanged over five successive runs. Leaching of metal or organic linker into the reaction solution was not detected during the course of reaction. A conversion of over 97% was achieved in the third run, and 80% conversion was still achieved in the fifth run.

Yaghi *et al*. examined the oxidative behavior of two vanadium-containing metal organic frameworks MIL-47 and MOF-48 for conversion of methane to acetic acid (AcOH). In MIL-47, $[VO(bdc)\cdot(H_2bdc)_{0.75}]$ the VO_6 octahedra are sharing opposite corners to make infinite SBUs that are linked together by benzene-1,4-dicarboxylate moieties form a hexagonal arrangement of 1D channel (Fig. 3).[92] The structure of MOF-48 analogue, $[VO(dmbdc)\cdot(H_2dmbdc)_{0.4}]$ (H_2dmbdc = 2,5-dimethylbenzene-1,4-dicarboxylic acid) was isoreticular to that of MIL-47. The methyl functionalities in MOF-48 point toward the center of the channels, where uncoordinated H_2dmbdc guest molecules were also observed. Both catalysts are thermally stable up to 425 °C and maintain their structural integrity during the recycling as evidenced by close correspondence of powder X-ray diffraction (PXRD) patterns of fresh and recycled catalysts. In the absence of CO, MIL-47 and MOF-48 catalysts gave the best yield (70% and 48% respectively) for acetic acid (AcOH) with 121 and 175 TON using $K_2S_2O_8$ as an oxidant at 80 C. In presence of CO, under same reaction condition TON increased to 490 and selectivity to 100% at 80 C. In presence of CO, the TON increased to 490 and 330 for MOF-48 and MIL-47 with 100% selectivity. With $VOSO_4$, only 210 TON was achieved under same reaction conditions. The higher yields and selectivity are associated with vanadium centers in an oxygen-dominated sphere and more hydrophobic pores of MOF-48. Their study showed promising evidence that the MOFs are active heterogeneous catalysts

for the conversion of methane to AcOH (TON = 490) and their performance exceeds that of other catalysts such as vanadium(IV) complexes (TON = 210).

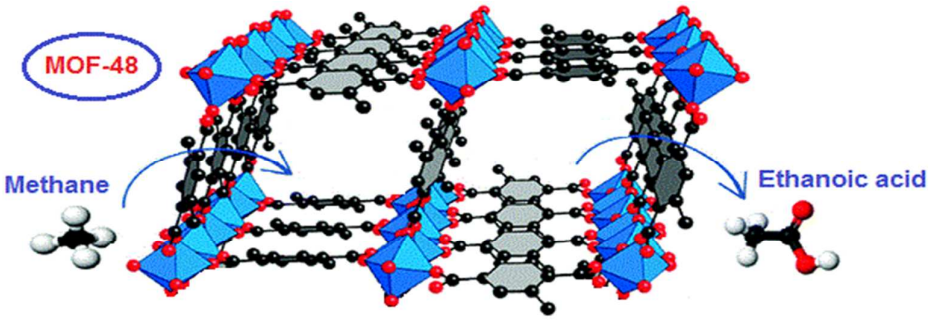

Fig. 3 Conversion of methane to AA in the absence and presence of CO. Reprinted with permission from ref. [92]. Copyright 2011 American Chemical Society.

Sreedhar and coworkers[93] explored the potential catalytic application of four different MOFs; $[Cu_3(btc)_2]$, [Cu(bdc)], $[Cu(2\text{-pymo})_2]$, and $[Cu(Im)_2]$ (H_3btc = benzene-1,3,5-tricarboxylic acid, 2-pymo = 2-hydroxypyrimidinalote, and Im = imidazolate) in the hydroxylation and nitration of aryl halides. 4-iodoanisole was selected as a model substrate for hydroxylation and also subjected to various reaction conditions. All MOFs catalyzed the reaction in moderate to excellent yields (20-94%). Very low yields 8%, 9%, and 10% were obtained with $Cu(OAc)_2$, CuI, and commercial CuO respectively. Cu-MOFs showed highly efficient catalytic activity compared to other known catalysts ($Cu(OAc)_2$, CuI, and commercial CuO). The reaction is highly sensitive to the amount of base (KOH) and ratio of solvent (DMSO/water) used. MOFs are highly unstable to the basic and polar conditions demanded for hydroxylation resulting in total destruction of framework forming copper oxide (CuO) nanoparticles (NPs). TEM images clearly showed the presence of CuO nano particles (10 nm). This limits the reusability of MOFs for hydroxylation but in case of nitration, FT-IR of fresh and used MOFs showed broad resemblance.

Ahn and coworkers reported the synthesis of two MOFs, $[Co_2(dobdc)]$ (M) and $[Co_2(dobdc)]$ (S) (H_2dobdc = 2,5-dihydroxybenzene-1,4-dicarboxylic acid) (Co-MOF-74) by microwave-heating method (M) and solvothermal method (S) respectively.[94] The average particle size of Co-MOF-74 (M) is smaller than the Co-MOF-74 (S) because of the short synthesis time which limits particle growth. The TGA patterns of Co-MOF-74 (S) showed a final weight

loss in temperature range of 280-300 °C and Co-MOF-74 (M) showed weight loss at a slightly higher temperature. The catalytic property of both MOFs was tested for the cycloaddition reaction of CO_2 to styrene oxide. Styrene oxide conversion steadily increased from 41 to 96% as the reaction time increased from 0.5 to 4 h at 100 °C and 2.0 MPa CO_2 (MPa = megapascal) over Co-MOF-74 (M and S) in chlorobenzene. Styrene oxide conversion was directly proportional to the reaction temperature and CO_2 pressure. Conversion of styrene, increased from 38 to 96% when temperature was increased from 60 to 100 °C, and the conversion decreased from 96 to 49% as the CO_2 pressure was reduced from 2.0 to 1.0 MPa. PXRD patterns of fresh and those after second and third runs showed identical patterns with same intensity. No significant effect of catalyst particle size was detected, and the Co-MOF-74(M) could be reused 3 times without loss of catalytic activity and structural deterioration.

Nguyen *et al.*[95] prepared a highly porous MOF-199 and investigated its activity for catalysis of Ullmann-type coupling reactions between aryl iodides and phenols to form diaryl ethers. To obtain the optimum conditions, influence of different factors affecting the reaction such as catalyst concentration, reaction temperature, use of different bases, solvent, different substrates, and reaction time were studied. The reaction of electron-rich phenols proceeded readily with high conversions; 94, 92, and 97% conversions as in case of phenol, *p*-cresol, and 2-methoxyphenol after 2 h, respectively. Lower conversions were observed with phenol having electron-withdrawing substituents, as in case of 4-chlorophenol and 4-cyanophenol, 63% and 8% conversion in 2 h, respectively. In order to confirm the catalyst recovery and reusability, the recovered catalyst was characterized by many techniques (FT-IR and TEM). The TEM results of reused catalyst indicated that the crystallinity of catalyst retained during the coupling reaction.

Jacqueline *et al.*[96] studied the use of $[Cu_3(btc)_2]$ as a catalyst for the generation of therapeutic NO from a biological substrate, *S*-nitrosocysteine (CysNO) without toxicity issues (Scheme

1). In the absence of MOF, no appreciable amount of NO was observed from a CysNO:CysH solution. The MOF is reusable without loss of activation over successive iterations of CysNO additions. This work shows for the first time the use of a MOF as a catalyst in the decomposition of *S*-nitrosothiols (RSNOs).

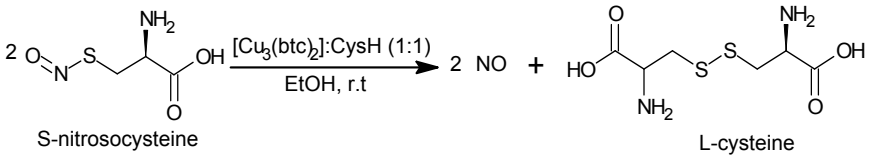

Scheme 1. Decomposition of CysNO to produce NO *via* $[Cu_3(btc)_2]$.

Chen *et al.*[97] constructed a new chiral indium(III)-MOF $[In(5\text{-}NH_2\text{-}ipa)_2]\cdot(TPP)\cdot 4H_2O$, (5-$NH_2$-ipa = 5-aminoisophthalate, TPP = tetraphenylphosphonium) solvothermally. The structure is developed by the In(III) ions adopting a 4-connected pattern by coordinating eight oxygen atoms from four 5-NH_2-ipa. The In-O distances range from 2.192(6) to 2.378(4) Å. Each ligand acts as a μ^2-linker to bridge two indium centers. The large open channels are fully occupied by the cationic guest species *i.e.*, TPP cation neutralize the anionic 3D framework developed by In(III)-5-NH_2-ipa coordination (Fig. 4). The guest (TPP cations) trapped into the open anionic framework is truly unusual and rarely observed in other MOFs. The catalytic activity of In-MOF toward the diethylzinc addition to benzaldehyde was tested after 24 h, the reaction led to a 54.6% conversion of benzaldehyde. PXRD patterns after catalysis is consistent with that of fresh catalyst revealing the good thermal stability of the catalyst. The TPP cation played three particular roles: (i) balancing charges and supporting frameworks, (ii) enhancing photoluminescence, and (iii) catalysis. The TPP cation might serve as a good template for the construction of new functional materials.

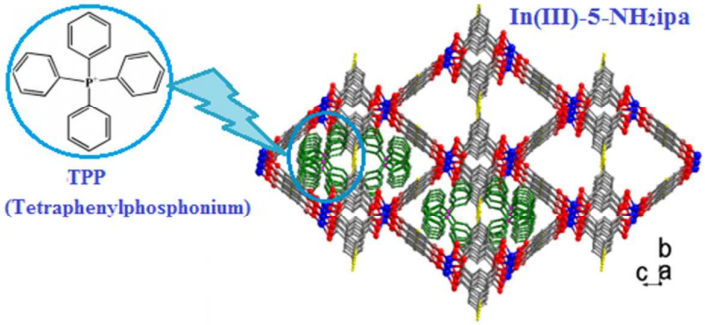

Fig. 4 3D open framework of Indium(III)-MOF containing TPP cationic guests in the channels. Reprinted with permission from ref. [97]. Copyright 2013 American Chemical Society.

An urea-containing MOF NU-601 having formula $[Zn_2(bipy)_2(1\text{-}4H)]$ (1-4H = 5,5'-(carbonyldiimino)dibenzene-1,3-dicarboxylic acid)[75] was synthesized and used as a catalyst in Friedel-Crafts reaction between pyrroles and nitroalkenes (Scheme 2). The initial experiments to catalyze the Friedel-Crafts reaction between *N*-methylpyrrole and (*E*)-1-nitroprop-1-ene with 10 mol% NU-601 (toluene at 23 °C) afforded no consumption of (*E*)-1-nitroprop-1-ene. To facilitate more H-bonding exchange, the reaction solvent (toluene) was changed to a more polar mixture (1:1, $MeNO_2$:THF). Under these reaction conditions (1.0 M reaction concentration and 60 °C), 98% consumption of (*E*)-1-nitroprop-1-ene was obtained after 36 h. The reaction was extended to different larger substrates as steric probes (size-exclusion catalysis experiments). When NU-601 was used, large substrate molecules showed significantly diminished yields *versus* small substrates, strongly concluding that catalysis occurs mainly within the pores. This approach is the first example of hydrogen-bond-donating (HBD) catalysis. The catalyst is stable and proved to be reusable for five cycles while retaining its crystallinity as determined by PXRD.

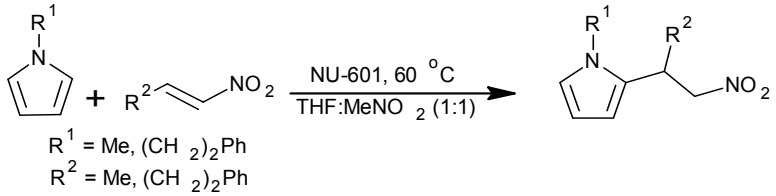

Scheme 2. Friedel-Crafts reaction between pyrroles and nitroalkenes.

Corma and coworkers[98] explored the catalytic behavior of MOFs like $[Cu_3(btc)_2]$, [Cu(bdc)], $[Cu(2\text{-}pymo)_2]$, and $[Cu(Im)_2]$ for a three-component coupling (amines, aldehydes, and alkynes to form the corresponding propargylamines). Two tandem reactions, including an

additional cyclization step (5-*exo*/*endo*-*dig* cyclization), lead to production of indoles (A) and imidazopyridines (B) (Scheme 3). For indole and imidazopyridine formation, the best result was obtained with [Cu(bdc)] among the other Cu-MOFs. In case of [Cu(bdc)], a complete conversion (97%) was attained for formation of imidazopyridine within 30 h. The catalyst undergoes a structural phase change during the course of reaction, passing from an active lamellar structure to an inactive lamellar structure. The catalytic activity can be reversed by refluxing in dimethylformamide (DMF) which recovers the active lamellar structure. The use of [Cu(bdc)] for this reaction also prevents the formation of Glaser/Hay condensation products of the alkyne. This is an additional advantage of [Cu(bdc)] with respect to other homogeneous copper catalysts such as copper chloride ($CuCl_2$) and copper acetate ($Cu(OAc)_2$) for which the use of an inert atmosphere is required. [Cu(2-pymo)$_2$] was found to be an active and selective catalyst for the tandem reaction to form indole affording 99% yield of propargylamine. The activity of [Cu(2-pymo)$_2$] was also comparable with other heterogeneous Cu-containing catalysts such as copper-exchanged USY zeolite that yielded 90% of propargylamine after 15 h. The catalyst deactivated after the first run not due to instability of MOF since its structure was fully preserved (as stated by PXRD), but due to adsorption of reaction products on the Cu-MOF that could not be fully removed by simple washing.

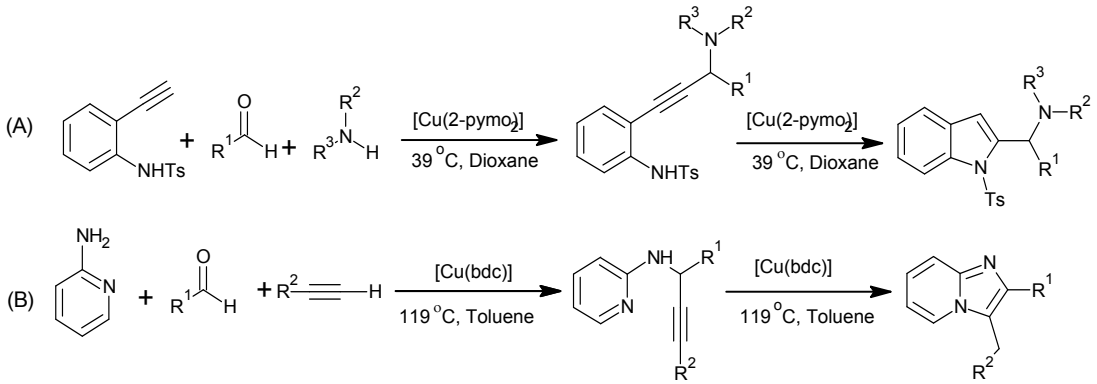

Scheme 3. (A) Indole formation through a three-component coupling and 5-*endo*-*dig* cyclization tandem reaction. (B) Imidazopyridine formation through a three-component coupling and 5-*exo*-*dig* cyclization tandem reaction.

MOFs have also been used as catalysts for the oxidation of organic compounds in the presence of oxidants like *tert*-butylhydroperoxide (TBHP), hydrogen peroxide (H_2O_2) and O_2. Aerobic oxidation of benzyl alcohols has been reported using $[Cu_3(btc)_2]$ catalyst in the presence of a base and catalytic amount of 2,2,6,6-Tetramethylpiperidinyloxy (TEMPO) in acetonitrile.[99] This catalyst showed moderate catalytic activity for benzyl alcohols but exhibited lower activity towards the oxidation of aliphatic, cyclic, and secondary alcohols. In addition to the lack of the general scope of $[Cu_3(btc)_2]$ in combination with TEMPO, a leaching test showed 1 ppm (parts per million) of copper and the catalyst itself undergoes some changes in its crystal structure as evidenced by XRD analysis. The benzoic acid formed during the reaction could lead to deactivation of the catalyst by coordination with the free metal centers (Scheme 4).

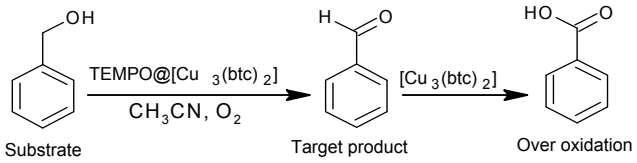

Scheme 4. Aerobic oxidation of benzyl alcohols by using $[Cu_3(btc)_2]$ catalyst.

3. Metal node

Metal,[100] its ions,[101] and transition metal complexes[102] have been extensively used as homogeneous catalysts for a large number of organic transformations. Recently heterogeneous catalysts have been developed based on MOFs where the metal atoms/clusters are located at the nodes in the structure and utilized as a catalyst in chemical transformation, especially as a Lewis-acid catalyst. The solvent remaining in the pores of framework during MOFs synthesis, can be removed by an activation procedure, generally heating is required to make pores available for guest molecules. When the catalytic activity is based on a metal than the channels inside MOFs, in that case microporous MOF catalysts assume the role as counterpart of homogeneous catalysts. A range of transition metal MOFs has been applied effectively for the catalysis of a variety of organic reactions (Table .1). Relationship between catalytic activities and metal centers is well predictable and has been addressed here with.

3.1 Unsaturated metal centers as reaction center

Two types of strategies are applied for the optimal catalytic activity: (i) introduction of organic groups to provide guest-accessible functional organic sites[103, 104] and (ii) formation of coordinative unsaturated metal sites.[105] If the metal centers are solvated (saturated), then an organic moiety incorporating a functionality for non-covalent interactions can bind the reactant(s) through H-bonding, π-π stacking, *etc*., leading to their activation. If the solvent is coordinated to metal atoms, its removal makes the metal atom more accessible. These MOFs are generally called as 'MOFs with open metal sites' or 'MOFs having unsaturated metal sites'.

As synthesized, MOFs are activated (removal of the coordinated solvent(s)) by heating, solvent exchange, and evacuation. Different metal ions like Ag(I), Co(II), Cu(II), Zn(II),Mn(II), Mg(II) Ni(II), Fe(II), Pd(II), Ti(III), Cr(III), Bi(III), Al(III), Sc(III), Ce(IV), Zr(IV)and V(III/IV) have been established as active sites (when unsaturated) in MOFs catalysis.[63, 77, 106-125] For examples, Volkmer *et al.* used the [Co(bpb)]·3DMF (H_2bpb = 1,4-bis(4′-pyrazolyl)benzene) containing tetrahedrally coordinated Co(II) sites (Table 1, entry 2) as the catalyst for cyclohexene oxidation,[126] a Cu-MOF $[Cu(H_2btec)(bipy)]_\infty$ (H_4btec= 1,2,4,5-benzenetetracarboxylic acid) with a coordinative unsaturated square-planar arranged Cu(II) center showed a high activity (Table 1, entry 3) and selectivity for epoxidation reactions of styrene and cyclohexene with *t*-BuOOH (*ter*-butyl hydroperoxide) as oxidant.[127]

Tao *et al.*[113] prepared a porous MOF, $[Cu_2I_2$(bttp-4)] (bttp-4 = benzene-1,3,5-triyl triisonicotinate), and investigated its catalytic activity for the three-component coupling of sulfonylazides, alkynes, and amines, leading to the formation of N-sulfonylamidines in appreciable yields. A range of functional groups including halide, alcohol, ester, and silyl were well tested in $[Cu_2I_2$(bttp-4)] catalyzed coupling reactions. Amines other than $(i\text{-Pr})_2$NH such as N-methylaniline (Ph(Me)NH) and diphenylamine (Ph_2NH) have also been tested, and the relative reactivity trend was $(i\text{-Pr})_2$NH > Ph(Me)NH > Ph_2NH. $[Cu_2I_2$(bttp-4)] can be recycled by simple filtration and reused at least four times without any loss in yield. The

unique structural features of the MOF, includes (i) active metal sites in the pore surface, (Table 1, entry 4) (ii) suitable framework channel size surrounded by rigid N-containing tripodal ligands, (iii) high porosity, and (iv) robustness endowing the MOF-[Cu_2I_2(bttp-4)] catalyst with versatile characteristics (Fig. 5). These features endow the catalyst with versatile characters such as unprecedented heterogeneous ligand-accelerated effect, size effect and recyclability for reuse of catalyst. Enhanced catalytic activity indicates that [Cu_2I_2(bttp-4)] could provide a platform to carry out reactions inside large cavities.

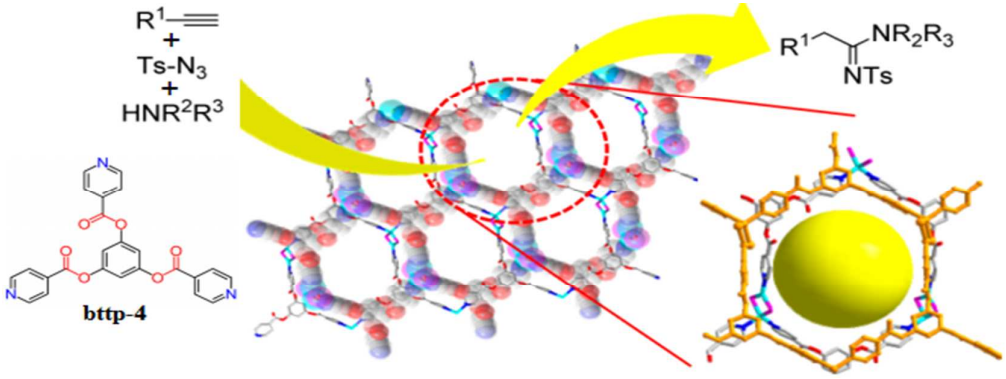

Fig. 5 Molecular structure of the ligand bttp-4, 1D channels in MOF−Cu_2I_2(bttp-4), and representation of catalytic behaviors. Reprinted with permission from ref. [113]. Copyright 2013 American Chemical Society.

Lijuan *et al*[128] synthesized $[Cu_2(bptc)(Im)_4(H_2O)(DMF)]_n$ (H_4bptc = Biphenyl-3,3,4,4-tetracarboxylic acid) by solvothermal method, and tested for the hydroxylation of phenols in the presence of H_2O_2 as an oxidant. To obtain optimum conditions, they investigated the effect of temperature, solvent, amount of catalyst and reaction time. Under the optimal conditions, experiments were carried out on a series of phenols with different substituents (methyl and tertiary butyl phenol). Oxidation of 2-methylphenol, and 3-methylphenol give corresponding benzoquinone with yield of 13%, and 7.2% respectively. However, the oxidation of 4-*tert*-butylphenol yielded just 1.6% in 4-*tert*-butyl-1,2-diphenol which may be due to steric effect of the *p*-substituted of *tert*-butyl group. The unsaturated Cu(II) sites in the framework played a decisive role in enhancing the catalytic performance (Table 1, entry 5) due to the formation of the powerful oxidative Cu-peroxo species between Cu(II) and H_2O_2 with a more powerful oxidative ability than H_2O_2 and coordination environment within the

framework. Cu-MOF showed high efficient catalytic activity as compared to free ligand, mixture of free ligand and $Cu(OAc)_2$, and $Cu(OAc)_2$.

Klemm and coworkers [121] used MOF $[Pd(2\text{-pymo})_2]_n{\cdot}3H_2O$ in the liquid-phase hydrogenation of 1-octene and cyclododecene. Shape/size selectivity was observed as up to a reaction time of 4 h, *i.e.*, 1-octene was hydrogenated, but not the more bulky molecule cyclododecene (Table 1, entry 6). Cyclododecene with a molecular diameter of about 9 Å was too large to enter the pores of $[Pd(2\text{-pymo})_2]_n{\cdot}3H_2O$. The XRD patterns of the reused catalyst showed no change even after the third run but a colour change of catalyst was observed from yellow to black indicating the formation of Pd^0 NPs. It was found and confirmed by XRD that Pd^0 NPs were formed and leached out of the MOF into the solution, due to this the shape-selective effect disappeared and the reaction was catalyzed by Pd^0 instead of $[Pd(2\text{-pymo})_2]_n{\cdot}3H_2O$. Therefore, the $[Pd(2\text{-pymo})_2]_n{\cdot}3H_2O$ was not long-times stable in liquid-phase hydrogenation catalysis because of the slow advancing reduction of the Pd^{2+} centers to Pd^0.

Menezes and coworker have reported the use of a porous 3D open-framework based on europium(III)-fumarate, $[Eu_2(fum)_3(H_2O)_4]{\cdot}(3H_2O)$, (fum = fumaric acid) as a catalyst to promote the addition of potassium allyltrifluoroborate to aldehydes.[129] The electronic nature of the different substituents in the aromatic aldehydes has little influence on the reaction. The high catalytic activity of Eu-MOF is due to the coordination of allyltrifluoroborate to Eu^{3+} ion (Table 1, entry 1). The catalyst is robust to a wide range of functional groups with aliphatic, aromatic, *α,β*-unsaturated, and heterocyclic aldehydes, being efficiently allylated in very high yields. For example, the allylation of 4-R-benzaldehyde (R = NO_2) gave the corresponding products in 93% yield. Other aromatic aldehydes having different substituents (R = CH_3, CH_3O, F, Cl, Br) afforded 84 to 91% yields (Scheme 5).

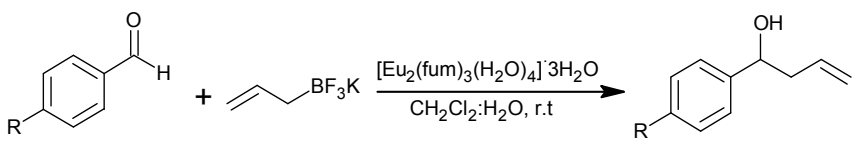

R = NO_2, CH_3, CH_3O, F, Cl, Br

Scheme 5. Allylation of substituted-benzaldehyde by potassium allyl-trifluoroborate catalyzed using Eu-MOF (10 mol%).

The catalytic activity of a series of isostructural MOFs CPO-27-M having formula [M_2(dobdc)] (where, M = Co, Mg, Mn, Ni, and Zn) using 2,5-dihydroxybenzene-1,4-dicarboxylic acid (H_2dobdc) have been studied for cyanosilylation of aldehydes with trimethylsilylcyanide, and also for the oxidation of styrene with *tert*-butylhydroperoxide. All MOFs are active in promoting the cyanosilylation of aldehydes but in case of styrene oxidation, only Co and Mn MOFs are active while others behave as initiators rather than catalyst (Table 1, entries 7 and 8). CPO-27-Mn exhibited the highest activity in comparison with the cobalt one for both reactions. CPO-27-Mn showed size selectivity and the catalyst could be recycled without losing its structural integrity and catalytic activity. The CPO-27-M presented good chemical stability during the course of reaction as confirmed by PXRD, making them good candidates for heterogeneous catalyst.[130]

Among several popular MOFs, mostly [Cu_3(btc)$_2$], [Fe(btc)] and [Cu(bdc)] are used as catalysts in various organic reactions due to their unsaturated metal sites.[85, 88, 98, 131] Corma *et al.*[131] presented for the first time that Cu-MOFs are active and regioselective catalysts for the 1,3-dipolar cycloaddition with activities and selectivity as high as when using homogeneous catalysts. They evaluated the behavior of four different copper MOFs [Cu(2-pymo)$_2$], [Cu(im)$_2$], [Cu_3(btc)$_2$] and [Cu(bdc)] as a "click" reaction catalyst and observed that these CuMOFs are highly active and fully regioselective for reactions between the benzyl azide and phenylacetylene in ethanol at 70 °C. The only product obtained was the 1,4-substituted triazole, being the reaction regioselective product, as expected for a copper-catalyzed 1,3-dipolar cycloaddition. According to the XRD patterns before and after the reaction, the crystalline structure of Cu-MOF was preserved and the catalyst could be reused for at least six consecutive runs without loss of activity and selectivity. The Cu-MOFs ([Cu(2-pymo)$_2$], [Cu(im)$_2$], [Cu_3(btc)$_2$] and [Cu(bdc)]) catalyzed the cycloaddition of benzyl azide and phenylacetylene giving a total yield of 1,4-triazole 99%, 99%, 37%, and 42%, respectively

(Fig. 6). It has been observed that copper(II) sites in MOFs such as [Cu(2-pymo)$_2$], [Cu(im)$_2$], surrounded by four diaza-heterocyclic nitrogen atoms (CuN_4) are generally more active catalysts than those MOFs having copper centers surrounded by four carboxylate oxygen atoms (CuO_4) such as [Cu_3(btc)$_2$] and [Cu(bdc)] (Table 1, entry 11).

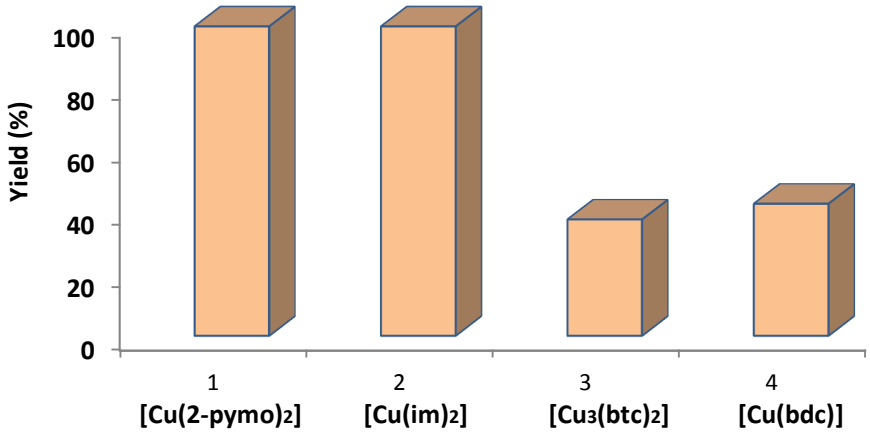

Fig. 6 Yields of 1,4-triazole over different Cu-MOFs from reaction of benzylazide and styrene.

Cyclopropanation of styrene has been carried out by Rocha *et al*. using a Cu-MOF of the formula [Cu(bipy)$_2$SO$_4$·6(H$_2$O)].[70] The structure of MOF consists of Cu(I) nodes linked by 4,4'-bpyridine into infinite chains, and sulfate groups connecting two neighboring chains, resulting in a 1-D double chain network. Guest water molecules established a complicated network of hydrogen bonding interactions with their neighboring oxygen and sulfur atoms, leading to the formation of a 3-D supramolecular framework. The thermal stability of MOF was studied in air from room temperature to 700 °C. TGA patterns of MOF showed the final weight loss in temperature range 195-460 °C. This MOF is a good heterogeneous catalyst for the cyclopropanation of styrene, with 72% *trans*-cyclopropane diastereoselectivity (Scheme 6), slightly higher than in the homogeneous phase reaction with the best-known catalyst (CuBox). The catalyst is recycled and reused for three consecutive cycles without a significant loss of catalytic activity, while the colour of the recycled catalyst is more greenish than the colour of the parent material.

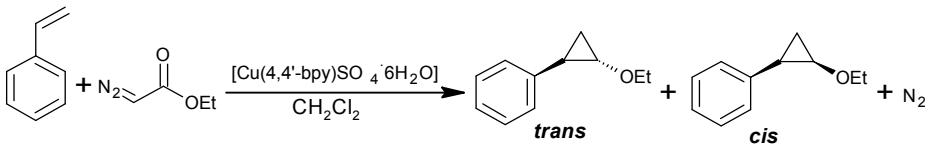

Scheme 6. Cyclopropanation of styrene with ethyldiazoacetate.

Recently, a novel MOF $[Cu_2(bpdc)_2(bipy)]$ (H_2bpdc = 4,4′-biphenyldicarboxylic acid) displayed a significant higher catalytic activity than other Cu-MOFs such as [Cu(bdc)], [Cu(bpdc)] and $[Cu_3(btc)_2]$ for the C-H arylation reaction of benzoxazole with aryl halides and heterocycles (Table 1, entry 12).[132] The C-H arylation reaction was carried out in DMSO at 120 ºC using 7.5 mol% of Cu-MOF catalyst. With *p*-substituted halo-benzene, the presence of an electron-withdrawing group led to significantly higher yield (> 90%) than the case of an electron-donating group. Moderate conversion, 32%, 39% and 46% were achieved for 4-methylthiazole, 2-chlorothiophene, and *N*-methylbenzimidazole respectively. The $[Cu_2(bpdc)_2(bipy)]$ displayed high efficient catalytic activity with 100% yield in comparison with other Cu-catalysts such as CuI, CuCl, $CuCl_2$ and $Cu(NO_3)_2$ with 80%, 77%, 54% and 15% yields respectively. In order to check the reusability and recoverability, the reused catalyst was characterized with FT-IR and XRD and showed the same patterns though slight differences in the diffractogram were observed.

In many reported MOFs, it has been observed that the catalytic performance is strongly dependent on the metal entities contained in the MOF. Studies along this line may open the opportunity of using mixed-metal MOFs to tune catalytic properties and to build up catalysts for multicomponent reactions.

3.2 Acidic MOF

Reusable and highly tolerant catalysts such as heterogeneous Lewis-acids are replacing rapidly the traditional approaches for acidic catalysis. Unlike the catalysis involving metal complexes, MOFs have inherent valuable advantages that no further support is needed for the heterogenization. The organo-micro environment provided by the framework allows the

metallic links to mimic enzyme catalysis. Removal of coordinated molecules from metal ions yield not only empty frameworks, but also could create Lewis-acidic characters which have promising applications in catalysis. MOFs have been used as highly effective Lewis-acid catalysts in many acid catalyzed reactions. MOFs designed from secondary building units *i.e.*, paddle-wheel clusters have shown Lewis type catalytic activities such as cyanosilylation,[133] terpene isomerization[37], alkene hydrogenation,[134, 135] cycloaddition of CO_2,[81] and alcohol aerobic oxidation.[136, 137]

Kumar *et al.*[138] synthesized a Cu-MOF [$Cu_3(btc)_2$] through an electrochemical route and used it as catalyst for chemical reduction of *p*-nitrophenol in the presence of an excess of sodium tetrahydroborate ($NaBH_4$). MOF is characterized by many techniques (XRD, TGA, and FT-IR) and the results reveal that supporting electrolyte and current density plays a crucial role in controlling the particle size and also improving the yield of MOF. The SEM and TEM studies showed that the morphology of the synthesized particles is cubic in nature and the particle size is ∼10-20nm. [$Cu_3(btc)_2$] proved to be an effective catalyst (Table 1, entry 15) for the chemical reduction of *p*-nitrophenol due to the enhanced catalytic properties (Cu active sites). The main advantage of the electro-synthetic route is that the Cu content is 32% higher than the previously reported value of 22% and the thermal stability is as high as 293 °C.

Lien *et al.*[139] prepared successfully a highly porous MOF-199 in solvothermal way. The thermal stability of MOF was studied in air from room temperature to 700 °C. The TGA patterns indicated that it is stable over 300 °C. MOF-199 is an efficient heterogeneous recyclable acid catalyst for the aza-Michael reaction of benzylamine with ethyl acrylate to form ethyl 2-(benzylamino)acetate (A) as the principal product being over 98-99% (Scheme 7). At longer reaction time, mono-addition product (A) containing N-H bond reacted further with excess ethyl acrylate to give the di-addition product (B). By employing 5 mol% MOF-199, a conversion of 89% was achieved after 1 h, and decreasing the catalyst concentration resulted in a drop of the reaction rate, though the reaction could still afford 88%, and 84%

conversion after 1 h at a catalyst concentration of 2.5 mol% and 1 mol%, respectively. To check the presence of Lewis center in MOF-199, the reaction was repeated in the presence of base (pyridine) leading to a dramatic drop in the reaction rate (with only 46%conversion). From this it is clear that Cu played active role in the aza-Michael reaction as Lewis-acid centre (Table 1, entry 16).

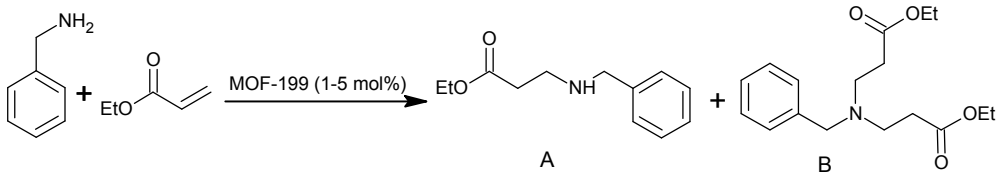

Scheme 7. aza-Michael reaction using the MOF-199 catalyst.

Two porous and robust MOFs, $Na_2[Nd_4(CO_3)L_4(DMF)_2(H_2O)_2]\cdot 2H_2O$ and $Na_2[La_4(CO_3)L_4(DMF)_2(H_2O)_2]\cdot 2H_2O$ (L_4 = tris(*p*-carboxylicacid)tridurylborane) were constructed by linking tetranuclear lanthanide.[140] The high-connectivity in Ln-MOFs featured significant thermal and hydrolytic stability and a large number of isolated Lewis-acid B(III) and Ln(III) sites on the pore surfaces. The central building block for this MOF is a tetranuclear [$Nd_4(\mu_4\text{-}CO_3)$] cluster. The four Nd ions are linked by a basic CO_3^{2-} to form a quadrangle. The carbonate atoms of the ligand and four Nd metal sites are coplanar with a crystallographic C_2 axis passing through center (Fig. 7b). Both MOFs are thermally stable; the TGA showed that both MOFs are stable up to 310 °C. Also chemical stability was checked by heating MOFs in boiling benzene, methanol and water for seven days and no noticeable change in PXRD patterns was observed. Nd-MOF found to be highly effective and reusable heterogeneous catalyst for carbonyl allylation reaction of aldehydes or ketones with tetraallyltin $(CH_2{=}CHCH_2)_4Sn$). Both aromatic and aliphatic aldehydes reacted smoothly with tetraallyltin to give the desired alcohols in good to high yields (Fig. 7a). In both cases, Diels-Alder reaction of 3-acryloyl-1,3-oxazolidin-2-one with cyclopentadiene, and Streker-type reaction of benzaldehyde, aniline and tributyltincyanide in water, the isolated products are much higher (53% and 46% respectively) than those of 1:1 mixture of $NdCl_3$ and tris(*p*-

carboxylicacid)tridurylborane. All reactions were co-catalyzed by B(III) and Nd(III) Lewis-acids (Table 1, entries 19, 20, and 21), and catalytic activities were much higher than those of the individual organo-boron and lanthanide counterparts and their mixture. The Nd-MOF verified to be a highly efficient and reusable solid acid catalyst for various organic reactions in water, establishing that its activity is much higher than those of the individual organic and inorganic counterparts.

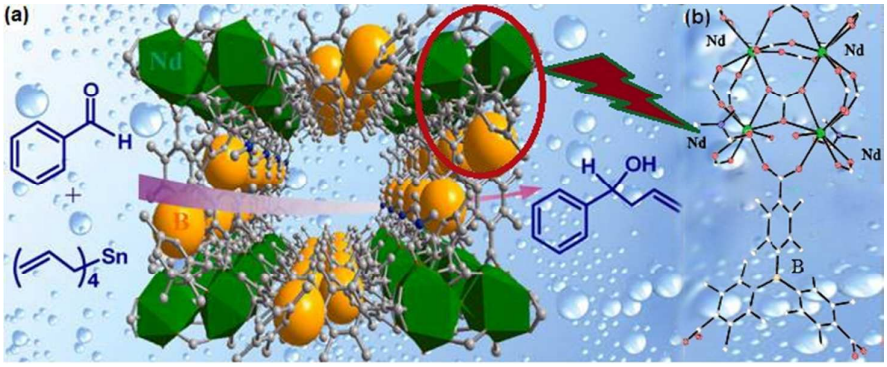

Fig. 7 (a) Catalytic allylation reaction using MOF in water (b) $[Nd_4(\mu_4\text{-}CO_3)]$ cluster with one ligand (Tris(p-carboxylic acid)tridurylborane. Reprinted with permission from ref. [140]. Copyright 2013 American Chemical Society.

Recently, Cu-MOF-74 ($[Cu_2(dobdc)]$) with unsaturated and accessible metal sites showed an amazing catalytic performance for the acylation of anisole with acetyl chloride as acid catalyzed reaction (Table 1, entry 22). The influence of different reaction variables affecting the yield such as catalyst concentration, reaction temperature, solvent, and time were studied. The catalyst showed high thermal stability and promising results for seven catalytic cycles. The TGA indicates that MOF is stable up to 375 °C with comparable thermal stability to [Cu(bdc)] that is slightly lower than Zn-MOF-74 which is stable up to 400 °C. For Cu-MOF-74, the yield was 100% as comparison to HKUST-1, HZSM-5 and Al-MCM-41 yields were 93%, 58% and 47% respectively. The catalytic activity of Cu-MOF-74 was highly efficient in comparison to other Cu-containing MOFs materials such as HKUST-1, and conventional inorganic acid catalyst such as aluminum-containing microporous zeolites such as Zeolite Socony Mobil-5 (HZSM-5) and mesoporous ordered materials such as Mobil composition of matter No.41 (Al-MCM-41).[141]

Mostly, the cyanosilylation reaction,[130, 142] esterification,[143] and isomerization reaction[106] are widely used as test reaction for the evaluation of the Lewis-acid[120] as well as Brønsted acid[144] catalysis of MOFs. The active metal sites should be easily accessible to substrate molecules and should be solvent free for optimal catalytic activity. Furthermore, the engineering of structural defects in MOFs may lead to the generation of a new group of MOFs with different acidity and hydrophobic properties than encountered in zeolites.

4. Organic functional linker

Accessibility of the functional groups on the organic bridging linker's can be tailored to the application in heterogeneous catalysis. MOFs with catalytic active functional organic sites (FOS, *i.e.*, catalysis takes place at the organic linker) have also been well established. Although these FOSs makes MOFs a promising class of new heterogeneous catalysts, still there is need to assess the catalytic activity, deactivation, and stability of MOFs. There are varieties of organic functional groups that serve as active sites during catalysis. Additionally, the organic moieties can also be further functionalized by reactive centers such as chiral basic groups[145] or metallo complexes[146] to provide guest accessible FOS.[147]

Gascon *et al.*[148] reported the inclusion of free sulfonic acid groups in two MOFs $[Cr_3OF(H_2O)_2(bdc\text{-}SO_3H)_3].nH_2O$ (HSO_3-MIL-101(Cr)) and HSO_3-MOF(Zr). The former HSO_3-MIL-101(Cr) was prepared from a mixture of $Cr(NO_3)_3{\cdot}9H_2O$ and mono sodium 2-sulfobenzene-1,4-dicarboxylic acid ($NaSO_3$-H_2bdc) in deionized water by heating at 190 °C for 24 h. HSO_3-MOF(Zr) was synthesized under the same conditions using of $ZrCL_4$ and mono potassium 2-sulfobenzene-1,4-dicarboxylic acid. The acidic properties, catalytic performance, deactivation and stability were critically evaluated. The crystallinity and reusability retain after four catalytic regeneration cycles demonstrating the higher chemical stability of these new MOFs. The turn-over frequencies (TOFs) and acidic performance of the MOFs were assessed in the esterification of acetic acid and *n*-butanol, in comparison with the benchmark catalyst Amberlyst-15 (A-15). HSO_3-MOF(Zr) displayed a high activity due to

the presence of sulfonic acid groups (Table 1, entry 23) and re-usability in the esterification and the catalyst deactivation due to the formation of sulfonic esters could be tackled by reactivation under acidic conditions

4.1 Basic MOF

By incorporating basic functional groups like amino,[38] pyridyl,[149] and amide[150] highly active solid basic catalysts can be obtained. Since, the incorporated basic functional group is an intrinsic part of the organic linker in the MOF, leaching does not occur, thereby resulting in a stable system.

Effect of substituents on linker containing electron-donating NH_2-group and electron-withdrawing NO_2-group in MOF $[Zr_6O_4(OH)_4(NH_2\text{-bdc})_6]$ (UiO-66-NH_2) and $[Zr_6O_4(OH)_4(NO_2\text{-bdc})_6]$ (UiO-66-NO_2) (NH_2-H_2bdc = 2-amino-benzene-1,4-dicarboxylic acid and NO_2-H_2bdc = 2-nitro-benzene-1,4-dicarboxylic acid) has been studied in the acetalization of benzaldehyde with methanol.[151] UiO-66 ($[Zr_6O_4(OH)_4(bdc)_6]$) is a zirconium based MOF built up from hexamers of eight coordinated $ZrO_6(OH)_2$ polyhedra and 1,4-benzene-dicarboxylate linkers forming a $[Zr_6O_4(OH)_4(CO_2)_{12}]$ cluster. The Lewis-acid activity decreased in order of UiO-66-NO_2 > UiO-66 > UiO-66-NH_2. The catalytic results showed that the insertion of NH_2-groups into the linker leads to an increase in the strength of basic sites in contrast to NO_2-groups which resulted in a decrease in basic strength catalytic activity and thus in catalytic activity for acetalization in the same order (Table 1, entry 25). Recently, the use of UiO-66-NH_2 as solid catalyst was reported for Knoevenagel condensation of aromatic aldehydes with ethyl cyanoacetate and malononitrile with afforded the reaction product with more than 90% conversion.[152] The Zr metal sites activate the aldehyde group so that the amino group may readily attack the aldehyde carbonyl group to generate an intermediate aldamine (Table 1, entry 24). This aldamino intermediate further facilitates not only the removal of the proton from the methylene carbon as a base but also coupling with the methylene carbon.

Similarly, the catalytic behavior of same isostructural MOFs having formula [M_2(dobdc)] (M = Co, Mg, Mn, Ni and Zn) (MOF-74-M or CPO-27-M) were investigated also for the Knoevenagel condensation and Michael addition. The catalytic activity of MOF-74-M was first evaluated for Knoevenagel reaction of benzaldehyde and malononitrile or cyanoacetate and the MOFs activity was found to be the metal-type dependent and following the order Ni > Cu > Mg > Zn > Co. Same trend of reactivity was observed in the Michael addition of ethyl cyanoacetate to methyl vinyl ketone. In Both reactions, Ni-MOF-74 displayed a satisfactory catalytic performance (Table 1, entries 9 and 10) due to the presence of phenolate oxygen atoms in dobdc coordinated to metal ions which are responsible for the deprotection of the methylene proton of the donor molecule. Both the basic property of phenolates and the coordinative unsaturated metal sites played an important role in the reaction. The basicity of Ni-MOF-74 was confirmed further by chemisorption of pyrrole and IR spectroscopy.[153]

Gascon *et al.*[38] prepared amino-MOFs [$Zn_4O(NH_2\text{-bdc})_3$] (IRMOF-3) and [$Al(OH)(NH_2\text{-bdc})(NH_2\text{-}H_2bdc)_{0.75}$] ($NH_2$-MIL-53(Al) and confirmed that the amino group is capable of performing base-catalyzed Knoevenagel condensation of benzaldehyde with ethyl cyanoacetate and ethyl acetoacetate. IRMOF-3 exhibited a high catalytic activity with a 100% selectivity to the condensation products that is far better than most active solid basic catalysts reported (Table 1, entry 26). The IRMOF-3 is stable under the reaction conditions, and could be reused without significant loss in activity. Although, the reaction rate is lower in the case of ethyl cyanoacetate but still the levels of conversion are higher than those reported for other basic catalysts under the same reaction conditions.

Hartmann *et al.*[154] constructed three different MOFs having amino groups at their organic linkers, [$Fe_3OCl(H_2O)_2(NH_2\text{-bdc})_3$] ($NH_2$-MIL-101(Fe)), [$Al_3O(DMF)(NH_2\text{-bdc})]\cdot nH_2O$ (NH_2-MIL-101(Al)) and [$Al_4(OH)_2(OCH_3)_4(NH_2\text{-bdc})_3$] (CAU-1). In order to screen MOFs for their air stability, the MOFs were stored at ambient atmosphere for 96 h at room temperature. No significant loss of porosity was observed in case of (NH_2-MIL-101(Al)), whereas corresponding Fe-derivative decomposed within several minutes. The new amino-

funtionalized MOFs were tested for the base catalyzed Knoevenagel condensation of benzaldehyde with malononitrile and ethyl cyanoacetate (Scheme 8). The MOF containing amino group, NH_2-MIL-101(Fe) and NH_2-MIL-101(Al) (Table 1, entry 27) proved to be excellent catalysts and benzylidenemalononitrile (BzMN) or ethyl (*E*)-α-cyanocinnamate yields of about 90% were obtained after three hours, while CAU-1 (CAU = Christian-Albrechts-University) exhibited a poor activity under the same reaction conditions. CAU-1 suffered from mass transport due to the small pore entrances (open apertures of 0.3–0.4 nm) to allow access for the reactant and product molecules. The catalytic activity of NH_2-MIL-101(Fe) and NH_2-MIL-101(Al) clearly shows that reaction takes place inside the pores because both MOFs have mesoporous cages with diameters of 2.9 and 3.4 nm respectively. These cages are easily accessible by the substrate molecules by windows of 1.2 and 1.6 nm, respectively. NH_2-MIL-101(Al) is stable during the reaction and can be recycled at least five times without loss of activity, as confirmed by PXRD and N_2-adsorption experiments.

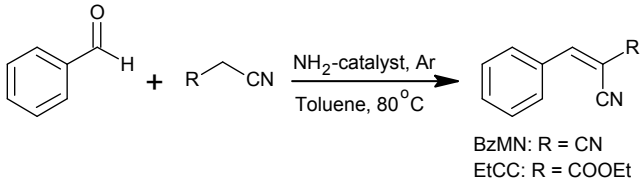

Scheme 8. Knoevenagel condensation of benzaldehyde with malononitrile (R = CN) and ethyl cyanoacetate (R = COOEt) yielding benzylidene malononitrile (BzMN) and ethyl (*E*)-α-cyanocinnamate (EtCC), respectively.

Acylamide is another widely used functional group, it has an electron acceptor (-NH moiety) site and electron donor (-C=O) site. In 2014, Zhou *et al.*[155] reported an acylamide-decorating MOF $[Cu_2(L)(DMA)_2]$ (H_4L = 5-(3,5-dicarboxybenzenamido)isophthalic acid, DMA = *N*,*N*-dimethylacetamide) exhibiting excellent catalytic activity in Knoevenagel condensation. The reaction of benzaldehyde with malononitrile and ethyl cyanoacetate was examined respectively. Malononitrile was found to be a good substrate, producing a conversion of about 76.5% compared to the ethylcyanoacetate that reacted negligibly. This observation suggests that the reaction occurs inside the cavity instead of on the outer surface as the larger substrate molecules (ethylcyanoacetate) fully blocked the pores (Table 1, entry 28). The

prepared MOF was found to be thermally stable up to 300 °C indicated by TGA. Similarly, the PXRD patterns of MOF were in good agreement before and after the reaction indicating the excellent thermal stability. Information about acyl-amide decorated MOFs is quite limited, due to the difficulty in producing guest accessible acylamide units on the pore surface as these groups are labile to interact with metal ions. Decorating MOF with different FOS enriches functional MOFs chemistry and will facilitate in future the MOFs with the best performance.

A catalogue of MOFs with proven catalytic activity is given in table 1, describing; (i) ligand and MOF (ii) the active catalytic center in MOFs (Metal, organic linker or both, *etc.*) and (ii) summery of reactions catalyzed with substrate.

Table 1. Catalogue of known catalytic MOFs with description of their catalytic centers and summery of reactions.

Entry	MOF linker	MOF	Active sites	Substrate(s)	Reaction(s)	Ref.
1.	fum	$[Eu_2(fum)_3(H_2O)_4](3H_2O)$	Eu(III)	Aldehydes and potassium allyltrifluoro borate	Allylation	129
2.	H_2bpb	$[Co(bpb]\cdot 3DMF$	Co(II)	Cyclohexene and TBHP Styrene,	Oxidation	126
3.	H_4btec bipy	$[Cu(H_2btec)(bpy)]_\infty$	Cu(II)	Cyclohexene and TBHP	Epoxidation	127
4.	bttp4	$[Cu_2I_2(bttp4)]$	Cu(II)	Sulfonylazides, Alkynes, and amines	Three-component coupling reaction	113
5.	H_4bptc	$[Cu_2(bptc)(Im)_4(H_2O)(DMF)]_n$	Cu(II)	Phenols and H_2O_2	Hydroxylation	128
6.	2-pymo	$[Pd(2\text{-}pymo)_2]_n\cdot 3H_2O$	Pd(II)	Cyclododecene and 1-octene	Hydrogenation	121
7.	H_2dobdc	CPO-27-M (M = Co, Mg, Mn, Ni and Zn)	Co(II) Mn(II)	Aldehydes and trimethylsilylcyanide	Cyanosilylation	130
8.	H_2dobdc	CPO-27-M (M = Co, Mn)	Co(II) Mn(II)	Styrene and TBHP	Oxidation	130
9.	H_2dobdc	Ni-MOF-74	Ni(II)	Benzaldehyde and malononitrile or cyanoacetate	Knoevenegal condensation	153

10.	H_2dobdc	Ni-MOF-74	Ni(II)	Ethyl cyanoacetate and methyl vinyl ketone.	Michael addition	153
11.	2-pymo Im H_3btc H_2bdc	$[Cu(2\text{-pymo})_2]$ $[Cu(Im)_2]$ $[Cu_3(btc)_2]$ [Cu(bdc)]	Cu(II)	Benzyl azide and phenylacetylene	1,3-dipolar cycloaddition "Click reaction"	131
12.	H_2bpdc, bipy	$[Cu_2(bpdc)_2(bpy)]$	Cu(II)	Benzoxazole and aryl halides.	C-H arylation	132
13.	H_3btc	$[Cu_3(btc)_2(H_2O)_3]\cdot_X H_2O$	Cu(II)	Benzaldehyde and cyanotrimethylsilane	Cyanosilylation	133
14.	H_3btc	$[Cu_3(btc)_2]$	Cu(II)	α−pinene oxide	Isomerization	37
15.	H_3btc	$[Cu_3(btc)_2]$	Cu(II)	*p*-nitrophenol and $NaBH_4$	Reduction	138
16.	H_3btc	MOF-199	Cu(II)	Benzylamine and ethyl acrylate	aza-Michael reaction	139
17.	H_3btc, H_2-bdc H_2ndc	[Fe(btc)] $[Fe_3O(bdc)_3X]$ (MIL-88B) $[Fe_3O(ndc)_3X]$ (MIL88C)	Fe(III)	α−pinene oxide	Isomerization	106
18.	DDQ	Cu-DDQ	Cu(II)	Benzaldehydes, Ketones and cyanotrimethylsilane	Cyanosilylation	142
19.	Tris(*p*-carboxylic acid)tridurylborane (H_3L)	$Na_2[Nd_4(CO_3)L_4(DMF)_2(H_2O)_2]\cdot 2HO$ $Na_2[La_4(CO_3)L_4(DMF)_4(H_2O)_2]\cdot 2H_2O$	Nd(III) B(III)	Aldehydes or ketones and tetraallyltin	Allylation	140
20.	Tris(*p*-carboxylic acid)tridurylborane (H_3L)	$Na_2[Nd_4(CO_3)L_4(DMF)_2(H_2O)_2]\cdot 2HO$ $Na_2[La_4(CO_3)L_4(DMF)_4(H_2O)_2]\cdot 2H_2O$	Nd(III) B(III)	3-acryloyl-1,3-oxazolidin-2-one and cyclopentadiene	Diels-Alder reaction	140
21.	Tris(*p*-carboxylic acid)tridurylborane (H_3L)	$Na_2[Nd_4(CO_3)L_4(DMF)_2(H_2O)_2]\cdot 2HO$ $Na_2[La_4(CO_3)L_4(DMF)_4(H_2O)_2]\cdot 2H_2O$	Nd(III) B(III)	Benzaldehyde, aniline and tributyltin cyanide	Strecker-type reaction	140
22.	H_2dobdc	Cu-MOF-74	Cu(II)	Anisole and acetyl chloride	Acylation	141
23.	$NaSO_3H_2$bdc KSO_3-H_2bdc	HSO_3-MIL-101(Cr) HSO_3-(Zr)MOF	Sulfonic acid group	Acetic acid and *n*-butanol	Esterification	148
24.	NH_2-bdc	UiO-66-NH_2	Amino group	Aromatic	Knoevenegal	152

				aldehydes and ethyl cyanoacetate or malononitrile	condensation	
25.	NH_2-H_2bdc NO_2-H_2bdc	UiO-66-NH_2 UiO-66-NO_2	Amino group Nitro group	Benzaldehyde and methanol	Acetalization	151
26.	NH_2-bdc	IRMOF-3 NH_2-MIL-53-Al	Amino group	Benzaldehyde and ethyl cyanoacetate or ethyl acetoacetat	Knoevenagel condensation	38
27.	NH_2-bdc	NH_2-MIL-101(Fe) NH_2-MIL-101(Al) CAU-1)	Amino group	Benzaldehyde and ethyl cyanoacetate or malononitrile	Knoevenagel condensation	154
28.	5-(3,5dicarboxy-benzene amido)-isophthalic acid (H_4L)	$[Cu_2(L)(DMA)_2]$	Amide group	Benzaldehyde and ethyl cyanoacetate or malononitrile	Knoevenagel condensation	155
29.	4-btapa	$[(Cd(4btapa)_2(NO_3)_2 \cdot 6H_2O \cdot 2DMF]_n$	Amide group	Benzaldehyde and malononitrile, ethyl or cyanoacetate or cyano-acetic acid *tert*-butyl ester	Knoevenagel condensation	150

4.2 Mixed Linker MOF

The new concept of incorporating mixed ligands/linkers as building struts in MOFs structures has been developed recently. This certainly tunes the physiochemical properties in the resulting MOF structures. The mixed-linker MOFs (MIXMOFs) are versatile, introducing multifunctional features within one MOF. Numerous studies have been carried out by varying two or more distinct functionalities in one MOF.[156] Catalysis with MIXMOFs has not been studied extensively, rather only few reports are available. Here we discuss some important MIXMOFs used in heterogeneous catalysis of organic reactions.

Kleist *et al.,* reported for the first time the catalytic activity of a MIXMOF having formula $[Zn_4O(bdc)_{3-x}(NH_2\text{-}bdc)_x]$ in the reaction of propylene oxide (PO) and carbon dioxide.[157] A new synthetic method was developed based on MOF-5 which allows the partial substitution

of benzene-1,4-dicarboxylate (bdc) linkers in MOF-5 by functionalized 2-aminobenzene-1,4-dicarboxylate (NH_2-H_2bdc). MIXMOF represent a promising class of materials for catalytic applications at a temperature as high as 300 °C which is verified by using the synthesis of propylene carbonate (PC) from propylene oxide and carbon dioxide as a test reaction. The MIXMOF showed an activity similar to the corresponding homogeneous reference compounds (NH_2-H_2bdc, H_2bdc and Zn salts) and could be recycled with modest loss in activity.

Similarly, another MIXMOF based on MOF-5 was constructed where 5% and 10% of benzene-1,4-dicarboxylate was substituted by 2-aminobenzene-1,4-dicarboxylate (Scheme 9), finally a loading of Pd was accomplished with $Pd(OAc)_2$.[47] The interaction between the amino groups and Pd leads to highly dispersed Pd species which do not form big particles enough to block the pores of MOF. At a temperature of 150 ^oC, the yield of CO oxidation amounted to 19%, 50% and 65% for the Pd catalysts Pd/MOF-5, Pd/5% and 10%-MIXMOF, respectively. The catalyst displayed good catalytic results in the oxidation of CO at elevated temperature (350 ^oC).

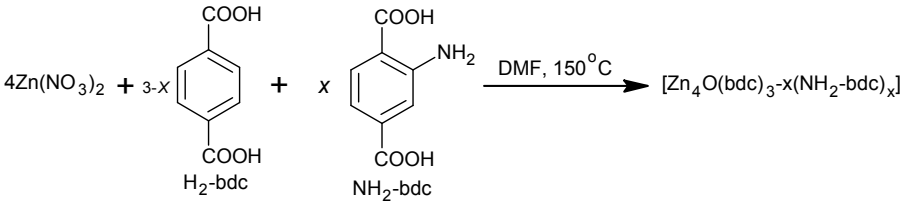

Scheme 9. Synthesis of MIXMOF from H_2bdc and NH_2-H_2bdc.

A MIXMOF based on the $[Cu_3(btc)_2]$ was prepared in which the benzene-1,3,5-tricarboxylate (H_3btc) linkers have been partially replaced by 10, 20, 30, 40, 50, and 90 mol% pyridine-3,5-dicarboxylate (H_2pydc).[50] The SEM of $[Cu_3(btc)_2]$ and $[Cu(btc)_{0.5}(pydc)_{0.5}]$ showed no significant alteration in the morphology. Both catalysts catalyzed the hydroxylation of toluene both in acetonitrile and under neat conditions. Different selectivity toward the desired *o*- and *p*-cresol and other oxidation products (benzaldehyde, benzyl alcohol, methylbenzoquinone) was observed for $[Cu_3(btc)_2]$ and the $[Cu(btc)_{0.5}(pydc)_{0.5}]$, respectively

(Scheme 10). It has been perceived that the reaction concentration had a striking and opposite influence on the product selectivity and conversion. Lower substrate concentrations led to an increased conversion and increased selectivity toward the side products. High selectivity for the products was achieved under solvent free condition.

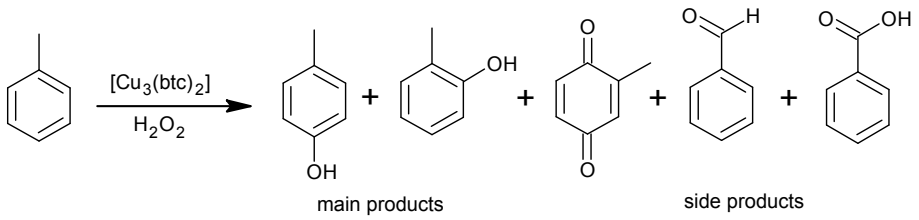

Scheme 10. Reaction scheme for the oxidation of toluene.

Huang *et al.*[158] constructed a MIXMOF *i.e.*, $[Al(OH)(bdc)_x(NH_2\text{-}H_2bdc)_{1-x}]$ based on MIL-53(Al) (x = 0.1; 0.5; 0.9) (Scheme 11) and finally Pd NPs were supported on the MIXMOF. It was also proved that amine-functionalized, mix-linker MIL-53(Al) exhibited a higher thermo stability than MIL-53(Al).[159, 160] The catalyst showed an efficient catalytic activity for the Heck reaction of *p*-subtituted arylhalides and styrene in DMF and in the presence of tri-ethylamine as base at 120 ^oC. Reaction between styrene and a variety of electron-rich substrates (such as *p*-methyl and *p*-methoxy arylbromide) proceeded smoothly and gave the corresponding coupling products in good to high yields (65% to 98%). The catalyst showed a remarkable activity after being recycled for five runs.

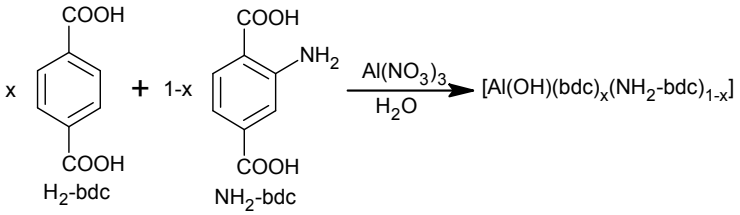

Scheme 11. Synthesis of MIXMOF, $[Al(OH)(bdc)_x(NH_2\text{-}bdc)_{1-x}]$ from H_2bdc and $NH_2\text{-}H_2bdc$.

5. Multifunctional MOF

MOFs are unique among the heterogeneous catalysts because of their potential to precisely install different catalytic centers within one MOF.[161] The overall structure, porosity, and active sites of MOFs can be planned and tuned through the careful choice of metal or metal-

containing building nodes and organic bridging ligands, depending on the specific applications. Some multi-functional MOFs have been developed capable of catalyzing different organic reactions (Table. 2).[53, 150, 162, 163] Bifunctional MOF containing unsaturated metal centers and metal NPs or functional linkers are also prepared and used as solid catalyst in organic transformations.[164, 165]

Li *et al.*[166] synthesized a novel hetero-bimetallic Pd/Y-MOF from K_2PdCl_4, 2,2-bipyrdine-5,5-dicarboxylic acid (H_2bpydc) and $Y(NO_3)_3{\cdot}6H_2O$ through a facile microwave irradiation method. The 3D extended framework is constructed by Y(III) coordinating to carboxylic groups on the Pd(bpydc)Cl_2 building blocks. The hetero-bimetallic MOF displayed high thermal stability up to 500 °C. Pd/Y-MOF exhibited higher catalytic activity than Pd(bpydc)Cl_2 in the Suzuki-Miyaura coupling reaction and Sonogashira reaction (Scheme 12) which might be due to (i) the highly dispersed Pd(II) sites in the layered structure of Pd/Y-MOF and (ii) the cooperative effect between Pd(II) and Y(III) (Table 2, entries 9 and 10). A series of arylhalides and 4-methylphenylboronic acid are used in Suzuki-Miyaura reaction. The catalytic activity follows the order Ar-I > Ar-Br > Ar-Cl which is attributed to the difficulty for enhancing the C-X bond. Presence of electron-rich substituents (methyl group, methoxy group) on arylhalides with 4-methylphenylboronic acid displayed a lower conversion (22%). However, the presence of electron-withdrawing substituents (nitro group) promotes the reaction due to the activation of C-X bond and conversion reaches 96%. Similar results are also observed in case of the Sonogashira coupling reaction of arylhalides and phenylacetylene. Pd/Y-MOF can be easily regenerated for reuse owing to the high stability of the framework formed by coordination of Y(III) with carboxylic groups. The XRD patterns indicate that the hetero-metallic MOF retains its original structure well after being used repetitively for three runs. Also the incorporation of Pd(II) into the crystal framework of Pd/Y-MOF prohibited the leaching of Pd (II) active species.

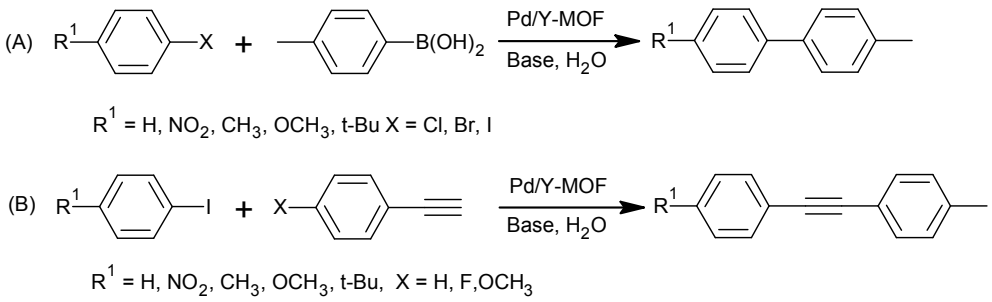

Scheme 12. Pd/Y-MOF-catalyzed (A) Suzuki-Miyaura reaction and (B) Sonogashira reaction.

MOFs have tunable structures that can be easily perceived for the possible assimilation of multiple functions within a given MOF through careful design. A bifunctional MOF (UiO -66-NH_2) containing Lewis-acid Zr^{4+}sites and basic amino groups used in aldol-condensation of heptanal with benzaldehyde was reported in 2011 by Vermoortele *et al*. Lewis-acid Zr^{4+} sites activate benzaldehyde and basic amino groups activate the methylenic group of the aliphatic aldehydes (Table 2, entry 7). The close proximity of Zr^{4+} Lewis-acid centers and basic amino groups inside the cages accelerates the aldol reaction and also suppresses the formation of by-products.[167] Zinc imidazole frameworks (ZIFs) based on imidazole linker and metallic nodes can adopt symmetrical porous analogous to zeolites. ZIF-8 has been synthesized from 2-methylimidazole and a Zn precursor. ZIF-8 exhibits a high surface area of 1400 m^2/g, thermal stability up to 420 °C, and pore diameters of about 11 Å. High catalytic activity of most famous ZIF-8, $[Zn(meIm)_2{\cdot}(DMF){\cdot}(H_2O)_3]$ (H-meIm = 2-methylimidazole) was observed in transesterification of triglycerides with alcohols which was due to Zn^{2+} Lewis-acid sites and Brønsted-acid sites (OH group) as well as basic-sites (NH groups and N^- moieties) (Table 2, entry 8).[168] Similarly, Zhu *et al.*[169] evaluated the catalytic activity of ZIF-8 in the cycloaddition of CO_2 to styrene oxide to form styrene carbonate. The catalytic study showed that the ZIF-8 is a bi-functional catalyst containing both acidic and basic sites, associated with the Lewis-acid Zn^{2+} ions and the basic imidazole groups, respectively (Table 2, entry 1). Lewis-acid Zn^{2+} sites and the nitrogen basic moieties from the imidazole linker

promoted the adsorption of carbon dioxide on the solid surface as well as the activation of the carbon-oxygen bonds.

Recently, a hetero-metallic MOF, CPO-27-Mn_xCo_{1-x} containing two different metals (Co-Mn) was tested for the cyanosilylation of different aldehydes with trimethylsilylcyanide. XRD analysis of CPO-27-$Mn_{0.57}Co_{0.43}$ and CPO-27-$Mn_{0.10}Co_{0.90}$ displayed that mixed-metal MOFs are isostructural with the parent MOFs (CPO-27-M). Catalytic results show that the catalytic activity of mixed-metal MOFs is situated between the parent MOFs CPO-27-Co and CPO-27-Mn and between the two mixed metal-MOFs. $Mn_{0.57}Co_{0.43}$ give the highest conversion for different benzaldehydes due to the higher content of Mn over Co (Table 2, entry 11).[130]

Another multi-functional porous coordination network (PCN-124) was synthesized by treating H_4pdai (H_4pdai = 5,5'-[(pyridine-3,5-dicarbonyl)bis-(azanediyl)]diisophthalate) with $Cu(NO_3)_2 \cdot 2.5H_2O$ in a mixed solvent of DMA:H_2O and HBF_4 at 75 °C for 2 days.[170] The MOF structure possesses a self-interpenetrated (3,36)-connected 3D structure and crystallizes in the space group *Im*3*m*. Its structure resembles with an isostructural MOF, PMOF-3, which was recently reported by Zhang.[171] PCN-124 is thermally stable up to 300 ºC as confirmed by TGA. The de-acetalization-Knoevenagel reaction was carried out using PCN-124 as catalyst. The weak Lewis-acidic open Cu^{2+} centers and Lewis-basic pyridine and amide groups in PCN-124 made this MOF convenient for one-pot tandem reactions (Table 2, entry 2). The first step, de-acetalization of dimethoxymethylbenzene to give benzaldehyde was catalyzed by Lewis-acidic Cu^{2+} ions and the second step, Knoevenagel condensation of benzaldehyde and malononitrile was catalyzed by base and amide groups. PCN-124 could be easily recovered and reused at least for three cycles without significant loss of activity as the PXRD patterns of the recycled PCN-124 was consistent with the fresh one.

Duan *et al.*[172] reported a new approach to construct a multifunctional lanthanide-organic framework (Tb-tca) by solvothermal reaction of H_3tca (tricarboxytriphenylamine) and

$Tb(NO_3)_3 \cdot 6H_2O$ in a mixture of solvents (DMF and ethanol) in a screw-capped vial at 100°C for 3 days (75% yield) (Fig. 8a). The synthesized MOF (Tb-tca) features a high activity due to high concentration of Lewis-acidic Tb^{3+} sites and Lewis-basic triphenylamine sites on its internal surfaces (Table 2, entry 3). TGA showed that Tb-tca is stable up to 200 °C. Tb-tca catalyzed both the Knoevenagel condensation of salicylaldehyde derivatives with malononitrile and cyanosilylation of different benzaldehydes and cyanotrimethylsilane (Fig. 8b) in a size-selective mode through basic and acidic catalytic sites, respectively. Only 2 mol% of Tb-tca led to over 90% and 70% conversion after 6 h reaction respectively.

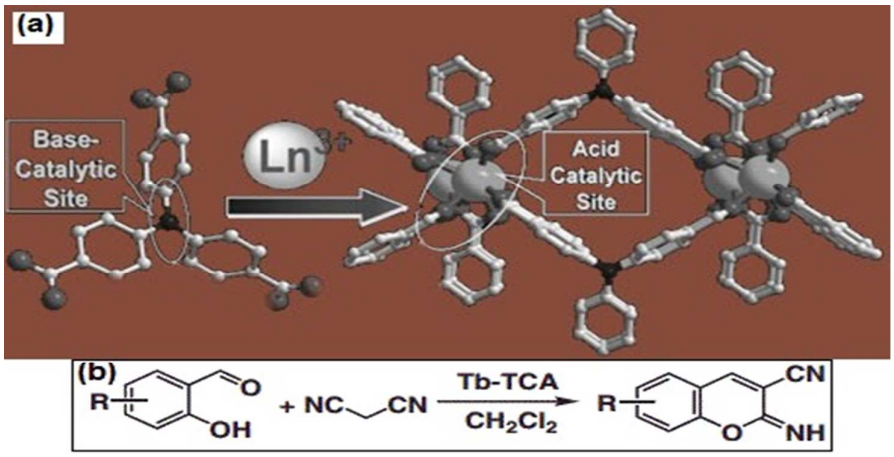

Fig. 8 (a) Perspective view of the channels with multifunctional MOF (Tb-TCA) with triphenylamine (basic sites) and Tb^{3+} (acidic sites). (b) Knoevenagel condensation catalyzed by Tb-TCA. Reproduced from Ref. [172].

In 2012, Kim and coworker reported a bifuntional MOF containing Lewis acid-Brønsted base sites, catalyzing a tandem Meinwald rearrangement-Knoevenagel condensation with remarkable substrate selectivity.[173] Similarly, they screened the catalytic activity of a number of MOFs UiO-66, UiO-66-NH_2, $[Mg_2(dobdc)]$ (Mg-MOF-74), $[Fe_3OCl(H_2O)_2(bdc)_3]$ (MIL-101(Fe)), $[Cu_3(btc)_2]$, ZIF-8, IRMOF-3 (IRMOF = Isoreticular Metal Organic Frameworks) and MOF-5 for the cycloaddition of CO_2 to different epoxide, and evaluated their catalytic activities correlated with the Lewis-acid/base properties of the MOFs. Yields of styrene carbonates from styrene oxides using the different catalysts were determined (Fig. 9).[174] An examination of the catalytic activities and acid-base characteristics of the MOF catalysts revealed that when both acidic and basic sites co-exist *e.g.*, MOFs UiO-66-NH_2, Mg-MOF-74

and UiO-66, they showed high catalytic activities for the CO_2 cycloaddition compared to others. The multi catalytic activity is due to the presence of NH_2-groups and oxygen atoms in these MOFs (Table 2, entry 5). UiO-66-NH_2 showed an excellent catalytic activity over the other MOFs. Three mechanisms have been proposed (Fig. 10), after complete investigation of the CO_2-TPD, NH_2-TPD profiles (TPD = temperature-programmed-desorption) and their catalytic activities. In the mechanism A: CO_2 is adsorbed on a Lewis-basic site and epoxide is adsorbed on adjacent Lewis-acid site leading to the reaction intermediate. While in the mechanism B, epoxide adsorption on Lewis-acidic site followed by a nucleophilic attack of the C-O bond of CO_2 leads to the intermediate formation. In the mechanism C, CO_2 is adsorbed on Lewis-basic site and inserted into the C-O bond of epoxides *via* a nucleophilic attack.

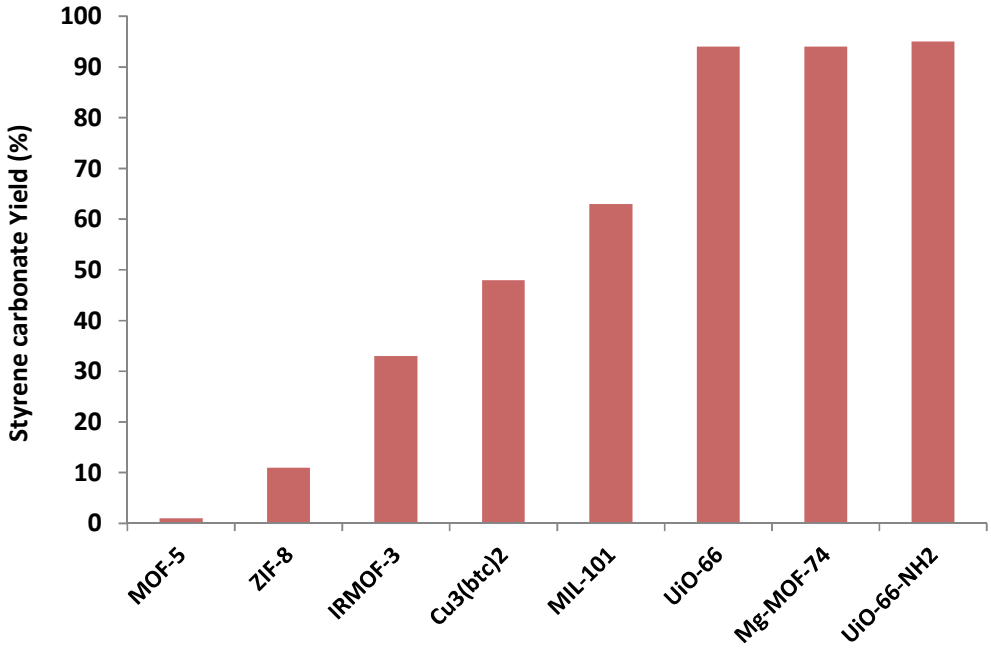

Fig. 9 Representation of yields of styrene carbonates from styrene oxides production with different MOFs. Reproduced from Ref. [174].

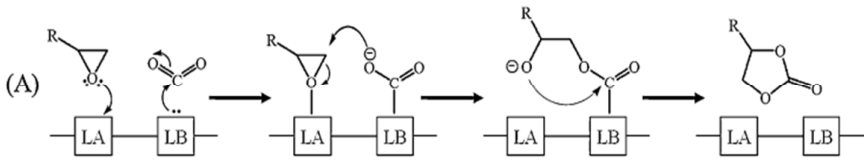

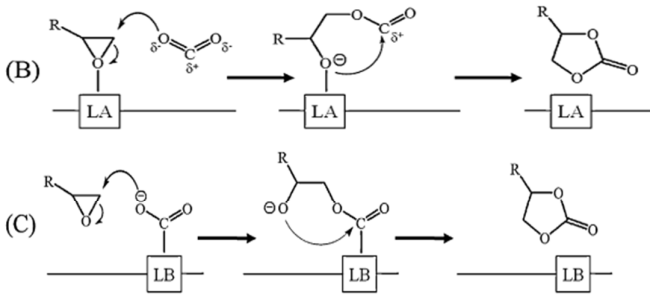

Fig. 10 Proposed mechanisms for cycloaddition of CO_2 to an epoxide. (A) Lewis-acid and base, (B) Lewis-acid, and (C) Lewis-base catalyzed. Reproduced from Ref. [174].

A list of multifunctional MOFs summarizes with proven multi-catalytic active sites such as metal-metal or metal-ligand or ligand-ligand is given in Table 2.

Table 2. List of multifunctional MOFs with reported catalytic properties.

Entry	Organic linker	MOF	Active sites	Substrate(s)	Reaction(s)	Ref.
1.	HmeIm	ZIF-8	Zn(II) Imidazole group	Styrene oxide	Cycloaddition of CO_2	169
2.	H_4pdai	PCN-124	Cu(II) pyridine and amide groups	Dimenthoxym ethylbenzene and malononitrile	De-acetaliza tion-Knoev enagel reaction	170
3.	H_3tca	Tb-tca	Tb(III) Triphenylamine	Salicylaldehyd e derivatives and malononitrile	Knoevenagel reaction	172
4.	H_3tca	Tb-tca	Tb(III) Triphenylamine	Different benzaldehydes and cyanotrimethy lsilane	Cyanosilylation	172
5.	NH_2 -H_2bdc H_2dobdc H_2bdc	UiO-66-NH_2 Mg-MOF-74 UiO-66	Oxygen atom Amino group	Different epoxides	Cycloaddition of CO_2	174
6.	H_2bdc	Pt/Pd @MIL-101 (Cr)	Cr(III) Pd II / Pt II	Carbonyl compounds	Reductive amination of carbonyl compounds	165
7.	NH_2 -H_2bdc	UiO-66-NH_2	Zr(IV) Amino group	Heptanal and benzaldehyde	Cross-aldol condensation	167
8.	HmeIm	ZIF-8	Zn(II) imidazole group	Triglycerides and alcohols	Transesterificati on	168
9.	H_2bpydc	Pd/Y-MOF	Pd(II) Y(III)	Aryl Halides and 4methyl phenylboronic acid	Suzuki-Miyaura coupling reactions	166
10.	H_2bpydc	Pd/Y-MOF	Pd(II) Y(III)	Substituted	Sonogashira reactions	166

				iodobenzene and substituted phenylacetylene		
11.	H_2dobdc	Mn_xCo_{1-x} MOFs	Co(II) Mn(II)	Different aldehydes andtrimethylsilylcyanide	Cyanosilylation	130

6. Immobilization of active guest specie within mesoporous MOF

The chemical flexibility of MOF structures has allowed a different set of strategies for building microenvironments within MOFs which allow immobilization of molecular catalysts and heterogenization of homogeneous catalysts. A broad consideration has been paid to immobilize active catalyst, transition metal complexes,[175, 176] and enzymes[177, 178] into MOFs that offer high surface areas with tunable and uniform pores.[102] Pore walls with functional moieties offer specific interaction for guests and avoid aggregation in solution as well. Mesoporous MOFs serve as new type of host material to immobilize active guest species such as microperoxidase (MP-11)[179] and *N*-hydroxyphthalimide (NHPI)[180] *etc.* for catalytic applications in the given organic solvents.

Ming and coworkers[179] were the first to evaluate the immobilization of MP-11 into a mesoporous MOF [Tb(tatb)(H_2O] (Tb = terbium and tatb = 4,4',4"-s-triazine-2,4,6-triyl-tribenzoic acid) consisting of nanoscopic cages, which pertained superior enzymatic catalysis performances. Mobil composition of matter No.41 (MCM-41) is a mesoporous material from a family of silicate and alumosilicate solids was also used for immobilization of MP-11. The catalytic activity of MP-11@Tb-mesoMOF, MCM-41 and MP-11@MCM-41 were tested in the oxidation of 3,5-di-*tert*-butyl-catechol (DTBC). MP-11@MCM-41 showed a high activity with 17.0% conversion, but the catalyst was deactivated due to the leaching of MP-11 during the assay. In contrast, MP-11@Tb-mesoMOF remained intact (no leaching evidence), and a relatively higher conversion of 48.7% was obtained. These results showed that the MP-11 catalyst was greatly stabilized through the mesoporous MOF host matrix.

Canivet *et al.*[181] performed a novel one-pot post functionalization of MOF, enabling the immobilization of an active organometallic catalyst in its cavities. For this purpose, NH_2-MIL-101(Fe) was chosen because of its high pore volume which is able to hold organometallic complexes. NH_2-MIL-101(Fe) can also be used as substrate along with the amino groups on its walls acting as a platform for post-synthetic functionalization. The imine condensation occurs in the presence of the [Ni(PyCHO)Cl_2] (PyCHO = 2-pyridine carboxaldehyde) methanolic solution to form the diimino nickel complex anchored into the MOF (Fig. 11). This new MOF catalyst Ni@NH_2-MIL-101(Fe) is very efficient in the triphasic ethylene dimerization forming selectively 1-butene. A higher selectivity for 1-butene is found in this methodology than that reported for molecular nickel diimino complexes.

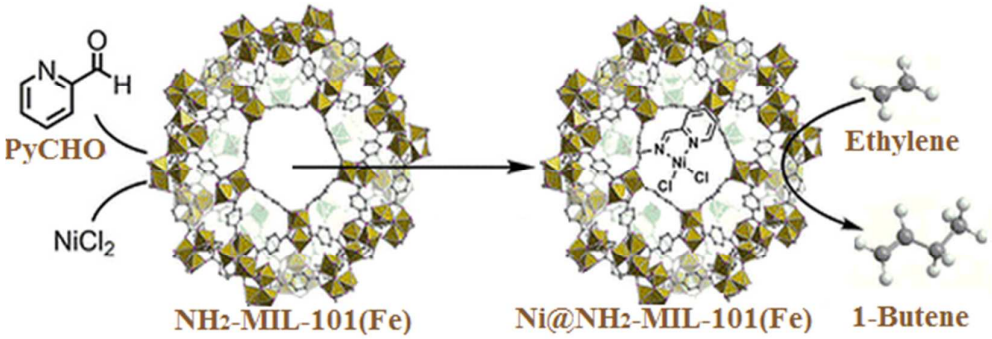

Fig. 11 Schematic representation of the synthesis and catalysis of the MOF-anchored Nickel complex Ni@(Fe)MIL-101. Reprinted with permission from ref. [181]. Copyright 2013 American Chemical Society.

The catalytic activity of NHPI/[Fe(btc)] in the aerobic oxidation of cycloalkenes was screened by Garcia and coworker.[180] NHPI was incorporated onto [Fe(btc)] by adsorption from a CH_2Cl_2 solution. The structure of [Fe(btc)] is composed of trimers of iron on tetrahedra sharing μ_3-O vertex linked by btc moieties. Two types of mesoporous cages were formed with windows of 5.5 and 8.6 Å respectively (Fig. 12a). After incorporation of NHPI, the surface area of [Fe(btc)] reduced from 840 to 24 m^2g^{-1} however the XRD patterns did not change. In presence of oxygen and [Fe(btc)] catalyst, no conversion of cyclooctene was observed. However, with NHPI/[Fe(btc)], 3.6% conversion to cyclooctene oxide was observed with 99% selectivity. Very high selectivity was achieved for the aerobic epoxidation with cyclooctene, while decreasing the ring size favored allylic oxidation.

Similarly, aerobic oxidation of cyclooctane was reported using NHPI/[Fe(btc)] as a heterogeneous catalyst under solvent free conditions.[182] It has been established that selectivity to cyclooctanol and cyclooctanone >90% could be achieved at 30% conversion within 6 h. After 6 h of reaction time, a decrease in the selectivity towards cyclooctanol and cyclooctanone was observed, because the primary reaction products can undergo further secondary reactions. After three consecutive uses, the stability of MOF structure was confirmed by comparison of its XRD patterns with the XRD pattern of the fresh MOFs.

Later, Garcia also evaluated the catalytic behavior of NHPI/[Fe(btc)] in the aerobic oxidation of benzyl amines and its derivatives.[183] The guest molecule NHPI initiated the auto-oxidation to generate the *N*-oxyl radical due to interaction of the N atom of NHPI and the O atom adjacent to Fe (Fig. 12b,c), which further abstract a hydrogen radical from the amine leading to the formation of an α-amino alcohol. The presence of the *N*-oxyl radical in the reaction was confirmed by electron spin resonance spectroscopy (ESR). By using NHPI/[Fe(btc)] as catalyst, the reaction rate was increased and a high conversion of benzyl amines to their corresponding benzyl imines was obtained at 100 °C with molecular oxygen. The catalyst displayed good activity in terms of conversion and selectivity and proved to be an efficient catalyst for the general synthesis of important benzylimine derivatives.

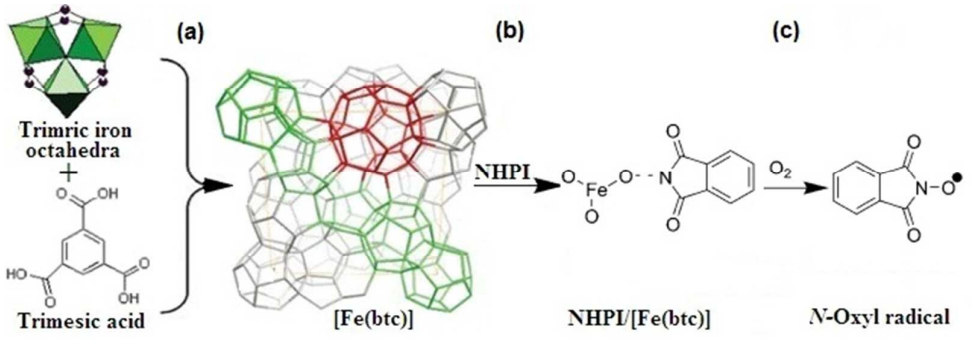

Fig. 12 (a) formation of MIL-101(Fe) from trimeric iron octahedral and trimesic acid (b) immobilization of guest molecule (c) formation of *N*-oxyl radical. Reproduced from Ref. [183].

Recently, a modified MOF, Im-MIL-101(Cr) (Im = Imidazole) was prepared by reaction of $[Cr_3OF(H_2O)_2(bdc)_3]\cdot nH_2O$ (MIL-101(Cr)) with methoxyacetyl chloride and further

substitution of chlorine with imidazole used as a support for immobilizing of Mn(tpp)Cl (tpp = tetraphenylporphyrin) afforded Mn(tpp)Cl@Im-MIL-101(Cr).[52] The XRD patterns confirmed that the crystallinity of MIL-101 is maintained after the modification. The catalyst showed a good activity in the oxidation of cyclooctene and gave cyclooctene oxide yield of 96%. In the case of cyclohexene, the major product was cyclohexene oxide (82%) and 2-cyclohexen-1-one was produced as a minor product (10%). Epoxidation of styrene yielded styrene oxide as the major product with only a small amount of benzaldehyde. Mn(tpp)Cl@Im-MIL-101(Cr) is highly active, stable and reusable for four consecutive runs without loss of catalytic activity as confirmed by XRD, FT-IR and solid state UV-vis.

Bromberg *et al.*[184] tailored the aluminum amino benzene-1,4-dicarboxylate MOFs, NH_2-MIL-53(Al) and NH_2-MIL-101(Al) with aluminum alkoxide (Al-*i*-Pro), a known catalyst for the Tischenko reaction. MOF/Al-*i*-Pro composites obtained by simple impregnation of the MOFs with a hydrocarbon solution of Al-*i*-Pro are stable due to the formation of bonds between the MOF carbonyls and Al-*i*-Pro. The uptake of acetaldehyde vapors and acrolein on MOFs and MOF/Al-*i*-Pro materials was approximately 5-fold and 2-fold higher than physisorption on carbon (wood origin) with a BET (Brunauer-Emmett-Teller) surface area of 2266 m^2g^{-1}, chemically activated with phosphoric acid, under saturated vapor conditions. The catalysis study showed that after 1 h of exposure of the catalyst to acetaldehyde vapors, the ratio of acetaldehyde to ethyl acetate was approximately 10:1. Following 8 h, the ratio was approximately 1:5. After 24 h, ethyl acetate comprised the majority of the product (> 95%) and isopropyl acetate as a minor product (approximately 5%) moreover crotonaldehyde was not found. But with NH_2-MIL-101(Al) and or NH_2-MIL-53(Al), after 24-h contact the ratio of acetaldehyde to crotonaldehyde was approximately 8:1 and ethyl acetate was not detected. A proposed mechanism for reaction of acetaldehyde dimerization is shown in Fig. 13. The modified MOF was recyclable, implying the possibility of practical applications.

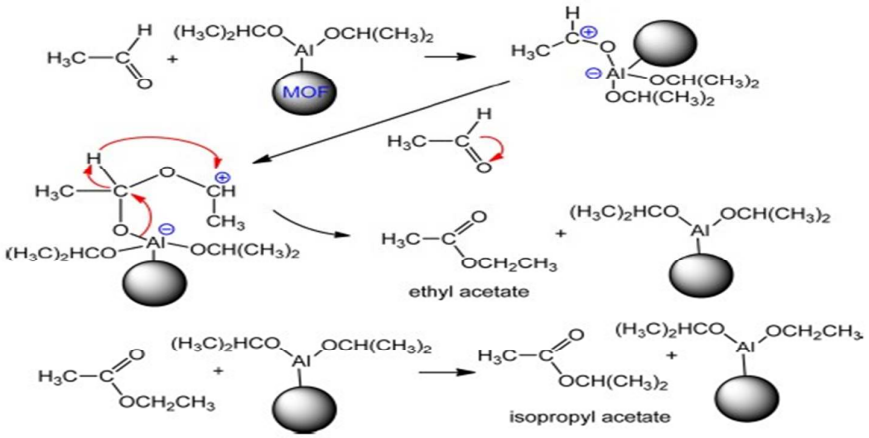

Fig. 13 Mechanism of MOF/Al-*i*-Pro-catalyzed Tischenko reaction of acetaldehyde dimerization. Reprinted with permission from ref. [184]. Copyright 2013 American Chemical Society.

For immobilization of polyoxometallates (POMs), efforts have been done and different methodologies have been deliberated using various solid supports to immobilize POMs *via* dative, covalent or electrostatic binding.[185-188] By using titanium, cobalt mono-substituted phosphotungstates and the Keggin anion $[PW_{12}O_{40}]^{3-}$, POMs@MIL-101 was prepared and used as catalyst for oxidative reactions with O_2 and H_2O_2.[189, 190] Furthermore, the inclusion of $H_3[PW_{12}O_{40}]$ in $[Cu_3(btc)_2]$ to prepare active heterogeneous catalysts has been recently investigated.[191, 192]

In 2013, Cunha-Silva and coworkers[193] prepared two novel hybrid composite materials, PW_{11}@MIL-101(Cr) and SiW_{11}@MIL-101(Cr), by the incorporation of the potassium salts of the polyoxotungstates, $[PW_{11}O_{39}]^{7-}$ (PW_{11}) and $[SiW_{11}O_{39}]^{8-}$ (SiW_{11}), into the porous MIL-101(Cr). The formation of PW_{11}@MIL-101(Cr) and the structural stability of MIL-101(Cr) after the inclusion are confirmed by ^{31}P solid state NMR and PXRD. The oxidation reactions of *cis*-cyclooctene, geraniol and *R*-(+)-limonene were carried out in acetonitrile (MeCN) with H_2O_2 (30 wt.%), using the PW_{11} and SiW_{11} as homogeneous catalysts and PW_{11}@MIL-101(Cr) and SiW_{11}@MIL-101(Cr) as heterogeneous catalysts. With heterogeneous catalyst, the conversion of *cis*-cyclooctene into 1-epoxycyclooctane was completed within 10 minutes (yield of 98% and TOF of 1922 mol $mol_{POM}^{-1}h^{-1}$). Using equivalent amount of homogeneous catalyst, conversion of *cis*-cyclooctene completed after 5 h of reaction (96% of yield).

The robustness, thermal and chemical stability of PW_{11}@MIL-101(Cr) and SiW_{11}@MIL-101(Cr), were established after catalytic experiments by several techniques. This provides an avenue for the immobilization of enzymes as heterogeneous biocatalysts for catalytic applications under various conditions.

7. Encapsulation of catalytic active specie inside MOF

MOFs have appeared as a novel class of catalysts, in which small catalytic active guest species such as POMs (polyoxometalates)[194] and metalloporphyrins[195] *etc.* have been successfully encapsulated. The micropore size of most MOFs precludes the entry of larger-sized enzymes and could result in only surface adsorption. Although, recent advances in mesoporous MOFs[196] may offer opportunities for enzymatic catalysis, the investigation of mesoporous MOFs for enzymatic catalysis applications has not been much exploited. Therefore, there is still plenty of room available in this research area for further developments.

7.1 Polyoxometalates

Polyoxometalates (POMs) offer numerous advantages as catalysts that make them economically and environmentally attractive. POMs are complex Brønsted acids that consist of heteropolyanions having metal-oxygen octahedra as the fundamental structural units. Encapsulation of POMs inside zeolitic cavities has been achieved by direct synthesis of the Keggin structures inside the zeolite cavities. Following a similar approach, Maksimchuk *et al.* impregnated different Ti and Co Keggin anions into the large cavities of MIL-101 and the catalytic performance was evaluated in the oxidation of alkenes using O_2 and H_2O_2 as oxidants. These catalysts could be reused many times without loss of activity and were stable under mild operation conditions.[197] A hetero-polyacid phosphotungstic acid (HPW) encapsulation in $[Cu_3(btc)_2]$ to afford $[HPW/Cu_3(btc)_2]$ has been assessed in an esterification reaction of acetic acid with 1-propanol. However, leaching of Cu^{2+} and hetero-polyacid was observed on using high mole ratio of acetic acid and 1-propanol (1:2).[192]

Gao and coworker[198] have designed and prepared three novel catalysts $PMo_{11}V$@HKUST-1, $PMo_{10}V_2$@HKUST-1 and PMo_9V_3@HKUST-1 *via* encapsulation of vanadium-doped Keggin polyoxometalates $PMo_{12-n}V_n$ into the framework HKUST-1. PXRD patterns of $PMo_{11}V$@HKUST-1, $PMo_{10}V_2$@HKUST-1, PMo_9V_3@HKUST-1, and HKUST-1 disclosed that the peaks for HKUST-1 were maintained in the modified MOFs, indicating that the crystallinity of HKUST-1 has not been disrupted. The catalytic activity of $PMo_{12-n}V_n$@HKUST-1 was tested for the hydroxylation of benzene to phenol, using ascorbic acid as the co-reductant with O_2. During hydroxylation of benzene to phenol, catalyzed by PMo_9V_3@HKUST-1, drastic oxygen consumption in the initial 20 min was observed. PMo_9V_3@HKUST-1 outperformed $PMo_{11}V$@HKUST-1 and $PMo_{10}V_2$@HKUST-1, achieving a phenol yield of 9.93%.

Kapteijn and coworkers[199] synthesized a composite (POM-MOF) by encapsulation of polyoxometalates into MIL-101(Cr), that was used because it has two types of quasi-spherical mesoporous cages limited by 12 faces for the smaller and by 16 faces for the larger. Large cavities of MIL-101(Cr) are accessible through 1.5 nm hexagonal windows, while medium cavities are accessible through 1.2 nm pentagonal windows (Fig. 14a). Zeo-type cavities (cages) of two different sizes, that are fully accessible together with high thermal and chemical stability make MIL-101 an excellent candidate for supporting catalytic species. The addition of H_3PW to MIL-101(Cr) yielded polyoxometalates encapsulated MIL-101(Cr) (Fig. 14b). The presence of coordinative unsaturated metal sites in MIL-101 allowed their use as a mild Lewis-acid and post functionalization *via* grafting of active species (POMs). The performance of the catalyst in the Knoevenagel condensation of benzaldehyde and ethyl cyanoacetate was excellent due to the presence of unsaturated metal sites (Lewis-acid site) and encapsulation of POMs (active catalyst). The encapsulated catalyst promoted the liquid phase acid-catalyzed esterification of acetic acid and *n*-butanol as well as the gas phase acid-catalyzed dehydration of methanol (etherification).

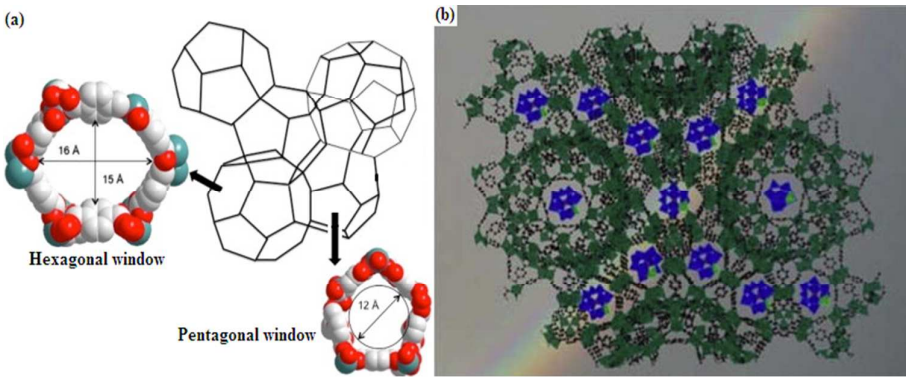

Fig. 14 (a) MIL-101(Cr) structure. (Left) Hexagonal windows; (center) zeo-type structure; and (right) pentagonal windows (b) POM encapsulated in MIL-101(Cr). Reproduced from Ref. [199].

In 2013, Hatton and coworkers have prepared hetero-polyacid functionalized alumino-2-aminoterephthalate MOFs (MOF/PTA composite) by using two MOFs (NH_2-MIL-101(Al) and $[Al(OH)(NH_2\text{-}bdc)](NH_2\text{-}H_2bdc)_{0.75}]$ (H_2N-MIL-53(Al)) with phosphotungstic acid (PTA) and employed them as a sorbent in the chemical conversion of acetaldehyde vapor.[200] The thermal stability of the MOFs was studied and the thermograms of NH_2-MIL-53(Al)/PTA and NH_2-MIL-101(Al)/PTA were similar with those of the parent MOF NH_2-MIL-101(Al). Both MOF and MOF/PTA showed equilibrium uptake of acetaldehyde from its saturated vapor phase exceeding 50 and 600 wt.% respectively, at 25 °C. The acetaldehyde vapor uptake occurs through the vapor condensation, with simultaneous conversion of acetaldehyde to crotonaldehyde. Higher-molecular-weight compounds (polymerization) were obtained from repeated aldol condensation.

Dang *et al.*[201] constructed a polyoxometalate-based lanthanide-organic framework, $[(Ho_4(dpdo)_8(H_2O)_{16}BW_{12}O_{40})\cdot 2H_2O](BW_{12}O_{40})_2\cdot(H_{1.5}pz)_2\cdot(H_2O)_{11}$ by a hydrothermal method using $HoCl_3\cdot 6H_2O$, 4,4'-bipyridine-*N,N'*-dioxide hydrate (dpdo), $HoH_2BW_{12}O_{40}\cdot nH_2O$, and hexahydropyrazine (pz). POM based lanthanide-MOF displayed good catalytic performance for phosphodiester bond cleavage in an aqueous solution. The catalyst is highly active, stable and reusable for three consecutive runs without loss of catalytic activity while retaining its crystallinity as determined by PXRD.

Song *et al.* examined the oxidative behavior of POM-MOF having formula $[Cu_3(btc)_2]_4[((CH_3)_4N)_4CuPW_{11}O_{39}H]\cdot 40H_2O$ prepared by encapsulation of $K_5CuPW_{11}O_{39}$

into MOF-199. The PXRD patterns and single crystal X-ray structure of POM-MOF reveal that the parent MOF-199 framework has been maintained. POM-MOF was capable of catalyzing the air-based oxidative decontamination of toxic sulfur compounds (Fig. 15).[202] Hydrogen sulfide was oxidatively converted to S8 by POM-MOF under ambient conditions in aqueous solution or gas phase. Similarly, the ability of POM-MOF to catalyze other aerobic oxidations, the conversion of volatile mercaptans to less toxic and odorous disulfides was also examined. 2-hydroxyethanethiol gives the highest conversion (95%) while bulky molecule *p*-toluenethiol gives less than a 30% yield of disulfides. Conversion decreases with increasing the mercaptan molecular weight. A size- and shape-dependent selectivity was observed in these reactions. The recycled POM-MOF catalyzes the aerobic oxidation of H_2S and alkanethiol for at least three cycles without significant activity loss. FTIR and powder XRD patterns of POM-MOF before and after the reaction are identical indicating that the both the structural component [$CuPW_{11}O_{39}$] and MOF-199 are stable.

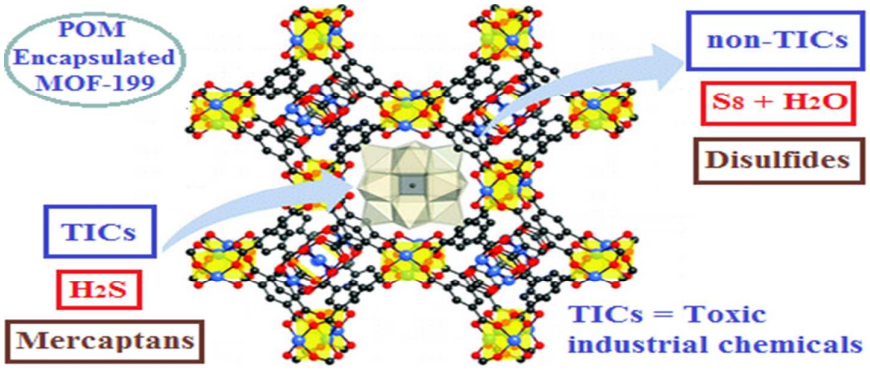

Fig. 15 Aerobic oxidation of thiols, mercaptans to S8, and disulphides catalyzed by POM-MOF. Reprinted with permission from ref. [202]. Copyright 2011 American Chemical Society.

7.2 Metalloporphyrins

Porphyrin and metalloporphyrin (MP) molecules have unique electronic structures, chemical and physical properties. MOFs that have permanent channels and cavities are used as catalyst supports.[64] There are a number of strategies to build porphyrin-containing MOF catalyst, such as using functional porphyrin molecules as organic linkers.[48, 203-206] It has also been demonstrated that cationic porphyrins can be encapsulated into the cavities of a zeolite-like MOF or HKUST-1[207, 208] using a "one-pot" self-assembly approach.

A robust anionic framework termed as rho-ZMOF was prepared from the reaction of $In(NO_3)_3 \cdot xH_2O$ and 4,5-imidazoledicarboxylic acid (H_3Imdc) in an DMF/CH_3CN mixture and in the presence of 5,10,15,20-tetrakis(1-methyl-4-pyridinio)porphyrintetra(*p*-toluenesulfonate) ($[H_2TMPyP][p\text{-tosyl}]_4$).[209] To assess catalytic activity of the MOF, oxidation of cyclohexane was performed at 60 °C using TBHP as oxidant. A total yield (from cyclohexane to cyclohexanol/cyclohexanone) of 91.5% and a noticeably high TON of 23.5 was observed as compared to other systems of supported metalloporphyrins (zeolites and mesoporous silicates). Cyclohexanol and cyclohexanone were the only products suggesting that this oxidation of cyclohexane is selective toward the formation of cyclohexanol and cyclohexanone and no further oxidation products were detected.

Two new porphyrin@MOFs catalysts have been synthesized through one-pot self-assembly approach by the reaction of 1,1-bis-[3,5-bis(carboxy) phenoxy]methane (H_4L) and $CuCl_2$ under solvothermal conditions in the presence of mesotetrakis[4-(nicotinoyloxy)phenyl] porphyrin (tnpp) and manganese complex of tnpp (Mn-tnpp) as shown in Fig. 16.[51] The resulting Cu-tnpp@MOF and Mn-tnpp@MOF solids were permanently porous, and presented good catalytic activity for the oxidation of 3,5-di-*tert*-butylcatechol to *o*-quinone in methanol usingH_2O_2. Results showed that the Cu-tnpp@MOF exhibited a higher catalytic activity than Cu-tnpp and pure MOF. Similarly, a microporous metal-organic material[208] containing Cd-tmpyp (tmpyp = meso-tetra(N-methyl-4-pyridyl)porphyrinetetratosylat) cations encapsulated in an anionic Cd (II) carboxylate framework , $[Cd_6(bpt)_4Cl_4(H_2O)_4]$ (H_3bpt = biphenyl-3,4′,5-tricarboxylate) resulted in a porphyrin-encapsulating MOF. The resulting catalyst showed excellent catalytic activity for the epoxidation of *trans*-stilbene. The porosity and stability of Cu- and Mn-tnpp@MOF solids after four catalysis cycles was confirmed by N_2-physiosorption and SEM measurement.

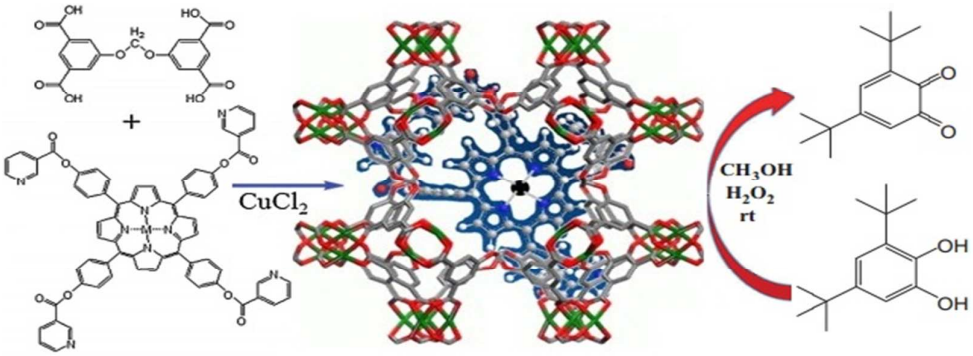

Fig. 16 Representation of encapsulation of porphyrin in MOF and oxidation of 3,5-di-*tert*-butylcatechol to *o*-quinone. Reproduced from Ref. [51].

8. MOF as a host for metal and metal oxides nanoparticles

The use of porous materials as supports for metal nanoparticles (MNPs) immobilization permits the production of specific surfactant-free active sites. This offers the advantages of controlling particle nucleation and growth to a nano size region in the confined cavities and reducing particle aggregation. MOFs are used as supports for MNP immobilization because of their rationally designed framework structures. Certain characteristics of MOF are required to get the desired immobilization of given MNPs. These includes, (i) sizes/volume, (ii) shapes, (iii) ease to modify the inner pore surfaces along with organic functionalities, and mode of electronic interaction between the MNPs and organic linkers. These parameters are considerably essential in controlling the uniform and limited growth of MNPs in their confined MOF's cavities producing highly reactive mono dispersed MNPs.[210-212] Different procedures have been developed for the introduction of MNPs into MOFs, including impregnation,[213] incipient wetness method,[214] deposition by solid grinding,[215] and immobilization of core–shell hetero-metallic NPs[59] on MOF by a sequential deposition–reduction method.[214, 216-218] There are three possible views in the literature to visualize MOF-immobilized MNP systems; (i) MNPs embedded within MOF nanopores designated as MNP@MOF,[219] (ii) MNPs immobilized onto porous surfaces of MOFs designated as MNP/MOF,[218] and (iii) construction of MOFs around pre-stabilized MNPs designated as PS-MNP@MOF. [220]

A uniform core-shell Pd@IRMOF-3 nanostructures were recently introduced, in which single Pd NPs cores are surrounded by an amino-functionalized MOF (IRMOF-3) shell *via* a facile mixed solvothermal method (Fig. 17 Bottom).[221] The nanocomposites showed high activity, enhanced selectivity, and excellent stability in the cascade reaction due to their unique core-shell structures. The core-shell nanocomposites could effectively and efficiently realize the cascade catalysis of Knoevenagel condensation of 4-nitrobenzaldehyde (**A**) and malononitrile to form intermediate products (**B**) *via* the alkaline IRMOF-3 shell coupled with subsequent hydrogenation of **B** using the Pd NP cores. For core-shell Pd@IRMOF-3, the hydrogenation selectivity is 86% while the Pd/IRMOF-3 and Pd NPs demonstrate a selectivity of 71% and 68%, respectively. The core-shell Pd@IRMOF-3 nanostructures showed superior selective hydrogenation, thus noticeably improving the yield of the products 2-(4-aminobenzylidene)-malononitrile (**C**) (Fig. 17 Top). Pd@IRMOF-3 exhibits high activity, enhanced selectivity, and excellent stability in cascade reaction with respect to conventional Pd/IRMOF-3.

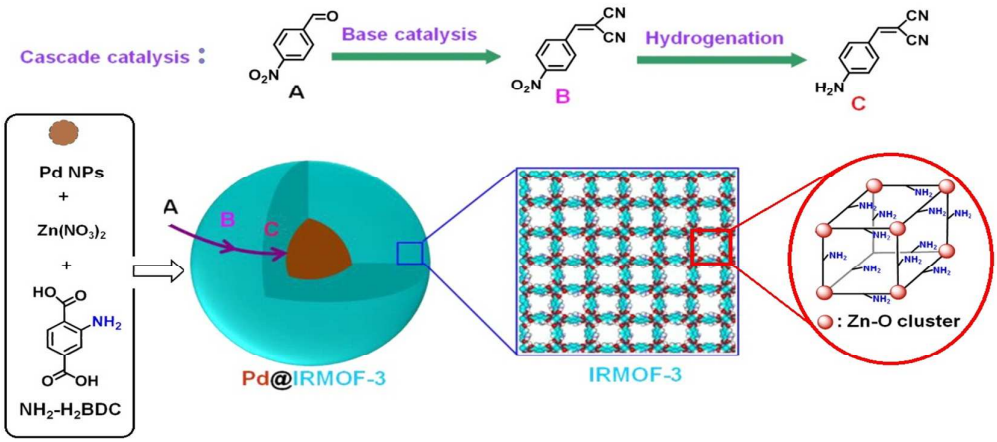

Fig. 17 Synthetic route for the core−shell Pd@IRMOF-3 hybrids *via* the mixed solvothermal method and model cascade reactions involving Knoevenagel condensation *via* the IRMOF-3 shell and subsequent selective hydrogenation through the Pd NP cores. Reprinted with permission from ref. [221]. Copyright 2014 American Chemical Society.

Similarly, Sun *et al.*[222] investigated the catalytic activity of Au NPs immobilized to [M(OH)(bdc)] (MIL-53(Cr)) and MIL-101(Cr) for selective oxidation of cyclohexane to cyclohexanone and cyclohexanol by molecular O_2. Only Au/MIL-53(Cr) and Au/MIL-101(Cr) maintain a selectivity above 80% and display a much higher yield compared with other supported Au catalysts (Au/TiO_2, Au/ZSM-5, Au/MCM-41, Au/MIL-96(Al), and

Au/MIL-110(Al)). Au NPs are the catalytic sites for the oxidation reaction and Au/MIL-53(Cr) and Au/MIL-101(Cr) exhibits superior catalytic performance to MIL-53(Cr) and MIL-101(Cr). Moreover, the catalytic property of Au NPs is directly related to particle size in nm. The confinement effect of MILs pore results in 2 nm Au NPs, which accounts for the higher selectivity of Au/MIL-101 than Au/MIL-53(Cr). XRD patterns of the Au-MIL-n-(Cr) (n = 53, 101) and recovered samples after reactions have no observable differences, which indicates Au-MIL-n-(Cr) (n = 53, 101 are very stable catalysts for the cyclohexane selective oxidation.

The catalytic activity of palladium NPs supported on amino functionalized MOF (H_2N-MIL-53(Al)) in Suzuki-Miyaura cross-coupling reaction was investigated by Hunag *et al.* (Scheme 13).[223] The parent MOF (H_2N-MIL-53(Al)) is thermally stable up to 400 ºC and stable in water and common organic solvents. The amino groups stabilize the Pd NPs and also prevent the agglomeration. The reactions proceeded very well with a broad variety of aryl bromides containing electron-withdrawing and electron-donating groups. Both the arylboronic acids with electron-donating (4-OMe-, 2-OMe-) and electron-withdrawing substituents (4-NO-, 4-CN-, 4-CF_3-, 4-CH_3CO-) produced good yields which decreased slightly for the sterically hindered arylboronic acids. Minor activity was observed for palladium supported MIL-53(Al) in the coupling of bromobenzene with phenylboronic acid under the same conditions. These catalytic results suggested that Pd/NH_2-MIL-53(Al) catalyst has high activity and good stability for the Suzuki-Miyaura cross-coupling reaction.

The reaction took place over the catalyst surface in a heterogeneous fashion and Pd NPs stabilized by the amine groups of the NH_2-MIL-53(Al) possessed a high chemical activity and good stability.

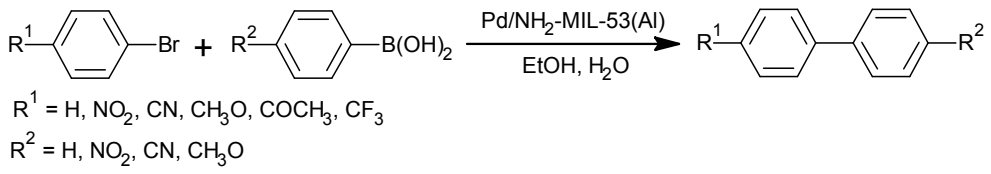

Scheme 13. Suzuki–Miyaura coupling reactions of different bromobenzene derivatives and arylboronic acid over supported palladium catalysts.

Park *et al.*[224] prepared the MOF-5(O_h) [$Zn_4O(bdc)_3$] from the reaction of $Zn(NO_3)_2$ with benzene-1,4-dicarboxylic acid (H_2bdc) in the presence of small amounts of 1,3,5-tris(4-carboxyphenyl)benzene (H_3btb), the structure of the new MOF is nearly alike to MOF-5, but has an octahedral morphology and a number of defect sites which are unique to functionalize with dangling carboxylates. This type defective MOF-5 produced by the above method is designated as MOF-5(O_h). Further, reaction of MOF-5(O_h) with $Pd(OAc)_2$ impregnate the metal ions, creating a heterogeneous catalyst (Pd(II)@MOF-5(O_h)) with surface area 2600 m^2g^{-1}. The Pd content of Pd(II)@MOF-5(O_h) was 2.3 wt.%. The catalytic activity of (Pd(II)@MOF-5(O_h)) toward C-H phenylation using diphenyliodoniumtetrafluoroborate has been examined (Scheme 14). The $Pd(OAc)_2$ catalyzed C-H arylation of naphthalene in nitrobenzene giving a total yield of 13% with 15:1 selectivity for the α-isomer over the β-isomer. Employing Pd(II)@MOF-5(O_h)) for longer reaction times (17 h) enhanced the yield slightly and lowered the selectivity (17% yield, α:β = 8:1).

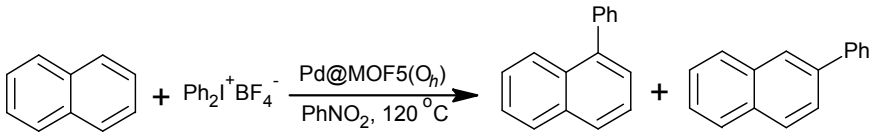

Scheme 14. Representation of .C-H arylation of naphthalene.

The amine-functionalized MOF $[Cr_3OF(H_2O)_2(bdc\text{-}NH_2)_3]\cdot nH_2O$ (NH_2-MIL-101(Cr)) was investigated for Pd NPs immobilization and tested for the Suzuki-Miyaura cross-coupling reaction.[225] Four different types of Pd@NH_2-MIL-101(Cr) were prepared with loadings of 4, 8, 12, and 16 wt.% Pd on NH_2-MIL-101(Cr). Excellent yield was achieved with 8% Pd@NH_2-MIL-101 (3 mol% Pd loading) without agglomeration of palladium. The structure of MIL-101(Cr) remained intact after Pd loading and no obvious changes were detected in PXRD patterns. To obtain optimum conditions for the coupling reaction, influence of temperature, bases, Pd loading, solvent and substrate polarity were investigated. The *p*-substituted phenyl bromides (*p*-methy, *p*-methoxy and *p*-ethoxy) were coupled within short reaction time (6 h in water and 30 minutes in water/EtOH) at room temperature. 2-

bromonaphthalene afforded 22% yield in water at ambient temperature and 97% after 2h in water/EtOH. This difference in yield is due to low solubility in water as compared to water/EtOH mixture. In case of bulky molecule, 9-bromoanthracene only a 19% yield was obtained. The coupling of arylchlorides with organic boranes required a higher temperature (80 °C) which disappointingly were more favorable for the formation of by-products (dehalogenation Ar-H and homocoupling Ar-Ar). The *p*-chlorobenzaldehyde and *p*-methoxyphenyl chloride reacted in water and good to excellent yields (70-99%) were obtained with little or no formation of by-products. Pd@NH_2-MIL-101(Cr) can be recycled 10 times without any change in catalytic performance.

Recently, Seayad *et al.*[226] reported a stable and active heterogeneous catalyst (Pd/ZIF-8) supported on ZIF-8 with polyvinyl alcohol (PVA) as stabilizer and hydrazine as the reductant. The Pd/ZIF-8 was used for the aminocarbonylation of both bromoarenes and iodoarenes in the presence of various amines under relatively mild operating conditions (Scheme 15). Further the scope of this aminocarbonylation reaction was extended to a wide variety of aryl bromides, amines and finally to different aryl iodides without the use of ligands. Aromatic primary amines and benzylamines (aniline 79% and benzylamine 68%) showed moderate yields compared with alkyl primary (*n*-hexylamine 84%), secondary (diethylamine 92%) and cyclic amines (morpholine 90%). In addition, the synthesis of a collection of pharmaceutically important compounds such as moclobemide (a generic drug), CX-546 (treatment of schizophrenia), procainamide (antiarrhythmic drug) and niketamide (a stimulant) was done successfully.

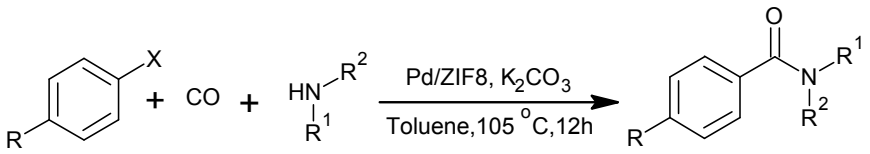

Scheme 15. Scope of the aminocarbonylation of aryl iodides with amines.

Yamashita and coworkers[227] immobilized the Pd NPs within the pores of metal organic frameworks [$Ti_8O_8(OH)(bdc)_6$] (MIL-125(Ti)) and amine-functionalized [$Ti_8O_8(OH)(NH_2$-

bdc)$_6$] (NH_2-MIL-125(Ti)) using ion exchange and photo-assisted deposition methods. There was no visible loss in homogeneity and crystallinity in XRD patterns after Pd loading suggesting that the integrity of MOFs frameworks retained. The resulting materials Pd/MIL-125(Ti) and Pd/NH_2-MIL-125(Ti) showed high efficient action for hydrogen production from formic acid (FA) at ambient temperature in comparison to titanium-based porous materials (Pd-TS-1 or Pd-TiMCM-41). Pd/NH_2-MIL-125(Ti) displayed the best catalytic performance generating 48.1 μmol and Pd-MIL-125 produced 17.8 μmol, in contrast to Pd NPs on Ti-containing porous support materials, namely, TS-1 and Ti-MCM-41 (Pd-TS-1 or Pd-TiMCM-41) generating only 1.7 μmol and 5.1 μmol, respectively (Fig. 18). The results showed that the average size of Pd NPs was not the most essential factor in attaining the high catalytic activity; it essentially was caused by the amine functional groups (Fig. 19). The amine groups in MOFs are known to prevent agglomeration of metal NPs, and the presence of amine enhance the catalytic activity for FA decomposition in other systems. The amine functionalized NH_2-MIL-125(Ti) is beneficial for an increased durability of the MOF in an aqueous environment.

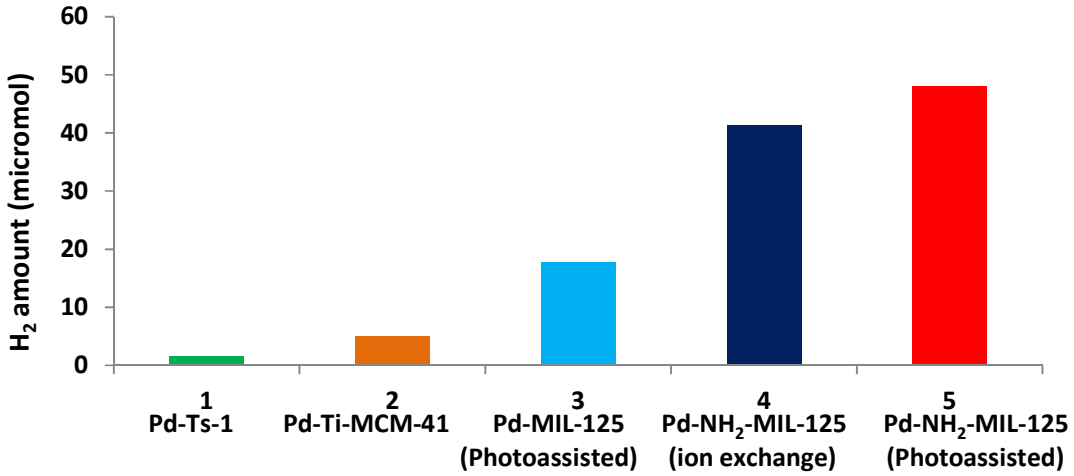

Fig.18 Generation of H_2 from formic acid using different Pd supported MOFs and Ti-containing porous supports. Reprinted with permission from ref. [227]. Copyright 2013 American Chemical Society.

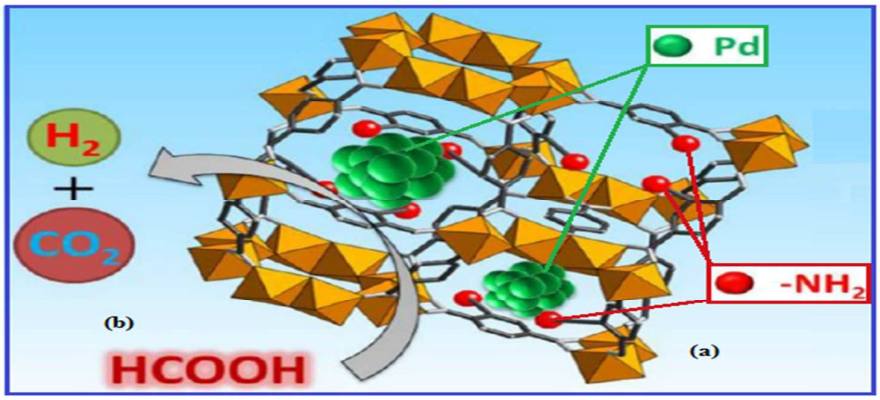

Fig. 19 (a) Schematic representation of Pd nanoparticles immobilized within pores of NH_2-MIL-125and (b) hydrogen production from formic acid (FA). Reprinted with permission from ref. [227]. Copyright 2013 American Chemical Society.

Upon investigating the selective hydroformylation of olefins with the highly porous and crystalline MIL-101(Cr) and rhodium supported MIL-101 (Rh@MIL-101), the later showed high activity.[228] In the hydroformylation of *n*-alk-1-enes, high conversion and selectivity to the corresponding *n*-aldehydes was achieved with rhodium loaded MIL-101(Cr). Total conversion of 33-55% after 1 h of reaction and 90% after 3 h of reaction was achieved for all used alkenes. The conversion decrease systematically in order: *n*-hex-1-ene > *n*-dec-1-ene > *n*-dodec-1-ene > *n*-oct-1-ene > *n*-hexadec-1-ene, after 1 h of reaction. Very low conversion was achieved with bulky *n*-hexadec-1-ene compared to *n*-dodec-1-ene. Structure selectivity was observed due to the catalytic active rhodium species located at the internal framework sites, and thereby conversion of bulky olefins to aldehydes was very slow.

MOFs and coordination polymers can also be used as heterogeneous single-site hydrogenation catalysts with loading of noble metals such as Rh^{1+}, Pd^{0}, Pd^{2+}, Pt^{0}, Pt^{2+} *etc.* A series of Pd@MIL-101(Cr) catalysts with different Pd loadings were prepared by incorporation of Pd NPs into the highly porous and hydrothermally stable MOF (MIL-101(Cr)) *via* an incipient-wetness impregnation method.[229] These catalysts were screened for the hydrogenation of 2,3,5-trimethylbenzoquinone (TMBQ) to 2,3,5-trimethylhydroquinone (TMHQ) into a high-pressure batch reactor (Scheme 16). The catalytic results revealed that the action of the MIL-101(Cr) catalysts was intimately associated with the Pd loading (1.0-2.0 wt.%) in MIL-101(Cr). Pd/MIL-101(Cr) gives 90% while Pd/C gives 65% yield of

TMHQ. The 2.0 wt.% Pd/MIL-101(Cr), displayed highly efficient catalytic activity and selectivity with excellent reusability amongst the other catalyst used for the above hydrogenation. In comparison with Pd/C catalyst that is currently used in the industrial hydrogenation of TMBQ to TMHQ, Pd/MIL-101(Cr) showed superior properties in terms of catalyst activity and stability, bringing a new opportunity for its industrial application.

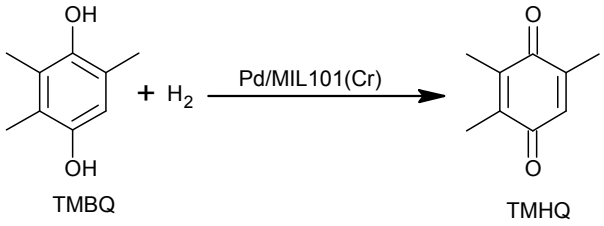

Scheme 16. Catalytic hydrogenation of TMBQ to TMHQ using Pd/MIL-101(Cr).

Isaeva *et al.*[230] studied the stereoselective hydrogenation of 2-butyne-1,4-diol into *cis*-2-butene-1,4-diol, using Pd supported MOFs such as MOF-5, IRMOF-3, and [Zn(pz25dc)$(DMF)_2$] (pz25dc = pyrazine-2,5-dicarboxylate) and host-guest materials (MOF-5) containing encapsulated calix[4]arenes of different structures used for Pd deposition. The use of MOFs for palladium deposition permitted controlling the catalytic performance in the selective partial hydrogenation of alkynes. High stereoselectivities were obtained with Pd loaded MOF-5 with respect to (2*Z*)-but-2-ene-1,4-diol (approximately 97%) (*cis*-2-butene-1,4-diol) and only a small amount of 4-hydroxybutanal was observed (around 1%) (Scheme 17). On further hydrogenation with a second mole of hydrogen, parallel reactions took place; *cis-trans* isomerization (2*E*)-but-2-ene-1,4-diol) and double bond shift (4-hydroxybutanal). With IRMOF-3 and a novel host–guest material containing calix[4]arene with nitrile groups as the Pd carriers, optimum ratio of alkynes/alkenes hydrogenation rates were achieved. Over Pd loaded IRMOF-3, isomerization of (2*Z*)-but-2-ene-1,4-diol into (2*E*)-but-2-ene-1,4-diol) and double bond shift was entirely avoided. X-ray fluorescence spectroscopy results showed no Pd leaching during the hydrogenation and XRD investigations confirmed the retention of MOFs structure after Pd deposition and also after catalysis. The catalyst stability was tested in three consecutive cycles and no deactivation in catalytic activity was observed.

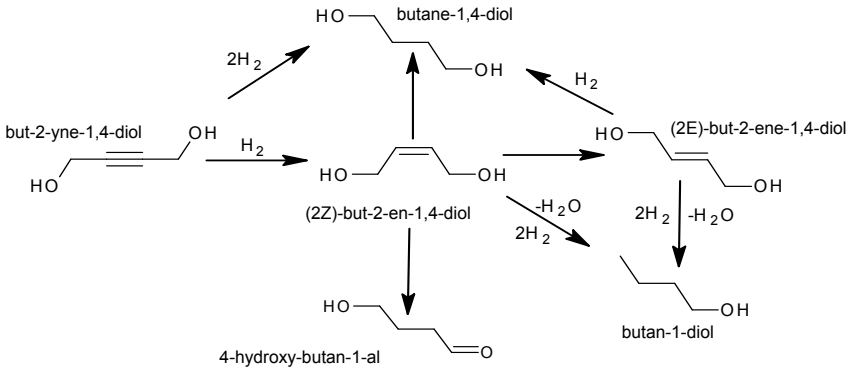

Scheme 17. 2-Butyne-1,4-diol hydrogenation.

MOF-5 is one of the representative MOFs having a BET surface area ranging from 260 to 4400 m^2g^{-1} based on the synthetic method and has a good thermal stability up to 400 °C. Zhao *et al.,* described the deposition of Ni NPs on MOF-5 by a facile wet impregnation strategy to prepare Ni/MOF-5.[231] Ni/MOF-5 exhibited an excellent catalytic activity for the hydrogenation of C=C bond. Using (2*E*)-but-2-enal (crotonaldehyde) as a probe molecule under mild reaction conditions conversion > 90.0% and selectivity > 98.0% was obtained (Scheme 18). By contrast, industrial catalyst Ni/SiO_2 showed only 83.06% conversion with 94.38% selectivity of butanal (butyraldehyde) under the same reaction conditions. Butan-1-nal was the main product with a small amount of butan-1-ol, but (2*E*)-but-2-en-1-ol (crotyl alcohol) was not detected.

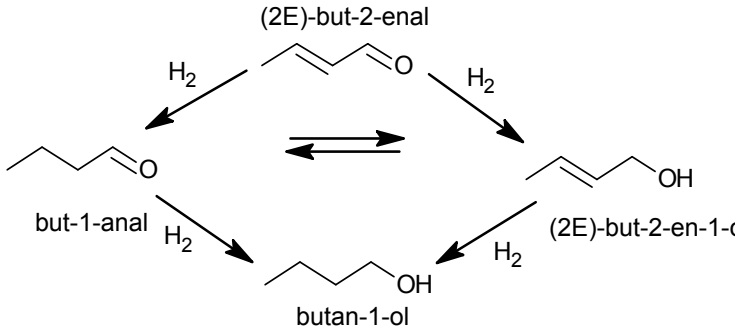

Scheme 18. The products of selective hydrogenation for crotonaldehyde.

Masoudinia and coworkers reported for the first time the development of a new efficient vanadium loaded $[Cr_3OF(H_2O)_2(bdc)_3]\cdot nH_2O$ (MIL-101-(Cr)), featuring a well-defined 3D, mesopore nano-rod structure exhibiting a very high catalytic activity for the oxidation of sulfides to sulfoxides and sulfones.[232] With this catalytic system, good to high yields of

oxidation products (78–98%) were obtained in desired times (0.5–3 h) indicating the high effectiveness of V@MIL-101(Cr) catalyst. V@MIL-101(Cr) also catalyzed the oxidation reaction of methylphenylsulfide and benzaldehyde at room temperature leading to the selective formation of methylphenylsulfoxide in good yield, whereas benzaldehyde remained unaffected. In addition, the use of V@MIL-101 makes this method simple, cost-effective, and attractive.

Liao *etal.*[233] reported the first example of using ZIF-8 as a host for preparing metal-oxide NPs (Co_3O_4) by a facile liquid-phase method. ZIF-8 was selected because it holds an intersecting 3D channel system, a large pore size (11.6 Å in diameter), and high thermal stability (>500 °C in N_2) as well as good chemical resistance to water and organic solvents. First, $Co(NO_3)_2{\cdot}6H_2O$ was introduced into the ZIF-8 by an impregnation method, the resulting composite that is designated as Co_3O_4@ZIF-8. ZIF-8 host was then removed by pyrolysis at 600 °C for 5 h under air. For the removal of ZnO which was formed from the decomposition of ZIF-8, remaining powder was dispersed in an NH_4Cl (5M)-$NH_3{\cdot}H_2O$ (2.5 M) aqueous solution. The nano metal oxide Co_3O_4 showed good catalytic activity and long-term stability in the low temperature oxidation of CO.

8.1 MOF as heterogeneous bimetallic NP catalyst

Over the past two decades, research efforts have been designed to plan novel MOF structures and studying their applications in molecular (gas) storage and separations/purifications.[234, 235] Because of the exceptional high surface area, porosity, and chemical tunability of MOFs, their logical application, especially when metal nanoparticles (MNPs) are embedded into their pores, becomes definite for the solid-state/heterogeneous catalysis[217, 236] To date, relatively scant data are available on MOF-supported bimetallic alloy NPs as catalysts for heterogeneous reactions. Moreover, it has been observed that due to the synergistic alloying effect of two metals, the catalyst displayed higher activity than their mono-metallic analogues.[237]

Gu *et al.*[238] employed a porous MOF (MIL-101(Cr)) and its amine grafted counterpart ethylenediamine (ED) as supports for preparing bimetallic NP catalysts. The bimetallic NP containing MOF were used as highly proficient catalysts in the generation of hydrogen from formic acid for chemical hydrogen storage. Pd/ED-MIL-101, Ru/Pd-MIL-101, Pt/ED-MIL-101 and Au/Pt/ ED-MIL-101 released 58, 14, 10, and 14% hydrogen from formic acid at 90 °C, respectively. MIL-101 and ED-MIL-101 were inactive at all for the decomposition of formic acid. Both Au-Pd/ED-MIL-101 and Au/Pd-MIL-101 also exhibited a high selectivity (100%) for dehydrogenation of formic acid.

Long *et al.*[239] demonstrated that bimetallic Au/Pd NPs immobilized to MIL-101(Cr) are active and selective in the oxidation of a variety of saturated C-H bonds (including primary, secondary, and tertiary) with molecular O_2. For the liquid-phase oxidation of cyclohexane, a conversion exceeding 40% was obtained (TOF: 19,000 h^{-1}) with > 80% selectivity to cyclohexanone and cyclohexanol under mild conditions. Moreover, due to the synergistic alloying effect of Au/Pd, the catalyst displayed higher activity than their mono-metallic counterparts and Au+ Pd physical mixture.

9. Synthetic chemical modification

Recently, the synthetic chemical modifications have been performed for decorating the MOF. By this technique, it is possible to introduce certain functionalities that are impossible or difficult to include through orthodox synthetic methods. MOFs can be functionalized *via* their metal nodes or organic linkers through whether pre-synthetic; the self-assembly of the MOF with the functionality already present [8] or post-synthetic approaches; the post-synthetic modification of the MOF after self-assembly network.[240] The chemical alteration of MOFs in the porous channels was first reported in 2000 by Kim *et al.*[241] in which the *N*-alkylation of the pyridyl groups in the MOFs occurred by adding an excess amount of iodomethane to a suspension of crystalline porous MOF material at room temperature, with the pore volume of

the MOF shrinking by 14%. Subsequently, many studies focused on different types of chemical modifications. An overview of these efforts is provided as follows.

9.1 Post-synthetic modification

Post-synthetic modification (PSM) of MOFs is a process in which framework species undergo chemical transformations while the overall framework structure is retained and even most of the time crystallinity is retained.[242, 243] PSM of MOFs assists the construction of novel MOFs with new physical and chemical properties that are not observable in original MOFs. Post-synthetic methods are synthetic alternative tools to achieve metal-binding sites or functional organic sites or both in MOFs. In this method, the metal ion and organic linkers are carefully selected to fabricate a MOF with favorable attributes capable enough to undergo modification, thereby a MOF can be further tuned after self-assembly.[146, 244-246]

Koner *et al.*[247] designed a new heterogeneous catalyst IRMOF-3-PI-Pd for a carbon-carbon coupling reaction by anchoring a Pd(II) Schiff base moiety into microporous MOF (IRMOF-3) in a post-synthetic method with pyridine-2-aldehyde (Fig. 20). The catalyst showed high activity toward the Suzuki and Stille cross-coupling reaction under mild reaction conditions. In case of Suzuki cross-coupling reaction, non-substituted iodobenzene and bromobenzene showed a comparable yield, which were higher than chlorobenzene. The reactivity of aryl bromides with electron-withdrawing substituents (CHO-, $COCH_3$-, NO_2-, CN-, COOH-, X-) was higher than that of electron-donating substituents (OH-, OMe-, NH_2-). The sterically hindered *ortho*-substituted substrate *o*-nitrobromobenzene gives a good yield of 2-nitrobiphenyl. For Stille cross-coupling reaction, desired products were obtained in good yields and TOFs of the reactions were high. Similar trends of reactions were observed as in the case of Suzuki reactions but the overall performance of IRMOF-3-PI-Pd in the Suzuki cross-coupling reaction was superior to the Stille cross-coupling reaction. In order to check the stability of catalyst, the recovered catalyst from both reactions was subjected to PXRD, FT-IR, and gas adsorption studies. Comparison of XRD, FT-IR and gas adsorption analysis

of fresh MOFs and the recovered one demonstrates the structural integrity of the catalyst retained after reactions.

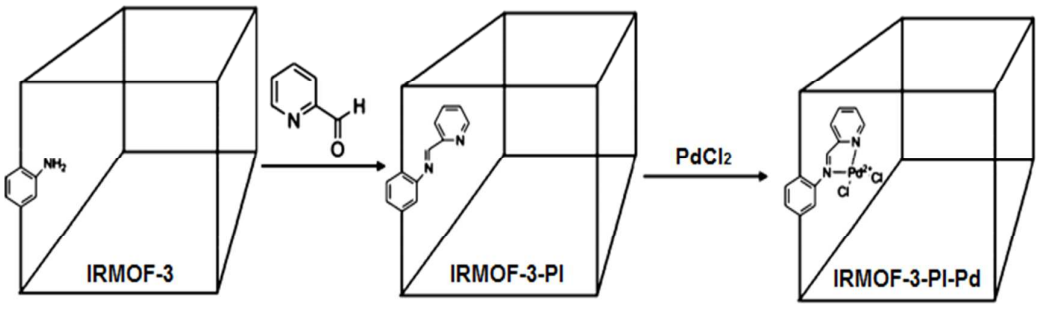

Fig. 20 Schematic demonstration of PSM of post-synthesis modification of IRMOF-3. Reprinted with permission from ref. [247]. Copyright 2013 American Chemical Society.

Wang *et al.*[22] prepared porous MOFs having general formula $[Zr_6(bpdc)_{6-x}(L)_x]$, by incorporation of Ir, Re, and Ru complexes into a porous MOF $[Zr_6O_4(OH)_4(bpdc)_6]$ (UiO-67) with a combination of 4,4-biphenyldicarboxylate (h_2bpdc) and ligands (H_2L_1-H_2L_6) (Fig. 21) in DMF at 100 °C. The MOFs obtained were phosphorescent and were employed in three photo-catalytic organic transformations (aza-Henry reaction, aerobic amine coupling, and aerobic oxidation of thioanisole) with very high activities. Post functionalized MOFs were efficient photo-catalysts for the aza-Henry reaction of tetrahydroisoquinoline and substituted tetrahydroisoquinoline (bromo and methoxy) with nitromethane (Fig. 22). The catalysts effectively catalyzed aerobic oxidative coupling of a series of primary amines (aniline, *p*-methylaniline and *p*-methoxyaniline) with 46-90% conversions within 3 hours. The photocatalyzed aerobic oxidation of thioanisole to methyl phenyl sulfoxide was also examined. A 72% conversion after 22 h was obtained which was comparable to that of corresponding homogeneous system (H_2L_6). The PXRD patterns of catalysts after the reaction were identical to that of fresh MOFs, indicating its stability under reaction conditions.

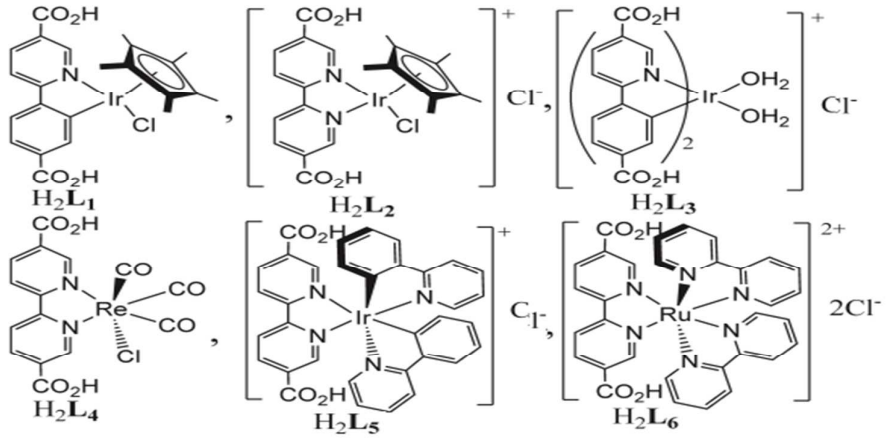

Fig. 21 Chemical structures of Ir, Re, and Ru complexes with ligands (H_2L_1-H_2L_6). Reprinted with permission from ref. 22. Copyright 2013 American Chemical Society.

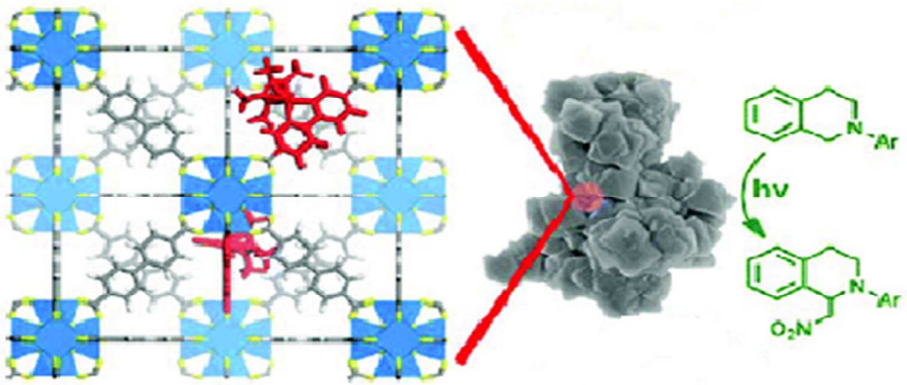

Fig. 22 Porous MOF [$Zr_6(bpdc)_{6-x}(L)_x$]and representation of catalytic behaviors. Reprinted with permission from ref. 22. Copyright 2011 American Chemical Society.

Cohen addressed a new sequential post functionalization method for the incorporation of carboxylic functionalities in NH_2-MIL-53(Al) by using different cyclic and aliphatic anhydrides (Fig. 23) and finally evaluated their catalytic activities for the methanolysis of epoxides.[248] The carboxylic acid groups residing in the framework were used as Brønsted acid catalytic sites for the methanolysis of epoxides. NH_2-MIL-53(Al)-AMMal facilitated the ring-opening of cyclopenteneoxide, cyclohexene oxide, styrene oxide, and *trans*-stilbene. Other carboxylate functionalized MIL possessing a weaker acidic group, NH_2-MIL-53(Al)-AMSuc, NH_2-MIL-53(Al)-AM1, and NH_2-MIL-53(Al)-AMCort did not carry out the same catalysis. The difference in catalytic activity originates from the difference in the acidity of the carboxylic acids. Unlike the succinic acid functionality, the maleic acid functionality contains a conjugated C=C bond, which stabilize the conjugate base resulting in higher acidity. Unfortunately, the recycled catalyst showed a significant reduction in catalytic

activity (95% compared to 10%) due to esterification of the carboxylic group which is due to MOF exposure to a large excess of methanol during the reaction.

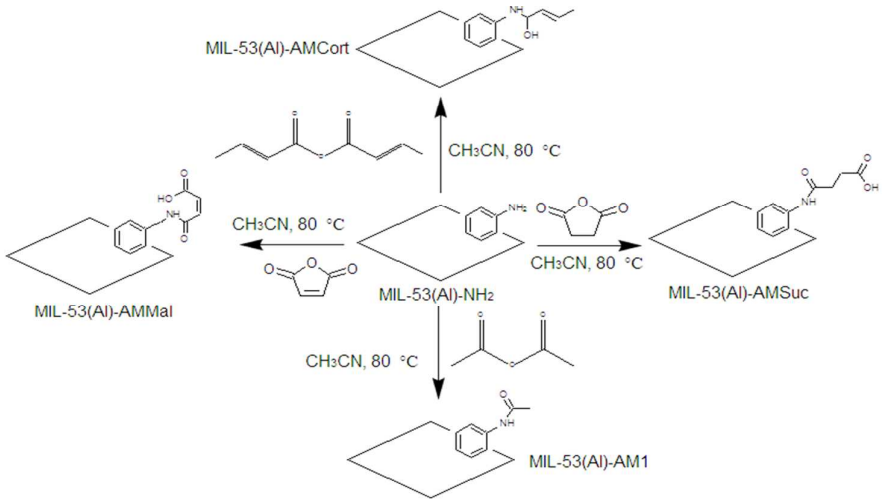

Fig. 23 Post-synthetic modification reactions performed on NH_2-MIL-53-(Al). Reprinted with permission from ref. [248]. Copyright 2011 American Chemical Society.

Iglesias and coworkers[249] developed an easy and efficient method for the synthesis of *N*-alkyl amines *via* reductive amination of aldehydes in the presence of hydrogen using a new hybrid catalysts IRMOF-3LIr and UiO-66-NH_2LIr (Ir = iridium; L = 6-((diisopropyl-amino)methyl) picolinaldehyde) that combines the catalytic activity of transition metal complexes with MOFs (IRMOF-3 and UiO-66-NH_2) (Fig. 24). IRMOF-3LIr and UiO-66-NH_2LIr were prepared by treating IRMOF-3 and UiO-66-NH_2 first with 6-((diisopropyl-amino)methyl) picolinaldehyde and then with an iridium complex $[IrCl(cod)]_2$. The stability of IRMOF-3LIr and UiO-66-NH_2LIr was examined by TGA. The modified MOFs showed thermal stabilities comparable to that of parent MOFs with decomposition temperatures near 350 °C in air. Under optimized reaction conditions, the scope of the reaction was explored with structurally and electronically varied aldehydes and diverse nitroarenes. Irrespective of the electronic nature of the substituents, aromatic aldehydes reacted sound to give the corresponding products. This procedure can be used to create a variety of N-alkyl amines in good to excellent yields. The simple catalyst preparation procedure, easy recovery, and reusability are expected to contribute its utilization for the development of benign chemical processes and products.

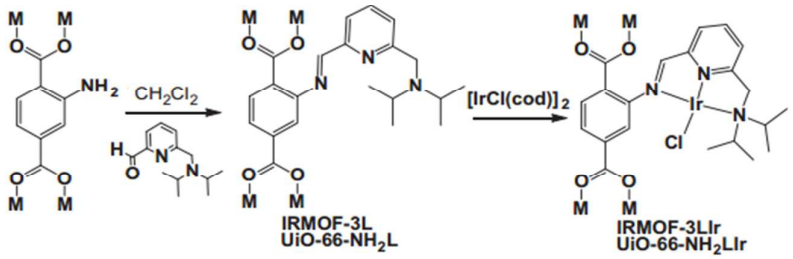

Fig. 24 Schematic representation of post-modification of IRMOF-3 and UiO-66-NH_2. Reproduced from Ref. [249].

A new sequential post-functionalization method was established by Juan-Alcaniz *et al.* for the incorporation of catalytic active metal complexes and NPs in MOFs.[250] In the first post-synthetic step, $[Cr_3OF(H_2O)_2(NO_2\text{-bdc})_3]\cdot nH_2O$ (NO_2-MIL-101(Cr)) was prepared under acidic conditions then reduction of the NO_2 moieties lead to the formation of $[Cr_3OF(H_2O)_2(NH_2\text{-bdc})_3]\cdot nH_2O$ (NH_2-MIL-101(Cr)). The second functionalization step consists of condensation of the amino groups of the ligand with ethyl chloro-oxoacetate, resulting in free oxamates attached to the organic linker. $Cu(NO_3)_2{\cdot}2.5H_2O$ and ED have been coordinated through the oxamate ligand, attaining loadings as high as 9 wt.%. [Cu/PMA-MIL-101(Cr)] and [CuEDA/PMA-MIL-101(Cr)] showing similar performance as the best reported copper MOFs (HKUST-1, $[Cu(2\text{-pymo})_2]$ and $[Cu(im)_2]$) in ‘‘click chemistry’’ catalysis (1,3-dipolar cycloaddition). Both catalysts yielded 100% conversion after 4 hour in ethanol and toluene as solvent. The catalysts were also active in propargylamine formation, achieving 60% conversion of phenyl acetylene after 17 h. The 6 wt.% loaded palladium-containing MOFs were tested for their catalytic activity in Suzuki-Miyaura coupling reaction of bromobenzene and phenyl boronic acid. A 60% bromobenzene conversion was achieved after 24 h with TOF value in the order of 10 h^{-1}.

Telfer[251] presented a thermo labile protecting group strategy for organ catalytic MOFs. The organo catalytic units are protected by a thermo labile protecting group during MOF synthesis and then unveiled by a simple post-synthetic heating step. By using *tert*-butoxycarbonyl protecting group for a proline moiety, the removal of which endows the resulting cubic Zn-IRMOF with a catalytic activity for aldol reaction of acetone and cyclopentanone with 4-nitro-benzaldehyde. Kristine *et al.*[65] introduced four metalated MOFs

(UMCM-1-AMlnpz, UMCN-1-AMlnsal, UMCM-1-AMFesal and UMCM-1-1AMCupz) by modifying the parent MOF (UMCM-1-NH_2) (UMCM = University of Michigan Crystalline Material) with different combinations of chelating groups and metal ions (Fig. 25). The four MOFs were analyzed by PXRD, TGA and N_2 gas adsorption. The PXRD patterns of modified MOFs were found to be identical to the parent MOF, indicating that the metalation had no effect on the structural stability of MOF. TGA results showed that the UMCM-1-AMlnpz and UMCN-1-AMlnsal were stable up to 400 °C. The MOFs were examined for *β*-azido and *β*-amino alcohol synthesis with epoxides of various sizes and shapes with two different nucleophiles, aniline and $TMSN_3$. MOFs, UMCM-1-AMlnpz, and UMCN-1-AMlnsal, act as robust, single-site catalysts with distinct selectivity for ring opening reactions of peroxides. Out of these four MOFs, the UMCM-1-AMlnpz displayed the highest conversion (78%), while UMCM-1-AMInsal, UMCM-1-AMFesal and UMCM-1-AMCupz showed appreciably poorer conversions of 56%, 30% and 11%, respectively. The PXRD patterns after catalysis indicated that the MOFs maintained their structural integrity.

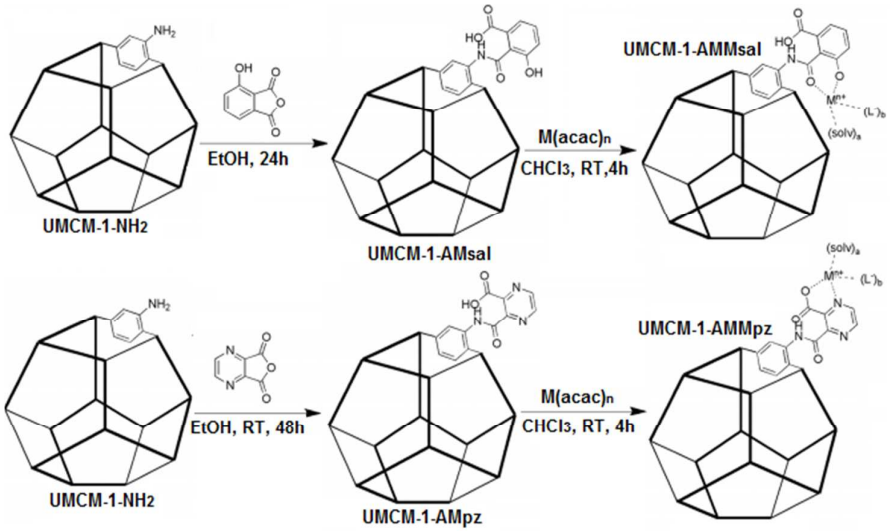

Fig. 25 Synthesis and post-synthetic modification of UMCM-1-NH_2. Reprinted with permission from ref. [65]. Copyright 2010 American Chemical Society

Four DAAP-MOFs were prepared by complexation of porous materials based on MOF (MIL-101(Cr)) with dialkylaminopyridines (DAAP) which were tested for the hydrolytic degradation of organo phosphorous esters such as diethyl-4-nitrophenyl phosphate (paraoxon) (Fig 26d).[252] MIL-101(Cr) has a 3D network of Cr atoms connected through

benzene dicarboxylate groups and generates two kinds of mesoporous cages that are accessible *via* 5 or 6 member ring windows. Two cages are built on a μ_3-O bridged trimeric Cr(III) cluster connected to three carboxylate moieties and one remaining coordination site occupied by a water molecule (Fig 26abc). The result shows that the catalytic activity of MOF-DAAP is 7 and 47-fold higher than the MIL-101 and DAAP, respectively. They proposed a mechanism for this hydrolytic reaction, where two reactive center *i.e*., Lewis-acid Cr(III) and electron-rich nucleophile (DAAP) are coordinately combined in one catalytic system, and the synergistic activation by the two reactive centers gave rise to a high reaction rate. This work introduced a promising approach toward formation of multifunctional MOF catalysts for various chemical transformations. The substrate selectivity observed with the MOF catalysts were distinct from those found with purely homogeneous catalysts. It illustrates clearly that the MOF pores create a specific environment for catalysis that can be used to generate novel patterns of selectivity. These results showed that PSM can be used to prepare energetic, selective, and robust catalysts.

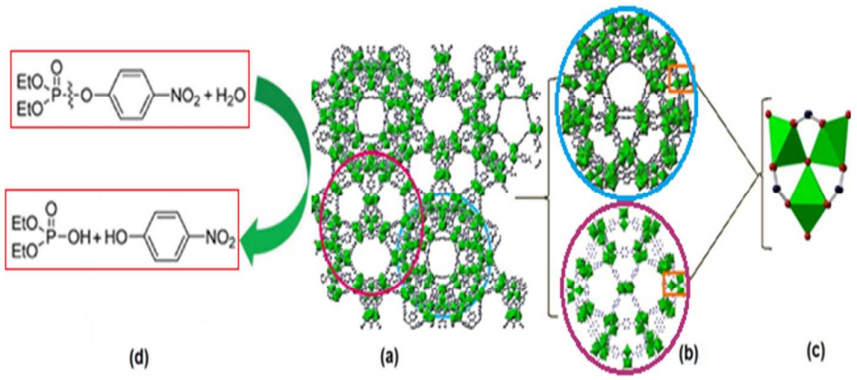

Fig. 26 Schematic representation of (a) unit cell of MIL-101 (b) polyhedral model view of two cages (c) unsaturated metal sites (Cr(III)cluster) (d) catalytic hydrolysis of paraoxon. Reprinted with permission from ref. [252]. Copyright 2013 American Chemical Society.

9.2 Post-synthetic exchange and post-synthetic deprotection

Synthetic modification refers to chemical transformations of the organic struts in MOFs to either unmask reactive functionalities [251, 253] or introduce functional groups [254] which are not created during the MOF synthesis and has become a familiar approach to engender extended frameworks. These include methods such as post-synthetic modification (PSM),[255, 256] post-

synthetic deprotection (PSD)[257] and post-synthetic exchange (PSE) (also termed SALE = solvent-assisted linker exchange).[258-262] In contrast, SALE allows the exchange of struts in readily accessible MOFs to construct frameworks with additional chemically diverse and useful properties. [258, 263] Both PSE and PSD have proved to be efficient approaches to access MOFs that could not be directly synthesized under solvothermal conditions. Compared with PSD, PSE is better. Because, in PSD deprotection protocols involve harsh experimental conditions that may demean the MOFs. In most cases, isolated metal-monocatecholato moieties have been achieved in a highly robust MOF by using these two fundamental post-synthetic strategies and were applied to catalyze the oxidation reactions and aromatizing ring-closing metathesis.

Nguyen and coworkers[264] constructed a V-CatBrO MOF through a combination of protecting groups (Me-, TBDMS-, *o*-NBn-, BOC-), post-synthetic deprotection (light or heat) and post-synthetic metallation with $VO(acac)_2$ (vanadyl acetylacetonate). TGA of prepared MOFs suggests that they have large solvent-accessible pores and high thermal stability (decompose at 450 °C). The as-synthesized MOFs were used for benzylic oxidation of a large substrate such as tetralin in the presence of TBHP as oxidant (Fig. 27). Tetralin was oxidized to tetralol and tetralone (1:3 molar ratios) at 45% total conversion in 24 h at 50 °C in chlorobenzene with minimal metal leaching in a non-coordinating solvent. This activity is equivalent to that of the homogeneous $VO(acac)_2$, whose products include more of the over-oxidized product tetralone (1:11 tetralol:tetralone) at comparable overall total conversion.

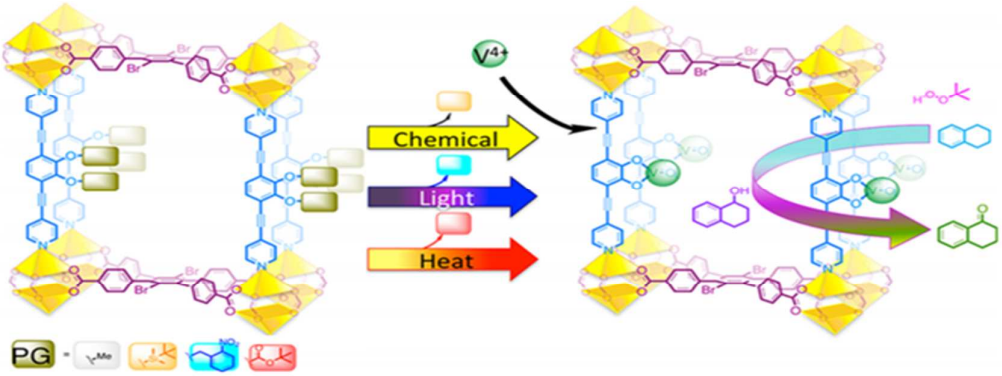

Fig. 27 A Schematic illustration of the synthesis of V-CatBrO MOF *via* postsynthesis. its deprotection followed by metallation. Reprinted with permission from ref. [264]. Copyright 2013 American Chemical Society.

Recently, Cohen[265] introduced metal-monocatecholato moieties in a highly robust MOF (UiO-66), by using two fundamentally different post-synthetic strategies (PSD and PSE). Metallation of the catechol functionality residing in the MOFs resulted in exceptional Fe-monocatecholato and Cr-monocatecholato species UiO-66-M-CAT (M = CrIII and FeII). The chemical robustness of UiO-66-Cr-CAT was confirmed by its incubation in aqueous solution for 24 h and its thermal stability up to 250 °C was also evidenced by TGA. As compared with PSD, PSE was a more facile and efficient functionalization approach to access MOFs that could not be constructed directly under solvothermal conditions. Secondary alcohol oxidation was studied with 2-heptanol as the test substrate using 1.3 equiv. of TBHP as an oxidant and chlorobenzene as a solvent at 70 °C (Fig. 28). Further the scope of reaction was extended to a wide variety of alcohols. Excellent yields (70-99%) were obtained with different secondary alcohols, including aliphatic, cyclic, and benzylic alcohols. Even a complex substrate 5*α*-cholestan-3*β*-ol was oxidized to the corresponding ketone in 12 h providing 99% yield.

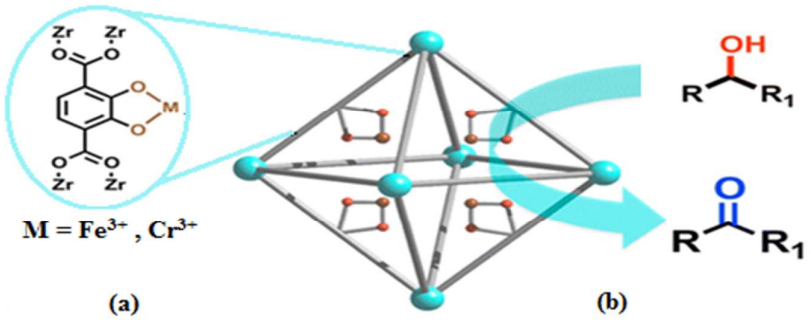

Fig. 28 Structure of UiO-66-CrCAT and UiO-66-FeCAT and oxidation of secondary alcohol. Reprinted with permission from ref. [265]. Copyright 2014 American Chemical Society.

For metathesis different metal complexes have been used, mostly ruthenium-based catalysts are highly valid such as first and second-generation Hoveyda-Grubbs catalysts, Grubbs' 1st generation catalyst and its NHC coordinated derivative.[266-268] Recently, Hupp[269] studied the use of Ru-based olefin metathesis catalyst inside a MOF to carry out a solid-state reaction in a post-synthetic fashion that cannot be accomplished in the solution phase. Br-YOMOF obtained from $Zn(NO_3)_2$ and two organic components: the tetracarboxylic acid ligand which forms 2D sheets with Zn^{2+} dimers and the dipyridyl strut which links the 2D sheets by

coordinating to the zinc paddlewheel clusters forming perpendicular pillars separating the 2D layers. By the use of SALE, tetravinyldipyridyl struts were incorporated into the Br-YOMOF architecture resulting in the production of solvent-assisted linker exchange MOF-14 (SALEM-14). In a dichloroethane (DCE) solution, exposure of SALEM-14 to the first generation Hoveyda-Grubbs (HG) catalyst at 120 °C led to the formation of the PAH-MOF-1 (Fig. 29). The MOF in SALEM-14 prevented the intermolecular olefin metathesis between the pillars in the presence of the first generation Hoveyda-Grubbs catalyst and favored the production of a polycyclic aromatic hydrocarbon (PAH), which can be released from PAH-MOF-1 under acidic conditions in dimethylsulfoxide. The main advantage of this kind of metathesis is that the MOF in SALEM-14 prevented the intermolecular olefin metathesis between the pillars in the presence of the first generation Hoveyda-Grubbs catalyst and favored the intramolecular olefin metathesis to get desired polycyclic aromatic hydrocarbons (PAH). The 2nd generation Hoveyda-Grubbs catalysts did not give the desired PAH. Due to combination of post-synthetic modification and solvent-assisted linker exchange (SALE) inside MOF, this kind of intramolecular chemical transformation became possible.

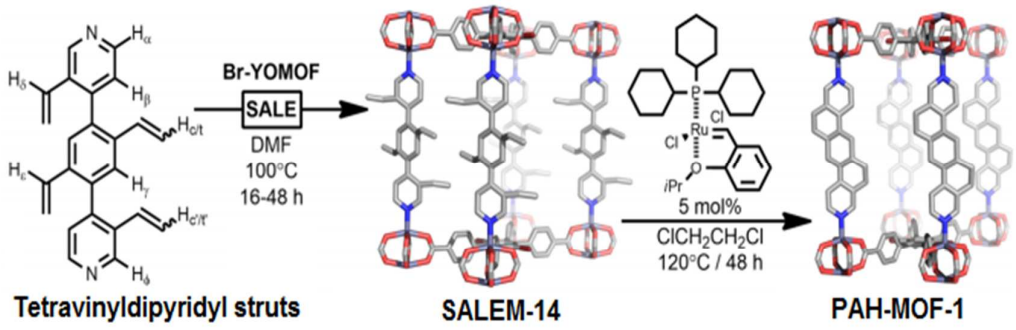

Fig. 29 Synthesis of SALEM-14 and Olefin Metathesis of tetravinyldipyridyl and SALEM-14. Reprinted with permission from ref. [269]. Copyright 2013 American Chemical Society.

Hupp *et al.*[263] also evaluated the systematic exchange of pillaring linkers as a means of accessing new versions of these materials. Dipyridyl-porphyrin Zn(II) (Zn-dipy) struts were replaced by M^2-dipy (M^2 = $2H^+$, Al(III), Sn(IV)), forming crystalline solid solutions of $Zn(Zn_{1-x}M_x)$RPM in variable ratios. In addition, post-synthetic metallation was done using Zn_2H-RPM, again with retention of crystallinity. The catalytic activity was tested for a

styrene oxide ring-opening reaction by trimethylsilylazide ($TMSN_3$). The conversion of styrene to the azide was 60%, with selectivity for the less hindered products.

Recent research has proved that synthetic modification of MOFs can be achieved and this strategy facilitates the generation of new MOFs with new physical and chemical properties that are not observable in the original robust MOFs. Given that, the large number of MOFs reported in the literature, and the vast number of suitable organic reactions accessible, there is a large scope for the marvelous opportunities to expand the systematic post-synthetic modification of MOFs regarding the catalytic protocols. These would lead to the ability to incorporate the additional functionalities, create diversity, and smart materials that can sense, transform certain guests, and change their physical properties.

9.3 Hydrophobization

Water poisoning is an often-encountered question in catalysis.[270-272] Indeed, catalytic reactions can be hindered or just limited due to poisoning effects originating from moisture in the air or from the water formed as the reaction product. Water molecules are irrevocably adsorbed on the catalytic sites, leading to catalyst deactivation. Hydrophobic properties can easily be integrated within a MOF. The inclusion of medium to long alkyl groups within MOF, shields the moisture-sensitive MOFs by turning it into a hydrophobic material. For example, the introduction of a methyl group coordinating with a nitrogen atom of the bipyridine-pillar linker in a carboxylate-based bridging MOF, shielded the metal ions from being attacked by water molecules, and thus, improving appreciably the water resistance of the MOF structure.[273] These hydrophobic groups can also protect MOFs from degradation upon contact with water. Cohen *et al.*[272] have tailored IRMOF-3 and [Al(OH)(bdc)] (MIL-53(Al)) by treatment with different alkyl anhydrides and finally determined their contact angle to observe the hydrophobic/philic properties of these materials. IRMOF-3-AM(1-5), IRMOF-3-AM*i*Pr, IRMOF-3-AM*i*Bu, MIL-53(Al)-AM-1, 4, 6 were prepared (Fig. 30). To evaluate changes in the moisture stability and hydrophobicity of the materials upon PSM, each sample of modified MOF was exposed to ambient air and immersed in water and finally

characterized using contact angle measurements, PXRD and SEM. The contact angle measurements proved that the incorporation of hydrophobic groups to IRMOF-3 and MIL-53(Al) stabilizes them to ambient air and direct contact with water. Among modified hydrophobic MOFs, IRMOF-3, IRMOF-3AMiPr showed high hydrophobicity and MIL-53(Al)-AM-4 and MIL-53(Al)-AM-6 presented to be super hydrophobic than others.

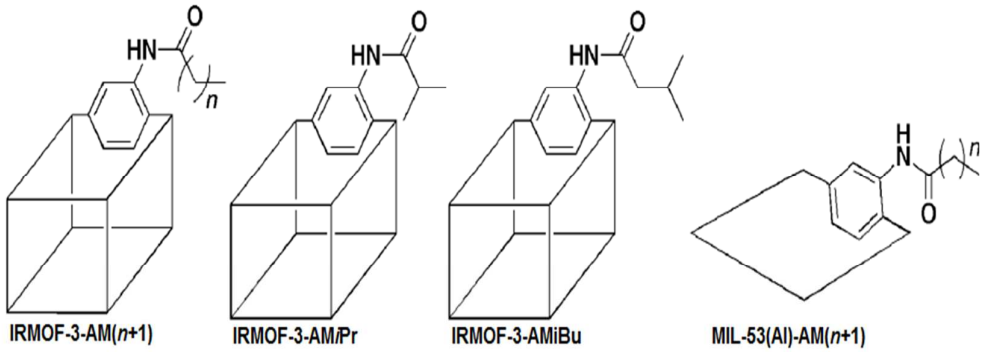

Fig. 30 Schematic representations of PSM of the IRMOF-3 and MIL-53(Al). Reprinted with permission from ref. [272]. Copyright 2010 American Chemical Society.

In order to prevent water-induced catalyst poisoning, Farrusseng developed a new water-repellent MOF by post-synthetic modification of SIM-1 (SIM = Substituted Imidazolate Material) with long alkyl chains into the very hydrophobic SIM-2(C_{12}) and used it as catalyst in Knoevenagel condensation (Fig 31a). SIM-1 belongs to the class of ZIF materials and is isostructural to ZIF-8 which is commercialized under the name BasoliteZ-1200. The MOF catalyst (SIM-2(C_{12})) showed the highest catalytic activity in the Knoevenagel condensation as compared to SIM-1 due to hydrophobic nature of the MOF.[274] In another way, they supported thin films of SIM-1 and SIM-2 on different support such as alumina disk and alumina beads and used the supported MOF catalysts for Knoevenagel condensation of benzaldehyde with malononitrile (Fig 31b). First, they immersed the alumina disk and beads in a solution of $Zn(NO_3)_2{\cdot}4H_2O$ and 4-methyl-5-imidazolecarboxaldehyde to get SIM-1 and finally to obtain (SIM-2(C_{12}))/alumina composite by immersing SIM-1 disk and beads in a solution of 7ml of anhydrous methanol containing dodecylamine. Surface tension properties were calculated by measuring the contact angle with a water droplet on SIMs disk and beads, which are directly interrelated to the catalytic activity of the MOF in reaction. By up-grading

of a supported MOF catalyst on alumina support through post-synthetic modification, the SIM-1 alumina beads showed a TOF = 1500 h^{-1}, while the equivalent SIM-1 beads displayed a TOF = 215 h^{-1} which corresponds to a 7-fold increase in reaction rate between benzaldehyde and malonitrile.[275]

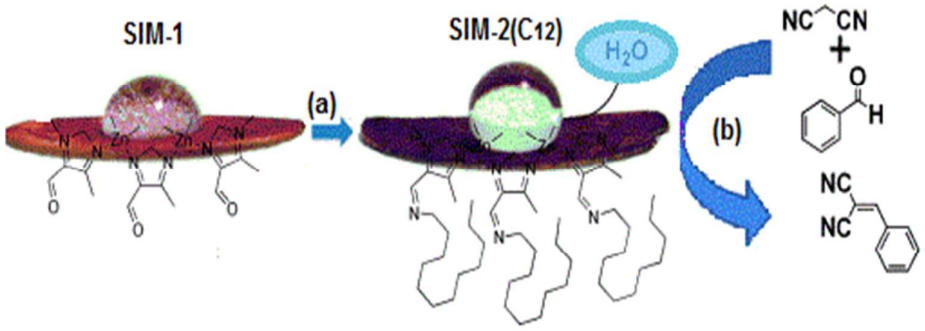

Fig. 31 (a) Post-synthetic modification of SIM-1 to SIM-2(C_{12}). (b) Knoevenagel condensation. Reproduced from ref. [274].

10. Heterogeneous Asymmetric catalysis

MOFs offer a highly tunable platform to engineer heterogeneous catalysts for important reactions, *e.g.*, asymmetric organic transformations, which cannot be achieved with conventional porous inorganic materials.[276] Homochiral MOFs are envisioned as a creative tool for a range of enantioselective applications, including the separation of optical isomers,[277] the promotion of catalytic enantioselective reactions and also for heterogeneous asymmetric transformations.[278] Homochiral MOFs are also proficient of stereoselective molecular recognition.[279] Homochiral MOFs are perfect candidates for the heterogeneous asymmetric catalytic conversions, since they can entail confined cavity's environment regarding to size and shape-selective restriction and caste a high enantioselectivity. Amongst the asymmetric MOF catalysts reported to date, approximately all of the efficient examples contain a privileged chiral ligand as a mean of the enantio-differentiation.[278] If a metal ion is present in a chiral environment then it can also acts as an asymmetric catalytic active moiety. Metal-based homochiral MOFs have been prepared and used as catalysts in organic reactions. Lin and coworkers are pioneers in this field.[280, 281] Similarly, chiral organic linkers based

heterogeneous asymmetric chiral MOF (CMOFs) catalysts have been constructed, having asymmetric catalytic activities.[282]

The first asymmetric catalysis using homochiral MOF was reported in 2000 by Kim[241] and first symmetric 1,1'-bi-2-naphthol (binol) based MOF in 2005 by Lin.[283] The post-synthetically generated Ti-binolate moiety in the chiral MOF was responsible for high *ee's* observed for diethylzinc additions to aromatic aldehydes. Subsequently, a Mn(salen) based MOF was used for asymmetric epoxidation of alkenes.[105] In 2010, a series of chiral MOFs (CMOFs) was prepared by reaction of well-defined Mn-salen complex with $Zn(NO_3)_2 \cdot 6H_2O$ in DMF and further screened for their catalytic activities in enantioselective epoxidation of different alkenes.[284] It has been observed that the epoxidation reaction rates depend on the CMOF open channel sizes, the larger the open channel dimensions the higher the reaction rate due to the easy diffusion of reactant and product molecules inside and outside the channels. Lin and coworker prepared a CMOF from the Mn-salen derived dicarboxylic acid with the $[Zn_4(\mu_4\text{-}O)(O_2CR)_6]$ secondary building units. The catalyst proved to be highly regio- and stereo-selective for alkene epoxidation and epoxide ring-opening reactions.[53]

Similarly, Cui *et al.*[285] constructed two chiral robust MOFs $[Cd_4(\text{Ni-salen})_4(DMF)_4] \cdot 4H_2O$ and $[Cd_4(\text{Co-salen})_4(DMF)_4(OAc)_4] \cdot 4H_2O$ based on dicarboxylate-functionalized Ni(salen) and Co(salen)(OAc) ligands. The TGA revealed that the MOFs are stable up to 350 ºC. The MOFs were checked as a solid catalyst for hydrolytic kinetic resolution (HKR) of epoxides. The reactions were carried out with a 0.7:1 molar ratio of water in tertahydrofuran (THF) or a mixed solvent of CH_3CN and CH_2Cl_2 at room temperature. A 0.5 mol% loading of Cd-MOF with regard to the racemic substrates afforded the resolved target epoxides in 87-98% *ee* and 54−57% conversions within 48 h. For 1- and 2-naphthyl glycidyl ethers, reaction carried out with 0.7 mol% catalyst loading gave 53 and 56% conversion and 95 and 94% *ee* within 48 h respectively (Scheme 19). Increasing reaction time from 48 h to 60 h led to 57 and 62% conversion with 95 and 94% *ee* respectively. The solid catalyst can be easily recycled and

reused without any loss of catalytic activity and enantioselectivity. PXRD indicated that catalysts retained their crystallinity after five cycles.

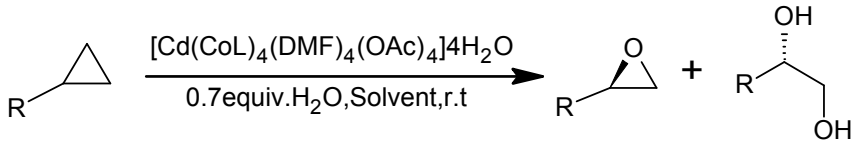

Entry	R	cat. Load (mol %)[a]	reaction time (h)	(*ee*) (%)[b]	Conv. (%)[c]	K_{rel}[d]
1	CH_2OPh	0.5	48	95	56	25
2	CH_2O (*o*-NO_2-C_6H_4)	0.5	48	92	54	27
3	CH_2O (*p*-Me-C_6H_4)	0.5	48	87	57	13
4	CH_2O (*p*-OMe-C_6H_4)	0.5	48	94	55	27
5	CH_2O (*o*-Me-C_6H_4)	0.5	48	97	54	43
6	CH_2O (*m*-Cl-C_6H_4)	0.5	48	98	55	41
7	CH_2O (1-naphthyl)	0.7	48/60	95/99	53/57	43/40
8	CH_2O (2-naphthyl)	o.7	48/60	94/99	56/62	23/40

Scheme 19. HKR of epoxides. Solvent: THF for entries 2,3 and 5; CH_2Cl_2/CH_3CN for other entries. [a] catalyst loading based on racemic epoxide. [b] *ee* values determined by HPLC. [c] isolated yield based on racemic epoxide. [d] K_{rel} = In[1 - c(1 + *ee*)] /In[1 - c(1 - *ee*)].

The first chiral Zr-MOF $[Zr_6O_4(OH)_4(binap)_6]$ based on 2,2-bis(biphenyl-phosphino-1,1-binaphthyl (binap) (Fig. 32a) and its post metallation with rhodium and ruthenium complexes to afford highly enantioselective catalysts for important transformation (Fig. 32b) has been reported by Lin *et al.*[286] The binap-MOF contains the $Zr_6O_4(OH)_4(O_2CR)_{12}$ cluster secondary building unit (SBU) and have the same framework topology as UiO-66 reported by Lillerud *et al.* in 2010.[287] Rh functionalized MOF proved to be an outstanding catalyst in conjugated addition of arylboronic acid to cyclohexanone and also in addition of $AlMe_3$ to *α,β*-unsaturated ketones to give chiral allylic alcohols (Fig. 32c, d). Rh-functionalized MOF displayed a high enantioselectivity in arylboronic acids addition up to >99% *ee* with an activity 3 times higher as the homogeneous control reaction. Ru-functionalized MOF is highly active in hydrogenation of *β*-keto esters and substituted alkenes with enantioselectivity up to 99% and 70% respectively. The post synthetically metalated binap-MOF offers a versatile family of single-site solid catalysts for a wide variety of asymmetric organic transformations.

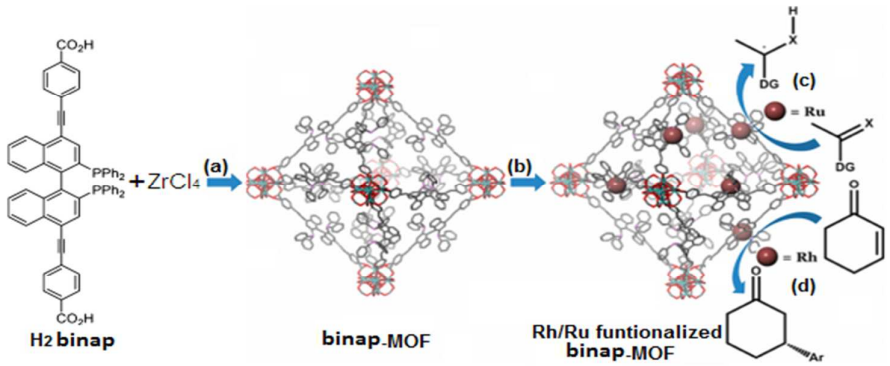

Fig. 32 (a) Synthesis of Zr-MOF based on a binap-derived dicarboxylate, (b) post-synthetic metallation, (c) asymmetric hydrogenation, and (d) asymmetric addition of aryl-boronic acid. Reprinted with permission from ref. [286]. Copyright 2014 American Chemical Society.

Ma *et al*. prepared a group of mesoporous CMOFs using eight different kinds of ligand (L_1-L_8), having general formula $[Cu_2L(S)_2]$ (L = chiral tetracarboxylate ligand derived from 1,1′-bi-2-naphthol and S is solvent) and further functionalized them with Ti(O-*i*-Pr)$_4$ (Scheme 20).[288] The catalysts displayed efficient activities for diethylzinc and alkynylzinc additions to aromatic aldehydes. The enantioselectivities of these reactions can be tailored by alteration of the channel size, which changed the diffusion rates of the organic substrates. Later they reported a 3D MOF based on binol-derived tetracarboxylate bridging ligand and dizinc SBUs and loaded with Ti(O-*i*-Pr)$_4$.[289] However, only modest enantioselectivity was obtained for Et_2Zn addition reactions with arylaldehydes.

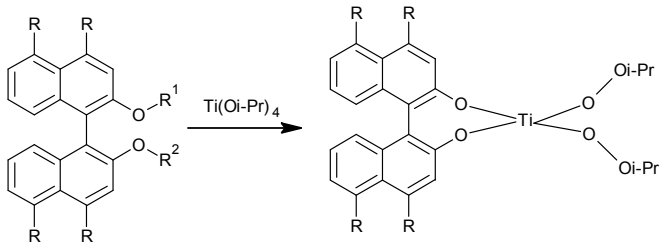

	L_1	L_2	L_3	L_4	L_5	L_6	L_7	L_8
R =	-COOH	-COOH	-CH=CH-COOH	-CH=CH-COOH	-C_6H_4-COOH	-C_6H_4-COOH	-CH=CH-C_6H_4-COOH	-CH=CH-C_6H_4-COOH
R^1=	H	Et	H	Et	H	Et	H	Et
R^2=	H	H	H	H	H	H	H	H

Scheme 20. Chemical structure of chiral tetracarboxylate ligands (L_1-L_8) derived from 1,1′-bi-2-naphthol and functionalization with Ti(O-*i*-Pr)$_4$.

Jeong *et al.*[290] synthesized a chiral porous MOF, (*S*)-KUMOF-1, $[(Cu_2(S)\text{-}\mathbf{L})_2(H_2O)_2)]$ (L = (*S*)-2,2'-dihydroxy-6,6'-dimethyl(1,1'-biphenyl)-4,4'-dicarboxylate) for asymmetric catalysis with potential catalytic sites exposed into the pore. They elucidated its catalytic activity in two reaction; the carbonyl-ene reaction with Zn/(*S*)-KUMOF-1 (KUMOF = Korea University Metal Organic Framework) after replacing the protons on biphenol on the organic links with $ZnMe_2$ and the hetero-Diels-Alder reaction with Ti/(*S*)-KUMOF-1 modified with Ti(O-*i*-Pr)$_4$. In case of Lewis-acid catalyzed carbonyl-ene reaction, product B was formed from A, as a single diastereomer after 3.5 h with higher yield 89%, 92% and 92% in presence of Zn/(*S*)-KUMOF-1 with 1.5:4.5, 3:9 and 6:18 MOF:$ZnMe_2$ ratios, respectively. On treatment with methoxy(trifluoromethyl)phenylacetic acid (MTPA) and pyridine in CH_2Cl_2, compound B transformed into C as a diastero mixture (Mosher ester) (Scheme 21a) and finally its optical activity was determined. It was observed that with increasing MOF:$ZnMe_2$ ratios from 1.5:4.5, 3:9 and 6:18, higher yields as well as a higher stereoselectivities (89% and 23% *ee*, 92% and 50% *ee* 92% and 50% *ee*) were obtained respectively. In hetero-Diels Alder reaction, product 3 obtained from reaction of 1 and 2 (Scheme 21b) was finally converted into product 4 by acid hydrolysis. Product 4 was formed with higher yield as well as a higher enantioselectivity (52% and 33% *ee* 77% and 48% *ee*, 79% and 55% *ee,* 80% and 55% *ee*) with 30:30, 30:45, 30:60 and 30:90 MOF:Ti(O-iPr)$_4$ ratios, respectively.

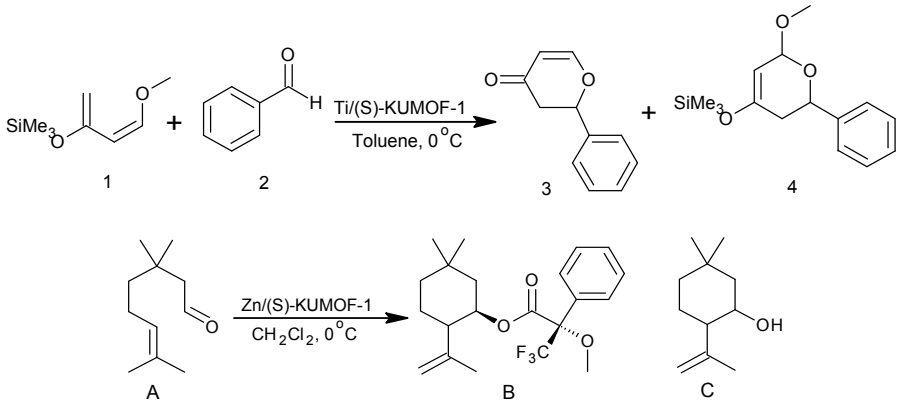

Scheme 21. (a) Enantioselective hetero-Diels–Alder reaction by Ti/(*S*)-KUMOF-1 and (b) carbonyl-ene reaction by Zn/(S)-KUMOF-1.

Recently, Duan and coworkers[291] used well recognized asymmetric organic catalyst L- and D-pyrrolidine to create CMOFs due to its high enantioselectivity in various enantioselective organic reactions, including C-C bond forming aldol and Michael reactions. By inclusion of the chiral group, L- or D-pyrrolidin-2-ylimidazole (PYI) and oxidation catalyst $[BW_{12}O_{40}]^{5-}$ into single framework, two enantiomorphs Ni-PYI1 and Ni-PYI2 were created *via* self-assembly, respectively (Fig. 33a, b). The coexistence of the chiral directors and the oxidants within a confined space provided a particular environment for the formation of reaction intermediates with high selectivity in a stereoselective fashion. Asymmetric dihydroxylation was monitored initially by using styrene and aqueous H_2O_2 (15%) as oxidant in CH_2Cl_2, along with ex-Ni-PYI1 (0.7% mol ratio) at 40 °C in a heterogeneous approach. The MOF performed excellent enantioselectivity (*ee* > 95%) for (R)-phenyl-1,2-ethanediol (Fig. 33c). Then, the use of catalyst was further extended to other substrates with similar activity and asymmetric selectivity. The result of catalysis showed that Ni-PYIs worked as an amphipathic catalyst for asymmetric dihydroxylation of aryl olefins with excellent stereoselectivity.

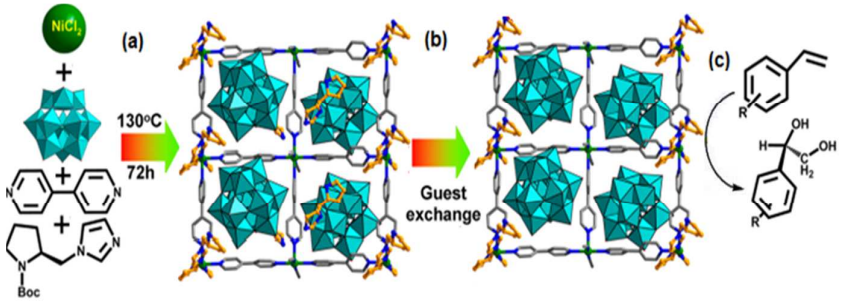

Fig. 33 Representation of (a) MOF synthesis, (b) guest exchange and (c) catalytic behavior. Reprinted with permission from ref. [291]. Copyright 2013 American Chemical Society.

Later the same authors reported two other homochiral MOFs Ce-MDIP1 and Ce-MDIP2, synthesized from the reaction of $Ce(NO_3)_3 \cdot 6H_2O$ and methylenediisophthalic acid (H_4MDIP) in the presence of L- and D-*N*-*tert*-butoxy-carbonyl-2-(imidazole)-1-pyrrolidine (BCIP) in water.[77] Asymmetric cynosilylation reaction of benzaldehyde was done in the presence of CH_3CN at room temperature giving (*S*)-2-phenyl-2(trimethylsilyloxy)acetonitrile with an *ee*

value up to 91%. Ce-MDIPs showed an efficient catalytic activity and high enantioselectivity for the asymmetric cyanosilylation of aromatic aldehydes (Scheme 22). While, another CMOF Cd-BTB having L-PYI (L-pyrrolidine-2-yl-imidazole) as a chiral adduct was used to catalyze the asymmetric Aldol reactions between different aldehydes and cyclohexanone with a better enantioselection.

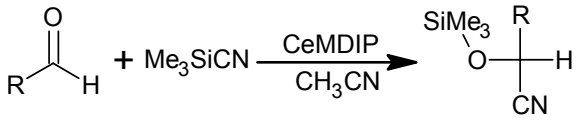

Entry	R	*ee* (%)[a]	
		Ce-MDIP1[b]	Ce-MDIP2
1	C_6H_5	93	94
2	*p*-OMe-C_6H_5	91	97
3	1-naphthyl	98	>98
4	2-naphthyl	>98	>98

Scheme 22. Results for the catalytic cyanosilylation of different carbonyl substrates in the presence of Ce-MDIPs. (The *ee* ratio was determined by HPLC analysis).

Mo *et al.*[292] reported the synthesis of an enantiopure tetracarboxylate 2,2-dihydroxy-1,1-biphenyl ligand (H_4L) to build a homochiral MOF $[Zn_4O(L)_{3/2}]\cdot 16H_2O\cdot 4THF$. TGA revealed that the MOF guest molecules could be easily removed in temperature range from 80-150 °C and decomposition of frameworks starts at 400 °C. After soaking $[Zn_4O(L)_{3/2}]\cdot 16H_2O\cdot 4THF$ in water for 2 days, PXRD indicated that sample retained its crystallinity. Mono- and dilithium salts, $[Zn_4O(L)_{3/2}]\cdot 16H_2O\cdot 4THF\text{-}Li(H_2O)_2$ and $[Zn_4O(L)_{3/2}]\cdot 16H_2O\cdot 4THF\text{-}Li_2(H_2O)_4$ were obtained from 1:2 and 1:4 molar ratios of $[Zn_4O(L)_{3/2}]\cdot 16H_2O\cdot 4THF$ (per formula unit) and *n*-BuLi, respectively.

After one proton exchange of the dihydroxyl group with Li(I) ions, the framework was highly efficient as catalyst for asymmetric cyanation of aldehydes with upto 99% *ee* and even recyclable. With di-lithium salt as catalyst, 90% conversion with 79% *ee* of the product was obtained, indicating that mono-lithium was more efficient and enantioselective than di-lithium. Aromatic aldehydes with an electron-withdrawing group and electron-donating group gave the required product quantitatively with enantioselectivities up to > 99% *ee*, and

81% *ee*, respectively. 3-Pyridylaldehyde and 2-furylaldehyde bearing a heterocycle gave excellent results up to > 99% *ee*. High enantioselectivity was obtained with the vinyl-type aromatic aldehyde such as cinnamaldehyde, affording 98% conversion and 98% *ee*. 1- and 2-naphthaldehydes were readily converted to the corresponding products with enantioselectivities of 94% and > 99% *ee*, respectively. In case of bulky substrate 9-anthralaldehyde a moderate conversion of 67% and enantioselectivity of 67% *ee* were attained (scheme 23). This method is appropriate for process chemistry to make sure a practical gram-scale cyanohydrin synthesis.

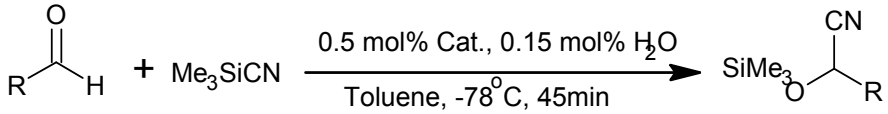

Entry	R	Conversion (%)[a]	Enantioselectivity (%)[b]
1	C_6H_5	97	98 (*S*)
2	*p*-Cl-C_6H_5	99	>99 (*S*)
3	*p*-Br-C_6H_5	99	92 (*S*)
4	*p*-NO_2-C_6H_5	99	>99 (*S*)
5	*m*-MeO-C_6H_5	99	81 (*S*)
6	2-fural	95	99 (*S*)
7	C_6H_4CH=CH	98	98 (*S*)
8	1-naphthyl	99	94 (*S*)
9	2-naphthyl	99	>99 (*S*)
10	9-anthral	67	67 (*S*)

Scheme 23. Cyanation of aldehydes catalyzed by $[Zn_4O(L)_{3/2}]\cdot 16H_2O\cdot 4THF\text{-}Li(H_2O)_2$. [a] Calculated by ^{1}HNMR.[b] Determined by HPLC.

Duan[293] devised two enantiomeric MOFs Zn−PYI1 and Zn−PYI2 by incorporating the stereoselective organo catalyst L- or D-pyrrolidin-2-ylimidazole (PYI) and a triphenylamine photoredox group into lanthanide-based MOFs Ho-TCA and MOF-150. First Zn-BCIP1 and Zn-BCIP2 are prepared by reaction of 4,4,4-tricarboxyltriphenylamine (H_3TCA) and $Zn(NO_3)_3.6H_2O$ in presence of L and D-*N*-*tert*-buttoxycarbonyl-2-(imidazole)-1-pyrrolidine (L-BCIP) in mixed solvent (DMF:EtOH) by solvothermal method and then deprotection of the proline unit in a dry DMF gave Zn-PYI1 and Zn-PYI2 using microwave irradiation. These heterogeneous asymmetric CMOFs have efficient catalytic activities for the photo-catalytic alkylation of different aliphatic aldehydes. The inclusion of a triphenylamine photoredox group (photocatalyst) and a stereoselective organo catalyst L- or D-pyrrolidin-2-ylimidazole (PYI) into the framework makes the enantioselection better to that of simply

mixing the corresponding MOFs with the chiral adduct. The reaction of phenylpropyl aldehyde and diethyl-2-bromomalonate as the coupling partners, along with Zn-PYI1 and a common fluorescent lamp displayed an excellent enantioselectivity (92% *ee*) and high reaction efficiency (74% in yield).

11. Stability of MOFs

MOFs have emerged as an interesting type of crystalline porous materials which mingle highly enviable properties, such as high surface areas, consistent micropores, along with thermal and chemical stability, making them ideal candidates for catalytic applications.[294,12] Catalysis is a prospective application of MOFs that is highly demanded for their chemical and thermal stability.[282] For a MOF to be broadly used as a catalyst for organic reactions, it must have (i) thermal stability, (ii) structural stability to activation, (iii) exceptional mechanical robustness, and (iv) chemical stability *i.e*., stable to the solvents, and reagents that the reaction demands.[295] Similarly, recyclability of MOF is an important and essential feature to be considered for use in industrial applications. MOF appropriateness for high-temperature catalysis would require assessment of stability over prolonged periods of time.

Frequent tests for assessing MOF stability include the comparison of the X-ray powder diffraction patterns, specific surface area, pore volume, and elemental analysis of the fresh MOF and the solid recovered after the catalytic reaction.[133, 296] The most common method for examining the stability of a MOF is a PXRD analysis of the bulk material after heating and/or evacuation, referenced to the calculated patterns of the host structure and then correlated with thermogravimetric analysis (TGA), in which framework stability is indicated by negligible weight loss between the temperatures of guest desorption and framework decomposition.

The thermal stability of a MOF is normally established by TGA or by diffractional thermal analysis (DTA), typically carried out in a flow of air or inert gas (N_2 or He) or in vacuum while increasing the temperature up to the complete destruction of the framework (typically up to 300-500 °C). As such, TGA measurements are most likely viewed as stability-screening

experiments rather than perfect experiments. Importantly, neither method of analysis is adequate on its own to show the ‘‘openness’’ of a material. In addition, corroborating evidence should be presented in the form of changes in elemental composition, and infrared (IR) and/or solid state nuclear magnetic resonance (NMR) spectra.

The comparatively low thermal stabilities of several earlier MOFs were often thought as a key barrier to their understanding as practicable heterogeneous catalysts in industrially valuable processes. Recent synthetic progresses have yielded many frameworks that have significant stability to high temperatures. Such improved framework thermal stability, and therefore the catalytically active species that they support, are important for the investigation of MOFs as heterogeneous catalysts and supports for catalytically active molecules such as POM, MP, and enzymes.

Several examples of MOFs with high thermal strength have been reported. For example, Chen *et al.* published Zn^{2+} MOFs with imidazolate ligands and zeolite topology that possessed high thermal stability, Eddaoudi *et al.* developed zeolite-like MOFs using indium and bis(bidentate) imidazoledicarboxylic acid ligands, and the Yaghi group also introduced zeolitic imidazolate frameworks (ZIFs), using Zn^{2+} and Co^{2+} and imidizolate linkers to construct a wide variety of highly stable frameworks that mimic zeolite topology, due to the metal ions adopting a tetrahedral environment while the imidazolates link them at angles similar to the oxides in zeolite minerals.[297-299]

The robustness and reactivity of MOFs are mostly dependent on metal-ligand interactions, where the metal-containing clusters are often susceptible to ligand substitution by water or other nucleophiles. Frameworks may also collapse upon thermal or vacuum treatment or simply over time. This instability confines the practical uses of many MOFs. In order to further enhance the stability of the framework, many different approaches, such as the utilization of high-valence metal ions or nitrogen-donor ligands, were recently investigated.

To further increase the chemical stability of MOFs, researchers can go further along the path of using high valence metal ions, such as Cr^{3+}, Fe^{3+}, and Zr^{4+}.[300] With all the coordination environments being equal, an increased charge will decrease labiality just by mounting the electrostatic interaction between the metal ions and the ligands. This trend can also be rationalized by the hard/soft acid-base principle, where soft acids like low-oxidation state metals form less stable coordination bonds with harder bases like the oxygen donors on carboxylate ligands. It is not just the charge of the metal ion that increases the stability but also the charge density. The smaller, hard ions with high charge density (*e.g.*, Cr^{3+} or Zr^{4+} *etc.*) are able to bond more strongly to carboxylates than larger, soft ions (*e.g.*, Co^{2+}or Zn^{2+} *etc.*) could.[301]

Increased chemical stability is also reported in UiO-66 and its isoreticular derivatives.[302] UiO-66 possesses $Zr_6O_4(OH)_4$ SBUs in which the Zr^{4+} ions have stronger interactions with carboxylate ligands than copper or zinc. Therefore, these SBUs are less susceptible to ligand substitution.[303] It is reported that the SBU is the key to the exceptional stability, and has the ability to reversibly change between a hydroxylated ($Zr_6O_4(OH)_4$) and a non-hydroxylated structure (Zr_6O_6). Both UiO-66 and UiO-67 are found to be stable up to 540 ºC based on TGA and up to 375 C based on temperature-programmed PXRD. It is stable to water and many organic solvents. Additionally, it can withstand high pressure without mechanical degradation, making it highly attractive as a support in fixed-bed flow reactors for gas-phase reactions.

Zhou *et al.* have synthesized single crystals of an extremely stable Zr-based MOF (PCN-222) with porphyrin-containing ligands that can themselves bind different metal ions, enabling a variety of catalytic activities, which was enabled both by the actual catalytic sites and by the high pore size. Additional to the catalytic active sites and the high pore size; the stability of PCN-222 to water and temperature makes it more attractive material. Its stability is not only limited to air and boiling water, but also extended to immersion in concentrated HCl for 24

hours. Similar Zr-MOFs PCN-224 and PCN-225 exhibited a different catalytic activities or pH-dependent florescence.[304, 305]

The porphyrinic organic linkers are mostly carboxylate based.[306] When relatively soft Lewis-acidic species are used as nodes (Zn^{2+}, Cu^{2+}, and Cd^{2+}), the weak coordinating bond makes the framework less resistant to the attack of reactive chemicals (solvents or reagents). To triumph such a weakness, clusters formed with harder Lewis-acidic metals (Zr^{4+} and Cr^{3+}) are selected as nodes, leading to porphyrinic MOFs with notably superior stability.[304] Fe^{3+} is an ideal substitute to Zr (IV) as the metal ion to construct nodes in MOFs due to its low toxicity, abundance, and its hard Lewis acid character, which results in stronger coordinating bonds with carboxylates and therefore more stable frameworks (Fig. 34).

Fig. 34 Representation of the stability of MOFs prepared from different metal ions (di, tri and tetravalent).

It has been observed that the use of poly-azolate-bridging ligands lead to frameworks with strong metal-nitrogen bonds, providing a better chemical and thermal stability compared to their carboxylate-based counterparts.[307] A number of pyrazolate-based MOFs have already been realized exhibiting an extraordinary and high stability compared with the tetrazolate- and triazolate-bridged frameworks. For example, 1,4-bis(1H-pyrazol-4-yl)benzene (1,4-H_2bdp) reacts with salts of cobalt(II) nickel(II) or zinc(II) to give MOFs having high thermal stability (420-460 ºC).[308] Using the 1,3-H_2bdp results in a double-walled Zn-MOFs of even greater thermal stability (500 ºC), which further shows chemical stability in a hot acidic solution (pH 3).

On the whole, the thermal and chemical stability profiles of pyrazolate-based frameworks are in fact significantly increased relative to the tetrazolate- and triazolate-bridged frameworks.

Similarly, $[Zn_3(btp)_2{\cdot}4CH_3OH{\cdot}2H_2O]$ (btp = 1,3,5-tris(1H-pyrazol-4-yl)benzene) is stable to heating in air up to at least 510 ºC, while $[Ni_3(btp)_2{\cdot}3DMF{\cdot}5CH_3OH{\cdot}17H_2O]$ is stable to heating in air to 430 ºC.[309]

Many MOFs are especially air- and moisture-sensitive following evacuation of the pores, leading to the need for careful handling under an inert atmosphere. In case of MOF-5, even slight exposure of the activated form to the air results in rapid deprivation of the crystallinity and loss of its surface area due to the hydrolysis of the Zn-O bonds.[310, 311]

The metal-ligand bond is usually the weakest point of a MOF, and hydrolysis of metal-ligand bond can lead to the displacement of the bond and collapse of the framework structure.[311] This was observed in the zinc-carboxylate based MOF-5, which is water sensitive and begins to lose the crystallinity upon disclosure to small amounts of moisture.[312]

It has been established that the essential zinc acetate clusters characteristic of the most zinc carboxylate MOFs, such as the IRMOF series and MOF-177, are most liable to hydrolysis.[313] The trinuclear chromium clusters set up in many of the MIL series are the most stable of the SBUs, while the copper paddle wheel carboxylate clusters found in HKUST-1 exhibit intermediate stability. MOFs containing Cr^{3+}, Al^{3+}, Fe^{3+}, and Zr^{4+} cations displayed a high degree of stability in water (Fig. 35). Specifically, MIL-53(M), (M = Cr^{3+}, Fe^{3+}, Al^{3+}) is a flexible framework that expands or contracts based on the absence or presence of water.[314, 315] Here, the structural transition is reversible, and the overall framework scaffold remains intact upon repeated exposure to water.

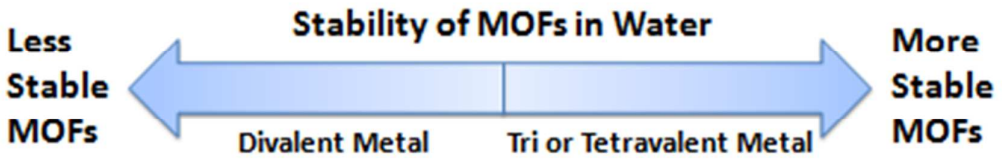

Fig. 35 A schematic representation of stability of MOFs in water with respect to divalent and tri or tetravalent metals.

Though future MOFs are developed for more extensive applications, their thermal stability and also chemical stability towards more varied chemicals should be determined, and application-built MOFs should be logically planned to be stable towards conditions as reaction demands.

12. Conclusions and remarks

Heterogeneous catalysis is one of the explored applications of metal-organic frameworks. A wide range of organic reactions has been catalyzed with MOFs from acid-base to redox categories. Pore size, morphology, and surface functionality of MOFs have been easily tuned upon selection of different metal ions and organic molecules making it possible to design MOFs for desired and specific catalytic applications. Compared with zeolites, MOFs have numerous advantages, such as multifunctional organic linkers, more choice of metallic nodes, ease of formation, high surface area and pore volume *etc*. Size, shape, and environment of pores in the MOF can be modified *via* chemical synthesis, which discriminates MOFs over other conventional nanoporous materials *i.e.*, zeolites and activated carbons *etc*. MOFs provide the tremendous means to recognize multifunctional catalysis along with a perfect connection between homogeneous and heterogeneous catalysis. MOF-based catalysis has alleviated the boundaries of homogeneous and heterogeneous systems while capturing the best features of each. The high porosity of MOFs allow for the fast mass transfer and interaction with substrates.

MOFs have been functionalized *via* their metal nodes and organic ligand through pre-synthetic and post-synthetic modifications to access MOFs which could not be directly synthesized under conventional methods. High porosity has been used not only as a reaction chamber but also more interestingly for the immobilization and encapsulation of active homogeneous catalyst, MNPs, organometallic complexes, polyoxometalates, porphyrins, and metalloporphyrin. Loading of MNPs into pores of MOFs makes them accessible by reactants for chemical transformations with improved catalytic performance of MOF reinforced MNPs

as composites. Hetero-bimetallic MOFs have shown enhanced catalytic activity than their mono-metallic analogues due to the alloying effect of two metals. Chiral and enantiopure organic molecules have been employed to form the chiral MOFs and notable catalytic activities have been observed in asymmetric reactions and enantiospecific separations. Especially the use of MOFs for shape, size, region-, and enantioselectivity has become one of the most important catalytic applications. The difference in catalytic activity between compounds with empty or filled channels concludes that catalysis does definitely take place inside the pores. Moreover, large substrates show significantly diminished yields *versus* small substrates, revealing that catalysis occurs mainly within the pores. One of the major drawbacks for the use of MOFs as catalysts is their relatively limited thermal and chemical stability. Only few systems have been established which are stable up to 500 °C. MOF-based catalysis cannot be performed for such reactions which have highly basic and polar conditions; this lead to destruction of framework as observed in nitration and hydroxylation of aryl halides. Further, in some cases the main product or side product formed leads to the deactivation of the MOF catalysts *e.g.*, by coordination with the free metal centers and diminishing the Lewis-acid character of the whole structure.

Open metal sites of MOFs may become hydrated on long time exposure to atmospheric moisture leading to catalyst deactivation/poisoning. These problems have been overcome by introduction of alkyl groups in the organic linker (hydrophobization of MOFs) which prevents MOFs from water poising making them water resistant. Utilization of high-valence metals as hard acids appears to be the most straightforward approach for the construction of stable MOFs by taking the advantage of the existing ligand database. In addition to this approach, the interactions between softer ligands (such as imidazolates, triazolates, tetrazolates, and other nitrogen containing heterocycle incorporated ligands) with softer metal ions (such as Zn^{2+} and Co^{2+}) can also be exploited in stable MOF synthesis.

The diversity of metal active sites in the framework of MOFs has led to a new strategy towards catalysis of various organic reactions. A large variety of organic reactions have been catalyzed by the unsaturated metal sites and also due to their Lewis or Brønsted-acid properties.

Leaching of metal from MOFs structure has been observed. As in case of liquid-phase hydrogenation of 1-octene, catalyzed by Pd^0 instead of $[Pd(2\text{-pymo})_2]_n \cdot 3H_2O$ due to leaching of Pd into the solution. Therefore, it is necessary to find out the stability of MOF and leaching of active metal species by comparing the crystal structure and surface area before and after the reactions. In most cases it has been seen that only XRD and thermogravimetric analysis are performed. The reacted MOF should also be characterized by different techniques; electron microscopic analysis, XRD, Fourier transform infrared (FTIR) spectroscopy to ensure its texture and morphology.

In principle, because of their composition, MOFs are more suited for being used in hydrocarbons and polar solvents; although in some cases water and alcohols can be used. XRD is a suitable technique to assess the structural stability. In some cases, minor changes in the XRD patterns, particularly in the relative intensity of some peaks, have been attributed to the presence in the interior of the MOF void space of organic species and not to a real destruction of the crystallinity. This can be assessed by determination of the microporosity of the used material after the reaction and observation of the isothermal gas adsorption data characteristic of MOFs.

MOFs provide an excellent playground for the development of heterogeneous catalytic systems. Many new kinds of MOFs with high thermal and chemical stability will appear as the research topic become more and more well-liked. The controllable topology and geometry of framework and tunable pore functionality render them highly attractive in future to various applications especially in catalysis. MOFs are still an evolving field, with plentiful prospects; many new materials are being prepared and the potential appears countless, but the

presentation of MOFs in industrially important technologies is still a mostly unexplored frontier.

List of acronyms and abbreviations:

Al-*i*-Pro	Aluminium-iso-propoxide
A-15	Amberlyst-15
BCIP	*N*-*tert*-butoxy-carbonyl-2-(imidazole)-1-pyrrolidine
BET	Brunauer–Emmett–Teller
binap	2,2-bis(biphenyl-phosphino-1,1-binaphthyl
binol	1,1'-bi-2-naphthol
bipy	4,4-bipyridine
BOC	*tert*-Butyloxycarbonyl
btp	1,3,5-tris(1H-pyrazol-4-yl)benzene
bttp-4	Benzene-1,3,5-triyl triisonicotinate
CAU	*Christian Albrechts* University
CMOF	Chiral Metal Organic Framework
CysNO	*S*-nitrosocysteine
DAAP	Dialkylaminopyridines
DDQ	*N*,*N*-dibenzoicacid-2,3-diaminoquinoxaline
DMA	*N*,*N*-dimethylacetamide
DMF	Dimethylformamide
Dpdo	4,4'-bipyridine-*N,N*'-dioxide hydrate
DTA	Diffractional thermal analysis
DTBC	3,5-di-*tert*-butyl-catechol
FA	Formic acid
H_2bdc	Benzene-1,4-dicarboxylic acid
1,4-H_2bdp	1,4-bis(1H-pyrazol-4-yl)benz ene
H_2bpb	1,4-bis(4′-pyrazolyl)benzene
H_2bpdc	4,4′-biphenyldicarboxylic acid
H_3bpt	Biphenyl-3,4′,5-tricarboxylate
H_4bptc	Biphenyl-3,3,4,4-tetracarboxylic cid
H_2bpydc	2,2-bipyrdine-5,5-dicarboxylic acid
H_3btc	Benzene-1,3,5-tricarboxylic acid
H_2dmbdc	2,5-dimethylbenzene-1,4-dicarboxylic acid
H_2dobdc	2,5-dihydroxybenzene-1,4-dicarboxylic acid

H_3Imdc	4,5-imidazoledicarboxylic acid
HKR	Hydrolytic kinetic resolution
HKUST	Hong kong university of science and technology's
H_4MDIP	Methylenediisophthalic acid
HmeIm	2-methylimidazole
H_2ndc	Naphthalenedicarboxylic acid
H_4pdai	5,5'-[(pyridine-3,5-dicarbonyl)bis-(azanediyl)]diisophthalate
H_2pydc	Pyridine-3,5-dicarboxylate
HPW	Hetero-polyacid phosphotungstic acid
H_3tca	Tricarboxytriphenylamine
HZSM-5	Zeolite Socony Mobil-5
ED	Ethylenediamine
ESR	Electron spin resonance spectroscopy
FA	Farmic acid
fum	Fumaric acid
FT-IR	Fourier transform infrared spectroscopy
FOS	Functional organic sites
Im	Imidazolate
IRMOF	Isoreticular Metal Organic Framework
KUMOF	Korea University Metal Organic Framework
L-bcip	L-*N*-*tert*-buttoxycarbonyl-2-(imidazole)-1-pyrrolidine
MCM	Mobil composition of matter
Me	Methyl
MIL	Matérial Institut Lavoisier
MNPs	Metal nano particles
MOFs	Metal-organic frameworks.
MOMs	Metal-organic materials
MP	Microperoxidase
MPa	Megapascal
MTPA	Methoxy(trifluoromethyl)phenylacetic acid
$NaBH_4$	Sodium borohydrate
$NaSO_3$-H_2bdc	Sodium 2-sulfobenzene-1,4-dicarboxylic acid
NH_2-H_2bdc	2-amino-benzene-1,4-dicarboxylic acid
NH_2-ipa	5-aminoisophthalate
NHPI	*N*-hydroxyphthalimide

NO_2-H_2bdc	2-nitro-benzene-1,4-dicarboxylic acid
NPs	Nanoparticles
NU	Northwestern University
PAH	Poly-cyclic aromatic hydrocarbons
PCN	Porous coordination network
POMs	Polyoxometalates
ppm	Parts per million
PSE	Post-synthetic exchange
PSD	Post-synthetic deprotection
PSM	Post-synthetic modification
PTA	Phosphotungstic acid
PVA	Polyvinyl alcohol
PYI	D-pyrrolidin-2-ylimidazole
2-pymo	2-hydroxyprimidinalote
SALE	Solvent-assisted linker exchange
SBUs	Secondary building units
SCM	Synthetic chemical modification
SEM	Scanning electron microscope images
SIM	Substituted Imidazolate Material
tatb	4,4',4"-*S*-triazine-2,4,6-triyl-tribenzoic acid
TBDMS	t-Butyldimethylsilyl (alcohol protection)
TBHP	*tert*-butylhydroperoxide
TEMPO	2,2,6,6-Tetramethylpiperidinyloxy
THF	Tetrahydrofuran
TMBQ	3,5-trimethylbenzoquinone
TMHQ	3,5-trimethylhydroquinone
tmpyp	Teso-tetra(N-methyl-4-pyridyl)porphyrinetetratosylate
$TMSN_3$	Trimethylsilylazide
tnpp	Mesotetrakis[4-(nicotinoyloxy)phenyl] porphyrin
TOF	Turn-over frequencies (TOF)
TON	Turn-over numbers
TPD	Temperature-programmed-desorption
TPP	Tetraphenylphosphonium
tpp	Tetraphenylporphyrin
UiO	University of Oslo

UMCM	University of Michigan Crystalline Material
XRD	X-ray diffraction
ZIF	Zinc imidazole framework

Acknowledgements

The authors would like to express their deep appreciation to Chinese Scholarship Council (CSC) for the financial support to A.H.C., N.A., and H.A.Y. for their PhD grants 2013GXZ988, 2012GXZ641, and 2012GXZ639, respectively. F.V. acknowledges the Chinese Central Government for an ‘‘Expert of the State’’ position in the program of ‘‘Thousand talents’’ and the support of the Natural Science Foundation of China (No. 21172027).

References

1. S. R. Batten, B. F. Hoskins and R. Robson, *J. Am. Chem. Soc.*, 1995, 117, 5385-5386.
2. S. Kitagawa, S. Kawata, Y. Nozaka and M. Munakata, *J. Chem. Soc., Dalton Trans.*, 1993, 1399-1404.
3. N. Ahmad, A. H. Chughtai, H. A. Younus and F. Verpoort, *Coord. Chem. Rev.*, 2014, 280, 1-27.
4. O. K. Farha, I. Eryazici, N. C. Jeong, B. G. Hauser, C. E. Wilmer, A. A. Sarjeant, R. Q. Snurr, S. T. Nguyen, A. O. z. r. Yazaydın and J. T. Hupp, *J. Am. Chem. Soc.*, 2012, 134, 15016-15021.
5. H. Deng, S. Grunder, K. E. Cordova, C. Valente, H. Furukawa, M. Hmadeh, F. Gándara, A. C. Whalley, Z. Liu and S. Asahina, *science*, 2012, 336, 1018-1023.
6. H. Furukawa, Y. B. Go, N. Ko, Y. K. Park, F. J. Uribe-Romo, J. Kim, M. O’Keeffe and O. M. Yaghi, *Inorg. Chem.*, 2011, **50**, 9147-9152.
7. Y.-G. Sun, X.-M. Yan, F. Ding, E.-J. Gao, W.-Z. Zhang and F. Verpoort, *Inorg. Chem. Commun.*, 2008, 11, 1117-1120.
8. D. J. Tranchemontagne, J. L. Mendoza-Cortés, M. O’Keeffe and O. M. Yaghi, *Chem. Soc. Rev.*, 2009, 38, 1257-1283.
9. Y.-g. Sun, X.-f. Gu, F. Ding, P. F. Smet, E.-j. Gao, D. Poelman and F. Verpoort, *Cryst. Growth Des.*, 2010, 10, 1059-1067.
10. Y.-G. Sun, M.-Y. Guo, G. Xiong, F. Ding, L. Wang, B. Jiang, M.-C. Zhu, E.-J. Gao and F. Verpoort, *J. Coord. Chem.*, 2010, 63, 4188-4200.
11. O. Yaghi and H. Li, *J. Am. Chem. Soc.* 1995, 117, 10401-10402.
12. O. M. Yaghi, M. O'Keeffe, N. W. Ockwig, H. K. Chae, M. Eddaoudi and J. Kim, *Nature*, 2003, 423, 705-714.
13. D.-J. Zhang, T.-Y. Song, J. Shi, K.-R. Ma, Y. Wang, L. Wang, P. Zhang, Y. Fan and J.-N. Xu, *Inorg. Chem. Commun.*, 2008, 11, 192-195.
14. S. Chaemchuen, N. A. Kabir, K. Zhou and F. Verpoort, *Chem. Soc. Rev.*, 2013, 42, 9304-9332.
15. S. Chaemchuen, K. Zhou, N. A. Kabir, Y. Chen, X. Ke, G. Van Tendeloo and F. Verpoort, *Microporous Mesoporous Mater.*, 2015, 201, 277-285.
16. L. E. Kreno, K. Leong, O. K. Farha, M. Allendorf, R. P. Van Duyne and J. T. Hupp, *Chem. Rev.*, 2011, 112 (2), 1105-1125.

17. P. Horcajada, T. Chalati, C. Serre, B. Gillet, C. Sebrie, T. Baati, J. F. Eubank, D. Heurtaux, P. Clayette and C. Kreuz, *Nat. Mater.*, 2010, 9, 172-178.
18. P. Horcajada, R. Gref, T. Baati, P. K. Allan, G. Maurin, P. Couvreur, G. Férey, R. E. Morris and C. Serre, *Chem. Rev.*, 2012, 112 (2), 1232-1268.
19. Y. G. Sun, G. Xiong, M. Y. Guo, F. Ding, L. Wang, E. J. Gao, M. C. Zhu and F. Verpoort, *J. Inorg. Gen. Chem.*, 2011, 637, 293-300.
20. M. Kurmoo, *Chem. Soc. Rev.*, 2009, 38, 1353-1379.
21. Y.-G. Sun, G. Xiong, M.-Y. Guo, F. Ding, S.-J. Wang, P. F. Smet, D. Poelman, E.-J. Gao and F. Verpoort, *Dalton T.*, 2012, 41 (25), 7670-7680.
22. C. Wang, Z. Xie, K. E. deKrafft and W. Lin, *J. Am. Chem. Soc.*, 2011, 133, 13445-13454.
23. N. Ahmad, H. A. Younus, A. H. Chughtai and F. Verpoort, *Chem. Soc. Rev.*, 2015, 44, 9-25.
24. U. Olsbye, S. Svelle, M. Bjørgen, P. Beato, T. V. Janssens, F. Joensen, S. Bordiga and K. P. Lillerud, *Angew. Chem. Int. Ed.*, 2012, 51, 5810-5831.
25. H. Furukawa, N. Ko, Y. B. Go, N. Aratani, S. B. Choi, E. Choi, A. Ö. Yazaydin, R. Q. Snurr, M. O'Keeffe and J. Kim, *Science.*, 2010, 329, 424-428.
26. N. Stock and S. Biswas, *Chem. Rev.*, 2011, 112, 933-969.
27. P. K. Thallapally, C. A. Fernandez, R. K. Motkuri, S. K. Nune, J. Liu and C. H. Peden, *Dalton T.*, 2010, 39, 1692-1694.
28. K. Tanabe and W. F. Hölderich, *Appl. Catal. A: Gen.*, 1999, 181, 399-434.
29. J. Caro, *Curr. Opin. Chem. Eng.*, 2011, 1, 77-83.
30. J. Liu, L. Chen, H. Cui, J. Zhang, L. Zhang and C.-Y. Su, *Chem. Soc. Rev.*, 2014. DOI: 10.1039/c4cs00094c.
31. W. Xuan, C. Zhu, Y. Liu and Y. Cui, *Chem. Soc. Rev.,* 2012, 41, 1677-1695.
32. J. F. Jenck, F. Agterberg and M. J. Droescher, *Green Chem.*, 2004, 6, 544-556.
33. P. Tundo, P. Anastas, D. S. Black, J. Breen, T. J. Collins, S. Memoli, J. Miyamoto, M. Polyakoff and W. Tumas, *Pure Appl. Chem.*, 2000, 72, 1207-1228.
34. M. Fujita, Y. J. Kwon, S. Washizu and K. Ogura, *J. Am. Chem. Soc.*, 1994, 116, 1151-1152.
35. F. X. Llabrés i Xamena, A. Abad, A. Corma and H. Garcia, *J. Catal.*, 2007, 250, 294-298.
36. S. S.-Y. Chui, S. M.-F. Lo, J. P. Charmant, A. G. Orpen and I. D. Williams, *Science.*, 1999, 283, 1148-1150.
37. L. Alaerts, E. Séguin, H. Poelman, F. Thibault-Starzyk, P. A. Jacobs and D. E. De Vos, *Chem. Eur. J.*, 2006, 12, 7353-7363.
38. J. Gascon, U. Aktay, M. D. Hernandez-Alonso, G. P. van Klink and F. Kapteijn, *J. Catal.*, 2009, 261, 75-87.
39. M. Opanasenko, A. Dhakshinamoorthy, J. Čejka and H. Garcia, *ChemCatChem.*, 2013, 5, 1553-1561.
40. J. Meeuwissen and J. N. Reek, *Nat. Chem.*, 2010, 2, 615-621.
41. D. Y. Hong, Y. K. Hwang, C. Serre, G. Ferey and J. S. Chang, *Adv. Funct. Mater.*, 2009, 19, 1537-1552.
42. Y. K. Hwang, D. Y. Hong, J. S. Chang, S. H. Jhung, Y. K. Seo, J. Kim, A. Vimont, M. Daturi, C. Serre and G. Férey, *Angew. Chem. Int. Ed.*, 2008, 47, 4144-4148.
43. F. L. i Xamena, F. Cirujano and A. Corma, *Microporous Mesoporous Mater.*, 2012, 157, 112-117.
44. G.-W. Li, J. Xiao and W.-Q. Zhang, *Chin. Chem. Lett.*, 2013, 24, 52-54.
45. W. Zhu, C. He, X. Wu and C. Duan, *Inorg. Chem. Commun.*, 2014, 39, 83-85.
46. N. B. Pathan, A. M. Rahatgaonkar and M. S. Chorghade, *Catal. Commun.*, 2011, 12, 1170-1176.
47. W. Kleist, M. Maciejewski and A. Baiker, *Thermochim. Acta.*, 2010, 499, 71-78.
48. M.-H. Xie, X.-L. Yang and C.-D. Wu, *Chem. Commun.*, 2011, 47, 5521-5523.

49. S. Biswas, M. Maes, A. Dhakshinamoorthy, M. Feyand, D. E. De Vos, H. Garcia and N. Stock, *J. Mater. Chem.*, 2012, 22, 10200-10209.
50. S. Marx, W. Kleist and A. Baiker, *J. Catal.*, 2011, 281, 76-87.
51. C. Li, W. Qiu, W. Long, F. Deng, G. Bai, G. Zhang, X. Zi and H. He, *J. Mol. Catal. A: Chem.*, 2014, 393, 166-170.
52. F. Zadehahmadi, S. Tangestaninejad, M. Moghadam, V. Mirkhani, I. Mohammadpoor-Baltork, A. R. Khosropour and R. Kardanpour, *J. Solid State Chem.*, 2014, 218, 56-63.
53. F. Song, C. Wang and W. Lin, *Chem. Commun.*, 2011, 47, 8256-8258.
54. D. H. Lee, S. Kim, M. Y. Hyun, J.-Y. Hong, S. Huh, C. Kim and S. J. Lee, *Chem. Commun.*, 2012, 48, 5512-5514.
55. R. Sen, D. Saha and S. Koner, *Catal. Lett.*, 2012, 142, 124-130.
56. X.-L. Yang and C.-D. Wu, *Inorg. Chem.*, 2014, 53, 4797-4799.
57. J. Hermannsdörfer and R. Kempe, *Chem. Eur. J.*, 2011, 17, 8071-8077.
58. H. Liu, Y. Li, R. Luque and H. Jiang, *Adv. Synth. Catal.*, 2011, 353, 3107-3113.
59. T. WU, P. ZHANG, J. MA, H. FAN, W. WANG, T. JIANG and B. HAN, *Chin. J. Catal.*, 2013, 34, 167-175.
60. W. Du, G. Chen, R. Nie, Y. Li and Z. Hou, *Catal. Commun.*, 2013, 41, 56-59.
61. G.-Q. Kong, S. Ou, C. Zou and C.-D. Wu, *J. Am. Chem. Soc.*, 2012, 134, 19851-19857.
62. L. Zhang, Z. Su, F. Jiang, Y. Zhou, W. Xu and M. Hong, *Tetrahedron.*, 2013, 69, 9237-9244.
63. X. Tan, L. Li, J. Zhang, X. Han, L. Jiang, F. Li and C.-Y. Su, *Chem. Mater.*, 2012, 24, 480-485.
64. A. Corma, H. Garcia and F. Llabrés i Xamena, *Chem. Rev.*, 2010, 110, 4606-4655.
65. K. K. Tanabe and S. M. Cohen, *Inorg. Chem.*, 2010, 49, 6766-6774.
66. A. Dhakshinamoorthy, M. Alvaro and H. Garcia, *Chem. Eur. J.*, 2010, 16, 8530-8536.
67. D. Britt, C. Lee, F. J. Uribe-Romo, H. Furukawa and O. M. Yaghi, *Inorg. Chem.*, 2010, 49, 6387-6389.
68. A. Dhakshinamoorthy, M. Alvaro and H. Garcia, *Appl. Catal. A: Gen.*, 2010, 378, 19-25.
69. W. Lu, D. Yuan, A. Yakovenko and H.-C. Zhou, *Chem. Commun.*, 2011, 47, 4968-4970.
70. F.-N. Shi, A. R. Silva and J. Rocha, *J. Solid. State. Chem.*, 2011, 184, 2196-2203.
71. L.-X. Shi and C.-D. Wu, *Chem. Commun.*, 2011, 47, 2928-2930.
72. L. T. Nguyen, C. V. Nguyen, G. H. Dang, K. K. Le and N. T. Phan, *J. Mol. Catal. A: Chem.*, 2011, 349, 28-35.
73. M. Deng, Y. Ling, B. Xia, Z. Chen, Y. Zhou, X. Liu, B. Yue and H. He, *Chem. Eur. J*, 2011, 17, 10323-10328.
74. N. T. Phan, K. K. Le and T. D. Phan, *Appl. Catal. A: Gen.*, 2010, 382, 246-253.
75. J. M. Roberts, B. M. Fini, A. A. Sarjeant, O. K. Farha, J. T. Hupp and K. A. Scheidt, *J. Am. Chem. Soc.*, 2012, 134, 3334-3337.
76. S. Horike, M. Dinca, K. Tamaki and J. R. Long, *J. Am. Chem. Soc.*, 2008, 130, 5854-5855.
77. D. Dang, P. Wu, C. He, Z. Xie and C. Duan, *J. Am. Chem. Soc.*, 2010., 132, 14321-14323.
78. T. Ladrak, S. Smulders, O. Roubeau, S. J. Teat, P. Gamez and J. Reedijk, *Eur. J. Inorg. Chem.*, 2010, 2010, 3804-3812.
79. J.-M. Gu, W.-S. Kim and S. Huh, *Dalton T.*, 2011, 40 (41), 10826-10829.
80. X. Zhang, F. Llabres i Xamena and A. Corma, *J. Catal.*, 2009, 265, 155-160.
81. E. E. Macias, P. Ratnasamy and M. A. Carreon, *Catal. Today.*, 2012, 198, 215-218.
82. A. Sachse, R. Ameloot, B. Coq, F. Fajula, B. Coasne, D. De Vos and A. Galarneau, *Chem. Commun.*, 2012, 48, 4749-4751.

83. E. Pérez-Mayoral and J. Čejka, *ChemCatChem.*, 2011, 3, 157-159.
84. A. Arnanz, M. Pintado-Sierra, A. Corma, M. Iglesias and F. Sánchez, *Adv. Synth. Catal.*, 2012, 354, 1347-1355.
85. A. Dhakshinamoorthy, M. Alvaro and H. Garcia, *Adv. Synth. Catal.,* 2010, 352, 3022-3030.
86. T. V. Vu, H. Kosslick, A. Schulz, J. Harloff, E. Paetzold, H. Lund, U. Kragl, M. Schneider and G. Fulda, *Microporous Mesoporous Mater.*, 2012, 154, 100-106.
87. P. Li, S. Regati, R. J. Butcher, H. D. Arman, Z. Chen, S. Xiang, B. Chen and C.-G. Zhao, *Tetrahedron Lett.*, 2011, 52, 6220-6222.
88. A. Dhakshinamoorthy, M. Alvaro and H. Garcia, *Adv. Synth. Catal.,* 2010, 352, 711-717.
89. M. Opanasenko, M. Shamzhy, M. Lamač and J. Čejka, *Catal. Today.*, 2013, 204, 94-100.
90. S. Gao, N. Zhao, M. Shu and S. Che, *Appl. Catal. A: Gen.*, 2010, 388, 196-201.
91. M. J. Vitorino, T. Devic, M. Tromp, G. Férey and M. Visseaux, *Macromol. Chem. Phys.*, 2009, 210, 1923-1932.
92. A. Phan, A. U. Czaja, F. Gándara, C. B. Knobler and O. M. Yaghi, *Inorg. Chem.*, 2011, 50, 7388-7390.
93. S. Priyadarshini, P. Amal Joseph, M. L. Kantam and B. Sreedhar, *Tetrahedron*, 2013, 69, 6409-6414.
94. H.-Y. Cho, D. Yang, J. Kim, S.-Y. Jeong and W.-S. Ahn, *Catal. Today.*, 2012, 185, 35-40.
95. N. T. Phan, T. T. Nguyen, C. V. Nguyen and T. T. Nguyen, *Appl. Catal. A: Gen.,* 2013, 457, 69-77.
96. J. L. Harding and M. M. Reynolds, *J. Am. Chem. Soc.*, 2012, 134, 3330-3333.
97. Y.-F. Chen, Y.-C. Ma and S.-M. Chen, *Cryst. Growth Des.*, 2013, 13, 4154-4157.
98. I. Luz, F. Llabrés i Xamena and A. Corma, *J. Catal.*, 2012, 285, 285-291.
99. A. Dhakshinamoorthy, M. Alvaro and H. Garcia, *ACS Catal.*, 2010, 1, 48-53.
100. S. J. Fretz, C. M. Hadad, D. J. Hart, S. Vyas and D. Yang, *j. Org. Chem.*, 2012, 78, 83-92.
101. M. T. Khan and A. E. Martell, *J. Am. Chem. Soc.*, 1967, 89, 4176-4185.
102. H. A. Younus, N. Ahmad, W. Su and F. Verpoort, *Coord. Chem. Rev.*, 2014, 276, 112-152.
103. R. Custelcean and M. G. Gorbunova, *J. Am. Chem. Soc.*, 2005, 127, 16362-16363.
104. R. Kitaura, K. Fujimoto, S. i. Noro, M. Kondo and S. Kitagawa, *Angew. Chem*, *Int. Ed.,* 2002, 114, 141-143.
105. S.-H. Cho, B. Ma, S. T. Nguyen, J. T. Hupp and T. E. Albrecht-Schmitt, *Chemical Commun.*, 2006, 2563-2565.
106. A. Dhakshinamoorthy, M. Alvaro, H. Chevreau, P. Horcajada, T. Devic, C. Serre and H. Garcia, *Cat. Sci. Tec.*, 2012, 2, 324-330.
107. L. Mitchell, B. Gonzalez-Santiago, J. P. Mowat, M. E. Gunn, P. Williamson, N. Acerbi, M. L. Clarke and P. A. Wright, *Cat. Sci. Tec.*, 2013, 3, 606-617.
108. K. Leus, M. Vandichel, Y.-Y. Liu, I. Muylaert, J. Musschoot, S. Pyl, H. Vrielinck, F. Callens, G. B. Marin and C. Detavernier, *J. Catal.*, 2012, 285, 196-207.
109. H.-Y. Cho, D.-A. Yang, J. Kim, S.-Y. Jeong and W.-S. Ahn, *Catal. Today.*, 2012, 185, 35-40.
110. M. Opanasenko, M. Shamzhy and J. Čejka, *ChemCatChem.*, 2013, 5, 1024-1031.
111. I. Luz, F. L. i Xamena and A. Corma, *J. Catal.*, 2012, 285, 285-291.
112. N. T. Phan, P. H. Vu and T. T. Nguyen, *J. Catal.*, 2013, 306, 38-46.
113. T. Yang, H. Cui, C. Zhang, L. Zhang and C.-Y. Su, *Inorg. Chem.*, 2013, 52, 9053-9059.
114. T. Yang, H. Cui, C. Zhang, L. Zhang and C. Y. Su, *ChemCatChem.*, 2013, 5, 3131-3138.

115. K. Gedrich, M. Heitbaum, A. Notzon, I. Senkovska, R. Fröhlich, J. Getzschmann, U. Mueller, F. Glorius and S. Kaskel, *Chem. Eur. J.*, 2011, 17, 2099-2106.
116. C. M. Miralda, E. E. Macias, M. Zhu, P. Ratnasamy and M. A. Carreon, *ACS Catal.*, 2011, 2, 180-183.
117. X. Jing, C. He, D. Dong, L. Yang and C. Duan, *Angew. Chem. Int. Ed.*, 2012, 51, 10127-10131.
118. R. Sen, D. Saha and S. Koner, *Chem. Eur. J.*, 2012, 18, 5979-5986.
119. D. Saha, R. Sen, T. Maity and S. Koner, *Dalton T.*, 2012, 41, 7399-7408.
120. F. Vermoortele, M. Vandichel, B. Van de Voorde, R. Ameloot, M. Waroquier, V. Van Speybroeck and D. E. De Vos, *Angew. Chem. Int. Ed.*, 2012, 51, 4887-4890.
121. S. Opelt, V. Krug, J. Sonntag, M. Hunger and E. Klemm, *Microporous Mesoporous Mater.*, 2012, 147, 327-333.
122. S. Schuster, E. Klemm and M. Bauer, *Chem. Eur. J.*, 2012, 18, 15831-15837.
123. M. Feyand, E. Mugnaioli, F. Vermoortele, B. Bueken, J. M. Dieterich, T. Reimer, U. Kolb, D. De Vos and N. Stock, *Angew. Chem. Int. Ed.*, 2012, 51, 10373-10376.
124. M. H. Xie, X. L. Yang and C. D. Wu, *Chem. Eur. J.*, 2011, 17, 11424-11427.
125. S. Biswas, M. Maes, A. Dhakshinamoorthy, M. Feyand, D. E. De Vos, H. Garcia and N. Stock, *J. Mater. Chem.*, 2012, 22, 10200-10209.
126. Y. Lu, M. Tonigold, B. Bredenkötter, D. Volkmer, J. Hitzbleck and G. Langstein, *J. Inorg. Gen. Chem.*, 2008, 634, 2411-2417.
127. K. Brown, S. Zolezzi, P. Aguirre, D. Venegas-Yazigi, V. Paredes-García, R. Baggio, M. A. Novak and E. Spodine, *Dalton T.*, 2009, 1422-1427.
128. L. Jian, C. Chen, F. Lan, S. Deng, W. Xiao and N. Zhang, *Solid. State Sci.*, 2011, 13, 1127-1131.
129. J. C. Freitas, C. K. de Oliveira, E. C. Cunha, I. Malvestiti, S. Alves Jr, R. L. Longo and P. H. Menezes, *Tetrahedron Lett.*, 2013, 54, 1558-1561.
130. H.-F. Yao, Y. Yang, H. Liu, F.-G. Xi and E.-Q. Gao, *J. Mol. Catal. A: Chem.*, 2014, 394, 57-65.
131. I. Luz, F. Llabrés i Xamena and A. Corma, *J. Catal.*, 2010, 276, 134-140.
132. H. T. Le, T. T. Nguyen, P. H. Vu, T. Truong and N. T. P, *J. Mol. Catal. A: Chem.*, 2014, 391, 74-82.
133. K. Schlichte, T. Kratzke and S. Kaskel, *Microporous Mesoporous Mater.*, 2004, 73, 81-88.
134. W. Mori, T. Sato, T. Ohmura, C. Nozaki Kato and T. Takei, *J. Solid State Chem.*, 2005, 178, 2555-2573.
135. W. Mori, S. Takamizawa, C. N. Kato, T. Ohmura and T. Sato, *Microporous Mesoporous mater.*, 2004, 73, 31-46.
136. C. N. Kato and W. Mori, *C. R. Chim.*, 2007, 10, 284-294.
137. C. N. Kato, M. Ono, T. Hino, T. Ohmura and W. Mori, *Catal. Commun.*, 2006, 7, 673-677.
138. R. S. Kumar, S. S. Kumar and M. A. Kulandainathan, *Microporous Mesoporous Mater.*, 2013, 168, 57-64.
139. L. T. Nguyen, T. T. Nguyen, K. D. Nguyen and N. T. Phan, *Appl. Catal. A: Gen*, 2012, 425, 44-52.
140. Y. Liu, K. Mo and Y. Cui, *Inorg. Chem.*, 2013, 52, 10286-10291.
141. G. Calleja, R. Sanz, G. Orcajo, D. Briones, P. Leo and F. Martínez, *Catal. Today.*, 2014, 227, 130-137.
142. Y. Zhu, Y.-M. Wang, S.-Y. Zhao, P. Liu, C. Wei, Y.-L. Wu, C.-K. Xia and J.-M. Xie, *Inorg. chem.*, 2014, 53, 7692-7699.
143. E. Y. Park, Z. Hasan, I. Ahmed and S. H. Jhung, *Bull. Korean Chem. Soc.*, 2014, 35, 1659-1664.
144. U. Ravon, G. Chaplais, C. Chizallet, B. Seyyedi, F. Bonino, S. Bordiga, N. Bats and D. Farrusseng, *ChemCatChem.*, 2010, 2, 1235-1238.

145. M. Padmanaban, P. Müller, C. Lieder, K. Gedrich, R. Grünker, V. Bon, I. Senkovska, S. Baumgärtner, S. Opelt and S. Paasch, *Chem Commun.*, 2011, 47, 12089-12091.
146. K. M. Taylor-Pashow, J. D. Rocca, Z. Xie, S. Tran and W. Lin, *J. Am. Chem. Soc.*, 2009, 131, 14261-14263.
147. K. S. Suslick, P. Bhyrappa, J.-H. Chou, M. E. Kosal, S. Nakagaki, D. W. Smithenry and S. R. Wilson, *Accounts. Chem. Res*, 2005, 38, 283-291.
148. J. Juan-Alcañiz, R. Gielisse, A. B. Lago, E. V. Ramos-Fernandez, P. Serra-Crespo, T. Devic, N. Guillou, C. Serre, F. Kapteijn and J. Gascon, *Cat. Sci. Tec.*, 2013, 3, 2311-2318.
149. B. Chen, L. Wang, Y. Xiao, F. R. Fronczek, M. Xue, Y. Cui and G. Qian, *Angew. Chem. Int. Ed.*, 2009, 48, 500-503.
150. S. Hasegawa, S. Horike, R. Matsuda, S. Furukawa, K. Mochizuki, Y. Kinoshita and S. Kitagawa, *J. Am. Chem. Soc.,* 2007, 129, 2607-2614.
151. M. N. Timofeeva, V. N. Panchenko, J. W. Jun, Z. Hasan, M. M. Matrosova and S. H. Jhung, *Appl. Catal. A: Gen.*, 2014, 471, 91-97.
152. Y. Yang, H.-F. Yao, F.-G. Xi and E.-Q. Gao, *J. Mol. Catal. A: Chem.*, 2014, 390, 198-205.
153. P. Valvekens, M. Vandichel, M. Waroquier, V. Van Speybroeck and D. De Vos, *J. Catal.*, 2014, 317, 1-10.
154. M. Hartmann and M. Fischer, *Microporous Mesoporous Mater.*, 2012, 164, 38-43.
155. R.-R. Cheng, S.-X. Shao, H.-H. Wu, Y.-F. Niu, J. Han and X.-L. Zhao, *Inorg. Chem. Commun.*, 2014, 46, 226-228.
156. H. Deng, C. J. Doonan, H. Furukawa, R. B. Ferreira, J. Towne, C. B. Knobler, B. Wang and O. M. Yaghi, *Science.*, 2010, 327, 846-850.
157. W. Kleist, F. Jutz, M. Maciejewski and A. Baiker, *Eur. J. Inorg. Chem.*, 2009, 2009, 3552-3561.
158. Y. Huang, S. Gao, T. Liu, J. Lü, X. Lin, H. Li and R. Cao, *ChemPlusChem.*, 2012, 77, 106-112.
159. S. Marx, W. Kleist, J. Huang, M. Maciejewski and A. Baiker, *Dalton T.*, 2010, 39 (16), 3795-3798.
160. Y. Jiang, J. Huang, S. Marx, W. Kleist, M. Hunger and A. Baiker, *J. Phys. Chem. Lett.*, 2010, 1, 2886-2890.
161. D. Zhao, D. J. Timmons, D. Yuan and H.-C. Zhou, *Acc. Chem. Res.*, 2010, 44, 123-133.
162. Y. Pan, B. Yuan, Y. Li and D. He, *Chem. Commun.*, 2010, 46, 2280-2282.
163. B. Li, Y. Zhang, D. Ma, L. Li, G. Li, G. Li, Z. Shi and S. Feng, *Chem. Commun.*, 2012, 48, 6151-6153.
164. F. Cirujano, F. L. i Xamena and A. Corma, *Dalton T.*, 2012, 41 (14), 4249-4254.
165. F. G. Cirujano, A. Leyva-Pérez, A. Corma and F. X. Llabrés i Xamena, *ChemCatChem.*, 2013, 5, 538-549.
166. J. Huang, W. Wang and H. Li, *ACS Catal.*, 2013, 3, 1526-1536.
167. F. Vermoortele, R. Ameloot, A. Vimont, C. Serre and D. De Vos, *Chem. Commun.*, 2011, 47, 1521-1523.
168. C. Chizallet, S. Lazare, D. Bazer-Bachi, F. Bonnier, V. Lecocq, E. Soyer, A.-A. Quoineaud and N. Bats, *J. Am. Chem. Soc.*, 2010, 132, 12365-12377.
169. M. Zhu, D. Srinivas, S. Bhogeswararao, P. Ratnasamy and M. A. Carreon, *Catal. Commun.*, 2013, 32, 36-40.
170. J. Park, J.-R. Li, Y.-P. Chen, J. Yu, A. A. Yakovenko, Z. U. Wang, L.-B. Sun, P. B. Balbuena and H.-C. Zhou, *Chem. Commun.*, 2012, 48, 9995-9997.
171. P. Zhang, B. Li, Y. Zhao, X. Meng and T. Zhang, *Chem. Commun.*, 2011, 47, 7722-7724.
172. P. Wu, J. Wang, Y. Li, C. He, Z. Xie and C. Duan, *Adv. Funct. Mater.*, 2011, 21, 2788-2794.

173. R. Srirambalaji, S. Hong, R. Natarajan, M. Yoon, R. Hota, Y. Kim, Y. H. Ko and K. Kim, *Chem. Commun.*, 2012, 48, 11650-11652.
174. J. Kim, S.-N. Kim, H.-G. Jang, G. Seo and W.-S. Ahn, *Appl. Catal. A: Gen.*, 2013, 453, 175-180.
175. F. Costa, C. Silva, M. Raposo, A. Fonseca, I. Neves, A. Carvalho and J. Pires, *Microporous Mesoporous mater.*, 2004, 72, 111-118.
176. K. V. Kovtunov, V. V. Zhivonitko, A. Corma and I. V. Koptyug, *J. Phys. Chem. Lett.*, 2010, 1, 1705-1708.
177. W.-L. Liu, S.-H. Lo, B. Singco, C.-C. Yang, H.-Y. Huang and C.-H. Lin, *J. Mater. Chem.*, 2013, 1, 928-932.
178. W. L. Liu, C. Y. Wu, C. Y. Chen, B. Singco, C. H. Lin and H. Y. Huang, *Chem. Eur. J.*, 2014, 20, 8923-8928.
179. V. Lykourinou, Y. Chen, X.-S. Wang, L. Meng, T. Hoang, L.-J. Ming, R. L. Musselman and S. Ma, *J. Am. Chem. Soc.*, 2011, 133, 10382-10385.
180. A. Dhakshinamoorthy, M. Alvaro and H. Garcia, *J. Catal.*, 2012, 289, 259-265.
181. J. Canivet, S. Aguado, Y. Schuurman and D. Farrusseng, *J. Am. Chem. Soc.*, 2013, 135, 4195-4198.
182. A. Dhakshinamoorthy, M. Alvaro and H. Garcia, *Chem. Eur. J.*, 2011, 17, 6256-6262.
183. A. Dhakshinamoorthy, M. Alvaro and H. Garcia, *ChemCatChem.*, 2010, 2, 1438-1443.
184. L. Bromberg, X. Su and T. A. Hatton, *Chem. Mater.*, 2013, 25, 1636-1642.
185. S. S. Balula, I. C. Santos, L. Cunha-Silva, A. P. Carvalho, J. Pires, C. Freire, J. A. Cavaleiro, B. de Castro and A. Cavaleiro, *Catal. Today.*, 2013, 203, 95-102.
186. O. Kholdeeva, N. Maksimchuk and G. Maksimov, *Catal. Today.*, 2010, 157, 107-113.
187. A. C. Estrada, I. C. Santos, M. M. Simões, M. Neves, J. A. Cavaleiro and A. Cavaleiro, *Appl. Catal. A: Gen.*, 2011, 392, 28-35.
188. P. A. Shringarpure and A. Patel, *Dalton T.*, 2010, 39 (10), 2615-2621.
189. N. V. Maksimchuk, K. A. Kovalenko, S. S. Arzumanov, Y. A. Chesalov, M. S. Melgunov, A. G. Stepanov, V. P. Fedin and O. A. Kholdeeva, *Inorg. Chem.*, 2010, 49, 2920-2930.
190. N. V. Maksimchuk, O. A. Kholdeeva, K. A. Kovalenko and V. P. Fedin, *Isr. J. Chem.*, 2011, 51, 281-289.
191. L. H. Wee, S. R. Bajpe, N. Janssens, I. Hermans, K. Houthoofd, C. E. Kirschhock and J. A. Martens, *Chem. Commun.*, 2010, 46, 8186-8188.
192. L. H. Wee, N. Janssens, S. R. Bajpe, C. E. Kirschhock and J. A. Martens, *Catal. Today.*, 2011, 171, 275-280.
193. C. M. Granadeiro, A. D. Barbosa, P. Silva, F. A. A. Paz, V. K. Saini, J. Pires, B. de Castro, S. S. Balula and L. Cunha-Silva, *Appl. Catal. A: Gen.*, 2013, 453, 316-326.
194. H. Yang, J. Li, H. Zhang, Y. Lv and S. Gao, *Microporous Mesoporous Mater.*, 2014, 195, 87-91.
195. E. Kockrick, T. Lescouet, E. V. Kudrik, A. B. Sorokin and D. Farrusseng, *Chem. Commun.*, 2011, 47, 1562-1564.
196. Q.-R. Fang, T. A. Makal, M. D. Young and H.-C. Zhou, *Comments Inorg. Chem.*, 2010, 31, 165-195.
197. N. Maksimchuk, M. Timofeeva, M. Melgunov, A. Shmakov, Y. A. Chesalov, D. Dybtsev, V. Fedin and O. Kholdeeva, *J. Catal.*, 2008, 257, 315-323.
198. H. Yang, J. Li, L. Wang, W. Dai, Y. Lv and S. Gao, *Catal. Commun.*, 2013, 35, 101-104.
199. J. Juan-Alcañiz, E. V. Ramos-Fernandez, U. Lafont, J. Gascon and F. Kapteijn, *Journal of Catal.*, 2010, 269, 229-241.
200. L. Bromberg, X. Su and T. A. Hatton, *ACS Appl. Mater. Interfaces.*, 2013, 5, 5468-5477.

201. D. Dang, Y. Bai, C. He, J. Wang, C. Duan and J. Niu, *Inorg. Chem.*, 2010, 49, 1280-1282.
202. J. Song, Z. Luo, D. K. Britt, H. Furukawa, O. M. Yaghi, K. I. Hardcastle and C. L. Hill, *J. Am. Chem. Soc.*, 2011, 133, 16839-16846.
203. O. K. Farha, A. M. Shultz, A. A. Sarjeant, S. T. Nguyen and J. T. Hupp, *J. Am. Chem. Soc.*, 2011, 133, 5652-5655.
204. A. Fateeva, P. A. Chater, C. P. Ireland, A. A. Tahir, Y. Z. Khimyak, P. V. Wiper, J. R. Darwent and M. J. Rosseinsky, *Angew. Chem*, *Int. Ed.,* 2012, 124, 7558-7562.
205. D. Feng, Z. Y. Gu, J. R. Li, H. L. Jiang, Z. Wei and H. C. Zhou, *Angew. Chem*, *Int. Ed.*, 2012, 124, 10453-10456.
206. M. Jahan, Q. Bao and K. P. Loh, *J. Am. Chem. Soc.*, 2012, 134, 6707-6713.
207. R. W. Larsen, L. Wojtas, J. Perman, R. L. Musselman, M. J. Zaworotko and C. M. Vetromile, *J. Am. Chem. Soc*., 2011, 133, 10356-10359.
208. Z. Zhang, L. Zhang, L. Wojtas, P. Nugent, M. Eddaoudi and M. J. Zaworotko, *J. Am. Chem. Soc.*, 2011, 134, 924-927.
209. M. H. Alkordi, Y. Liu, R. W. Larsen, J. F. Eubank and M. Eddaoudi, *J. Am. Chem. Soc*., 2008, 130, 12639-12641.
210. M. Meilikhov, K. Yusenko, D. Esken, S. Turner, G. Van Tendeloo and R. A. Fischer, *Eur. J. Inorg. Chem.*, 2010, 2010, 3701-3714.
211. A. Dhakshinamoorthy and H. Garcia, *Chem. Soc. Rev*, 2012, 41, 5262-5284.
212. H. R. Moon, D.-W. Lim and M. P. Suh, *Chem. Soc. Rev.*, 2013, 42, 1807-1824.
213. F. Wu, L.-G. Qiu, F. Ke and X. Jiang, *Inorg. Chem. Commun.*, 2013, 32, 5-8.
214. M. Sabo, A. Henschel, H. Fröde, E. Klemm and S. Kaskel, *J. Mater. Chem.*, 2007, 17, 3827-3832.
215. T. Ishida, M. Nagaoka, T. Akita and M. Haruta, *Chem. Eur. J.*, 2008, 14, 8456-8460.
216. S. Hermes, F. Schröder, S. Amirjalayer, R. Schmid and R. A. Fischer, *J. Mater. Chemi.*, 2006, 16, 2464-2472.
217. H.-L. Jiang, T. Akita, T. Ishida, M. Haruta and Q. Xu, *J. Am. Chem. Soc.*, 2011, 133, 1304-1306.
218. H.-L. Jiang, B. Liu, T. Akita, M. Haruta, H. Sakurai and Q. Xu, *J. Am. Chem. Soc.*, 2009, 131, 11302-11303.
219. A. Aijaz, A. Karkamkar, Y. J. Choi, N. Tsumori, E. Rönnebro, T. Autrey, H. Shioyama and Q. Xu, *J. Am. Chem. Soc.*, 2012, 134, 13926-13929.
220. G. Lu, S. Li, Z. Guo, O. K. Farha, B. G. Hauser, X. Qi, Y. Wang, X. Wang, S. Han and X. Liu, *Nat. Chem.*, 2012, 4, 310-316.
221. M. Zhao, K. Deng, L. He, Y. Liu, G. Li, H. Zhao and Z. Tang, *J. Am. Chem. Soc.*, 2014, 136, 1738-1741.
222. Z. Sun, G. Li, L. Liu and H.-o. Liu, *Catal. Commun.*, 2012, 27, 200-205.
223. Y. Huang, Z. Zheng, T. Liu, J. Lü, Z. Lin, H. Li and R. Cao, *Catal. Commun.*, 2011, 14, 27-31.
224. T.-H. Park, A. J. Hickman, K. Koh, S. Martin, A. G. Wong-Foy, M. S. Sanford and A. J. Matzger, *J. Am. Chem. Soc.*, 2011, 133, 20138-20141.
225. V. Pascanu, Q. Yao, A. Bermejo Gómez, M. Gustafsson, Y. Yun, W. Wan, L. Samain, X. Zou and B. Martín-Matute, *Chem. Eur. J.*, 2013, 19, 17483-17493.
226. T. T. Dang, Y. Zhu, J. S. Ngiam, S. C. Ghosh, A. Chen and A. M. Seayad, *ACS Catal.*, 2013, 3, 1406-1410.
227. M. Martis, K. Mori, K. Fujiwara, W.-S. Ahn and H. Yamashita, *J. Phys. Chem. C.*, 2013, 117, 22805-22810.
228. T. Van Vu, H. Kosslick, A. Schulz, J. Harloff, E. Paetzold, M. Schneider, J. Radnik, N. Steinfeldt, G. Fulda and U. Kragl, *Appl. Catal. A: Gen.*, 2013, 468, 410-417.
229. X. Zhao, Y. Jin, F. Zhang, Y. Zhong and W. Zhu, *Chem. Eng. J.*, 2014, 239, 33-41.

230. V. Isaeva, O. Tkachenko, E. Afonina, L. Kozlova, G. Kapustin, W. Grünert, S. Solov'eva, I. Antipin and L. Kustov, *Microporous Mesoporous Mater.*, 2013, 166, 167-175.
231. H. Zhao, H. Song and L. Chou, *Inorg. Chem. Commun.*, 2012, 15, 261-265.
232. R. Fazaeli, H. Aliyan, M. Moghadam and M. Masoudinia, *J. Mol. Catal. A: Chem.*, 2013, 374, 46-52.
233. W. Wang, Y. Li, R. Zhang, D. He, H. Liu and S. Liao, *Catal. Commun.*, 2011, 12, 875-879.
234. H.-L. Jiang, Y. Tatsu, Z.-H. Lu and Q. Xu, *J. Am. Chem. Soc.*, 2010, 132, 5586-5587.
235. X. Gu, Z.-H. Lu and Q. Xu, *Chem. Commun.*, 2010, 46, 7400-7402.
236. H.-L. Jiang and Q. Xu, *Chem. Commun.*, 2011, 47, 3351-3370.
237. F. Schröder, S. Henke, X. Zhang and R. A. Fischer, *Eur. J. Inorg. Chem.*, 2009, 2009, 3131-3140.
238. X. Gu, Z.-H. Lu, H.-L. Jiang, T. Akita and Q. Xu, *J. Am. Chem. Soc.,* 2011, 133, 11822-11825.
239. J. Long, H. Liu, S. Wu, S. Liao and Y. Li, *ACS Catal.*, 2013, 3, 647-654.
240. Z. Wang and S. M. Cohen, *Chem. Soc. Rev.*, 2009, 38, 1315-1329.
241. J. S. Seo, D. Whang, H. Lee, S. Im Jun, J. Oh, Y. J. Jeon and K. Kim, *Nature.*, 2000, 404, 982-986.
242. B. Hoskins and R. Robson, *J. Am. Chem. Soc.*, 1990, 112, 1546-1554.
243. Z. Wang and S. M. Cohen, *J. Am. Chem. Soc.*, 2007, 129, 12368-12369.
244. C. J. Doonan, W. Morris, H. Furukawa and O. M. Yaghi, *J. Am. Chem. Soc.,* 2009, 131, 9492-9493.
245. T. Gadzikwa, O. K. Farha, K. L. Mulfort, J. T. Hupp and S. T. Nguyen, *Chem. Commun.*, 2009, 3720-3722.
246. S. J. Garibay, Z. Wang, K. K. Tanabe and S. M. Cohen, *Inorg. Chem.*, 2009, 48, 7341-7349.
247. D. Saha, R. Sen, T. Maity and S. Koner, *Langmuir.*, 2013, 29, 3140-3151.
248. S. J. Garibay, Z. Wang and S. M. Cohen, *Inorg. Chem.*, 2010, 49, 8086-8091.
249. M. Pintado-Sierra, A. M. Rasero-Almansa, A. Corma, M. Iglesias and F. Sánchez, *J. Catal.*, 2013, 299, 137-145.
250. J. Juan-Alcañiz, J. Ferrando-Soria, I. Luz, P. Serra-Crespo, E. Skupien, V. P. Santos, E. Pardo, F. X. Llabres i Xamena, F. Kapteijn and J. Gascon, *J. Catal.*, 2013, 307, 295-304.
251. D. J. Lun, G. I. Waterhouse and S. G. Telfer, *J. Am. Chem. Soc.*, 2011, 133, 5806-5809.
252. S. Wang, L. Bromberg, H. Schreuder-Gibson and T. A. Hatton, *ACS Appl. Mater. interfaces.*, 2013, 5, 1269-1278.
253. D. Rankine, A. Avellaneda, M. R. Hill, C. J. Doonan and C. J. Sumby, *Chem. Commun.*, 2012, 48, 10328-10330.
254. A. M. Shultz, A. A. Sarjeant, O. K. Farha, J. T. Hupp and S. T. Nguyen, *J. Am. Chem. Soc.,*2011, 133,13252-13255.
255. S. M. Cohen, *Chem. Rev.*, 2012, 112 (2), 970-1000.
256. A. Demessence, D. M. D'Alessandro, M. L. Foo and J. R. Long, *J. Am. Chem. Soc.,* 2009, 131, 8784-8786.
257. A. M. Shultz, O. K. Farha, D. Adhikari, A. A. Sarjeant, J. T. Hupp and S. T. Nguyen, *Inorg. Chem.*, 2011, 50, 3174-3176.
258. O. Karagiaridi, W. Bury, A. A. Sarjeant, C. L. Stern, O. K. Farha and J. T. Hupp, *Chem. Sci.*, 2012, 3, 3256-3260.
259. M. Kim, J. F. Cahill, Y. Su, K. A. Prather and S. M. Cohen, *Chem. Sci.*, 2012, 3, 126-130.
260. M. Kim, J. F. Cahill, H. Fei, K. A. Prather and S. M. Cohen, *J. Am. Chem. Soc.,* 2012, 134, 18082-18088.

261. H. Fei, J. F. Cahill, K. A. Prather and S. M. Cohen, *Inorg. Chem.*, 2013, 52, 4011-4016.
262. S. Jeong, D. Kim, X. Song, M. Choi, N. Park and M. S. Lah, *Chem. Mater.*, 2013, 25, 1047-1054.
263. S. Takaishi, E. J. DeMarco, M. J. Pellin, O. K. Farha and J. T. Hupp, *Chem. Sci.*, 2013, 4, 1509-1513.
264. H. G. T. Nguyen, M. H. Weston, A. A. Sarjeant, D. M. Gardner, Z. An, R. Carmieli, M. R. Wasielewski, O. K. Farha, J. T. Hupp and S. T. Nguyen, *Cryst. Growth Des.*, 2013, 13, 3528-3534.
265. H. Fei, J. Shin, Y. S. Meng, M. Adelhardt, J. r. Sutter, K. Meyer and S. M. Cohen, *J. Am. Chem. Soc*, 2014, 136, 4965-4973.
266. F. B. Hamad, T. Sun, S. Xiao and F. Verpoort, *Coord. Chem. Rev.*, 2013, 257, 2274-2292.
267. A. M. Lozano-Vila, S. Monsaert, A. Bajek and F. Verpoort, *Chem. Rev.*, 2010, 110, 4865-4909.
268. R. Drozdzak, N. Nishioka, G. Recher and F. Verpoort, *Macromol. Symp.,* 2010, 293, 1-4.
269. N. A. Vermeulen, O. Karagiaridi, A. A. Sarjeant, C. L. Stern, J. T. Hupp, O. K. Farha and J. F. Stoddart, *J. Am. Chem. Soc.*, 2013, 135, 14916-14919.
270. G. Di Carlo, G. Melaet, N. Kruse, L. F. Liotta, G. Pantaleo and A. M. Venezia, *Chem. Commun.*, 2010, 46, 6317-6319.
271. J.-Y. Park, Z.-M. Wang, D.-K. Kim and J.-S. Lee, *Renew. Energ.*, 2010, 35, 614-618.
272. J. G. Nguyen and S. M. Cohen, *J. Am. Chem. Soc.,* 2010, 132, 4560-4561.
273. D. Ma, Y. Li and Z. Li, *Chem. Commun.*, 2011, 47, 7377-7379.
274. J. Canivet, S. Aguado, C. Daniel and D. Farrusseng, *ChemCatChem.*, 2011, 3, 675-678.
275. S. Aguado, J. Canivet, Y. Schuurman and D. Farrusseng, *J. Catal.*, 2011, 284, 207-214.
276. B. Kesanli and W. Lin, *Coord. Chem. Rev.*, 2003, 246, 305-326.
277. P. Li, Y. He, J. Guang, L. Weng, J. C.-G. Zhao, S. Xiang and B. Chen, *J. Am. Chem. Soc.*, 2014, 136, 547-549.
278. L. Ma, C. Abney and W. Lin, *Chem. Soc. Rev.*, 2009, 38, 1248-1256.
279. C. Valente, E. Choi, M. E. Belowich, C. J. Doonan, Q. Li, T. B. Gasa, Y. Y. Botros, O. M. Yaghi and J. F. Stoddart, *Chem. Commun.*, 2010, 46, 4911-4913.
280. O. R. Evans, H. L. Ngo and W. Lin, *J. Am. Chem. Soc.*, 2001, 123, 10395-10396.
281. Y. Liu, W. Xuan and Y. Cui, *Adv. Mater.*, 2010, 22, 4112-4135.
282. M. Yoon, R. Srirambalaji and K. Kim, *Chem. Rev.*, 2011, 112 (2), 1196-1231.
283. C.-D. Wu, A. Hu, L. Zhang and W. Lin, *J. Am. Chem. Soc.*, 2005, 127, 8940-8941.
284. F. Song, C. Wang, J. M. Falkowski, L. Ma and W. Lin, *J. Am. Chem. Soc.,* 2010, 132, 15390-15398.
285. C. Zhu, G. Yuan, X. Chen, Z. Yang and Y. Cui, *J. Am. Chem. Soc*., 2012, 134, 8058-8061.
286. J. M. Falkowski, T. Sawano, T. Zhang, G. Tsun, Y. Chen, J. V. Lockard and W. Lin, *J. Am. Chem. Soc.,* 2014, 136, 5213-5216.
287. M. Kandiah, M. H. Nilsen, S. Usseglio, S. Jakobsen, U. Olsbye, M. Tilset, C. Larabi, E. A. Quadrelli, F. Bonino and K. P. Lillerud, *Chem. Mater.*, 2010, 22, 6632-6640.
288. L. Ma, J. M. Falkowski, C. Abney and W. Lin, *Nat. Chem.*, 2010, 2, 838-846.
289. L. Ma, C. D. Wu, M. M. Wanderley and W. Lin, *Angew. Chem*, *Int. Ed*., 2010, 122, 8420-8424.
290. K. S. Jeong, Y. B. Go, S. M. Shin, S. J. Lee, J. Kim, O. M. Yaghi and N. Jeong, *Chem. Sci.*, 2011, 2, 877-882.
291. Q. Han, C. He, M. Zhao, B. Qi, J. Niu and C. Duan, *J. Am. Chem. Soc.*, 2013, 135, 10186-10189.

292. K. Mo, Y. Yang and Y. Cui, *J. Am. Chem. Soc.,* 2014, 136, 1746-1749.
293. P. Wu, C. He, J. Wang, X. Peng, X. Li, Y. An and C. Duan, *J. Am. Chem. Soc.,* 2012, 134, 14991-14999.
294. K. S. Park, Z. Ni, A. P. Côté, J. Y. Choi, R. Huang, F. J. Uribe-Romo, H. K. Chae, M. O'Keeffe and O. M. Yaghi, *P. Natal. Acad. Sci.*, 2006, 103, 10186-10191.
295. M. Zhang, M. Bosch, T. Gentle III and H.-C. Zhou, *CrystEngComm*, 2014, 16, 4069-4083.
296. A. Dhakshinamoorthy, M. Alvaro and H. Garcia, *J. Catal.*, 2009, 267, 1-4.
297. R. Banerjee, A. Phan, B. Wang, C. Knobler, H. Furukawa, M. O'Keeffe and O. M. Yaghi, *Science.*, 2008, 319, 939-943.
298. X. C. Huang, Y. Y. Lin, J. P. Zhang and X. M. Chen, *Angew. Chem. Int. Ed.*, 2006, 118, 1587-1589.
299. Y. Liu, V. C. Kravtsov, R. Larsen and M. Eddaoudi, *Chem. Commun.*, 2006, 1488-1490.
300. M. Zhang, Y. P. Chen, M. Bosch, T. Gentle, K. Wang, D. Feng, Z. U. Wang and H. C. Zhou, *Angew. Chem. Int. Ed.*, 2014, 126, 834-837.
301. H. Chevreau, T. Devic, F. Salles, G. Maurin, N. Stock and C. Serre, *Angew. Chem. Int. Ed.*, 2013, 52, 5056-5060.
302. J. H. Cavka, S. Jakobsen, U. Olsbye, N. Guillou, C. Lamberti, S. Bordiga and K. P. Lillerud, *J. Am. Chem. Soc*., 2008, 130, 13850-13851.
303. L. Valenzano, B. Civalleri, S. Chavan, S. Bordiga, M. H. Nilsen, S. Jakobsen, K. P. Lillerud and C. Lamberti, *Chem. Mater.*, 2011, 23, 1700-1718.
304. D. Feng, W.-C. Chung, Z. Wei, Z.-Y. Gu, H.-L. Jiang, Y.-P. Chen, D. J. Darensbourg and H.-C. Zhou, *J. Am. Chem. Soc*., 2013, 135, 17105-17110.
305. H.-L. Jiang, D. Feng, K. Wang, Z.-Y. Gu, Z. Wei, Y.-P. Chen and H.-C. Zhou, *J. Am. Chem. Soc*., 2013, 135, 13934-13938.
306. D. Feng, H.-L. Jiang, Y.-P. Chen, Z.-Y. Gu, Z. Wei and H.-C. Zhou, *Inorg. Chem.*, 2013, 52, 12661-12667.
307. A. Demessence and J. R. Long, *Chem. Eur. J.*, 2010, 16, 5902-5908.
308. H. J. Choi, M. Dinca and J. R. Long, *J. Am. Chem. Soc*., 2008, 130, 7848-7850.
309. V. Colombo, S. Galli, H. J. Choi, G. D. Han, A. Maspero, G. Palmisano, N. Masciocchi and J. R. Long, *Chem. Sci.*, 2011, 2, 1311-1319.
310. S. S. Kaye, A. Dailly, O. M. Yaghi and J. R. Long, *J. Am. Chem. Soc*., 2007, 129, 14176-14177.
311. J. J. Low, A. I. Benin, P. Jakubczak, J. F. Abrahamian, S. A. Faheem and R. R. Willis, *J. Am. Chem. Soc*., 2009, 131, 15834-15842.
312. L. Huang, H. Wang, J. Chen, Z. Wang, J. Sun, D. Zhao and Y. Yan, *Microporous Mesoporous Mater*, 2003, 58, 105-114.
313. K. A. Cychosz and A. J. Matzger, *Langmuir*, 2010, 26, 17198-17202.
314. T. R. Whitfield, X. Wang, L. Liu and A. J. Jacobson, *Solid. State. Sci*, 2005, 7, 1096-1103.
315. T. Loiseau, C. Serre, C. Huguenard, G. Fink, F. Taulelle, M. Henry, T. Bataille and G. Férey, *Chem. Eur. J.*, 2004, 10, 1373-1382.